ALTERNATE REPRESENTATIONS OF DYNAMIC PROPERTIES AND LOADING

by

Caner Gülenç

B.S., Civil Engineering, Dokuz Eylül University, 2010

Submitted to Kandilli Observatory and Earthquake Research Institute
in partial fulfillment of the requirements for the degree of
Master of Science

Graduate Program in Earthquake Engineering

Boğaziçi University

2014

ALTERNATE REPRESENTATIONS OF DYNAMIC PROPERTIES AND LOADING

APPROVED BY:

Assoc. Prof. Gülüm Tanırcan (Thesis Supervisor)	…….
Prof. M. Nuray Aydınoğlu (Thesis Co-supervisor)	…….
Prof. Erdal Şafak	…….
Prof. Sinan D. Akkar	…….
Assit. Prof. İhsan E. Bal (Istanbul Technical University)	…….

DATE OF APPROVAL: 20.06.2014

To my family,

ACKNOWLEDGEMENTS

First of all, I would like to express my appreciation to Prof. Nuray Aydınoğlu for his profound knowledge and experience shared with me during preparation of this thesis. His extraordinary excitement and passion for science have always kept my motivation at top level. Our long conversations have not been only beneficial to learn the topics covered by this thesis but also helpful to complete the shortcomings associated to my basic structural engineering knowledge. That has been a great chance to study with him.

I would like to thank my co-advisor Assoc. Prof. Gülüm Tanırcan for her support and encouragement. I have also received help from Prof. Erdal Şafak and Prof. Sinan Akkar about signal processing and Fourier analysis. Their valuable contributions are gratefully acknowledged.

I would like to thank professors from Dokuz Eylül University, Ömer Zafer Alku, Mustafa Düzgün and Dr. Özgür Bozdağ for their leadership to be accepted from Kandilli Observatory and Earthquake Research Institute.

Special thanks to Dr. Cüneyt Tüzün, who has contributed to me about being a part of Kandilli Observatory, given his time and patience since the day I came to İstanbul. Another special thanks goes to Dr. Eren Vuran since he has been a brother for me rather than a lecturer. Lastly, I would like to thank Dr. Göktürk Önem for sharing his time and knowledge in structural engineering, when I could not understand the topics comprehensively.

I would like to express my sincere gratitude to my friends in our department; Okan İlhan, Zeynep Coşkun and Sedef Kocakaplan. Whenever I confused with the details, they have given me useful advices and opened up my horizon.

I would like to specify my deepest gratitude to my father that I lost six years ago and my mother. Undoubtedly, neither this thesis nor my beautiful life would have been possible, without their efforts and amenities provided to me. Also, I wish to thank to my

sister and brother, who have always been supporting to me in every respect, giving anything I need during my life. Sure that I would be a miserable guy without my dear family.

Finally, I would like to express my sincere appreciation to my beloved fiancée Nihan Erkoyuncu for her extraordinary patience, endurance and love throughout the four year period of our relationship.

ABSTRACT

ALTERNATE REPRESENTATIONS OF DYNAMIC PROPERTIES AND LOADING

This study covers three main topics, which are directly related to dynamic behaviour of structures, namely, representation of mass, damping and loading. These three properties of equation of motion are generally represented by widely accepted approaches. In this thesis, such representations are discussed via comparisons with infrequently used representations and viability of them is investigated. For case study, 50-story core wall structure is chosen.

First topic discussed here is mass representation. Indisputably, the most accepted assumption for mass representation is lumped mass approach, which is very practical to construct the matrix or, at least, easy to understand the concept of. Another representation, not common one, consistent mass approach derived by a similar procedure in the method for derivation of stiffness coefficients. Consistent mass matrix has off-diagonal terms as distinct from lumped mass matrix. Since the core wall has a continuous form, it is reasonable to represent its mass distribution with consistent mass approach, which takes into account coupling terms. Effects of consistent mass representation on dynamic response of a 50-storey core-wall tall building are investigated.

Second one is damping property which may be evaluated as one of the most controversial aspects of structural dynamics. As it is not possible to derive a damping matrix from the element cross section properties and material properties directly, proportional viscous damping matrix is generally used instead, which is defined in terms of modal damping ratios at certain anchor frequencies. However, viscous damping model has a significant deficiency associated with the energy mechanism. Studies based on experimental data show that dissipated energy per cycle of an oscillating system is essentially independent of the excitation frequency as opposed to dependency inherent in

the viscous damping model. Such damping model is called rate-independent or structural damping, which is conveniently modelled in the frequency domain through complex stiffness matrix. One of the aims of this study is to observe the effects of such an alternate damping model on the linear seismic response of a tall building. To this end, a 50-story core-wall tall building system is investigated. Drift and total acceleration response characteristics for a set of earthquake records are obtained from the analyses conducted through Fourier Transform.

Last concept, probably the most innovative idea of this study, is related to loading part of equation of motion. It has been long applied that ground accelerations are used directly as force by multiplying floor masses, eventually, relative response quantities are obtained. The underlying idea of this loading concept is based on pseudo-static transmission assumption, which presumes that base displacement, in any time instant, is transmitted throughout building statically and naturally, such movement does not deform the structure. One of the aims of this study is to investigate viability of this concept. The motivation is based on the idea that if the building is tall enough, is it possible to be transmitted of base displacements throughout the building without generating any significant deformation? For this reason, absolute response and relative response quantities of the 50-story core-wall are obtained by using acceleration and displacement loading concepts respectively. Comparative results are given at the end.

ÖZET

ALTERNATİF DİNAMİK PARAMETRELERİN VE DEPREM YÜKLEMESİNİN DEPREM DAVRANIŞINA ETKİLERİ

Bu çalışma, yapıların dinamik davranışını doğrudan etkileyen kütle, sönüm ve deprem yüklemesi parametrelerinin alternatif modellerini kapsamaktadır. Hareket denkleminin bu üç terimi, genellikle tüm dünyada kabul gören bazı temel yaklaşımlarla temsil edilmektedir. Bu tez kapsamında, dinamik parametrelerin temsilleri için farklı yaklaşımlar kullanılmış ve yapıların sismik tepkisine olan etkileri karşılaştırmalı olarak incelenmişlerdir.

Bu özelliklerden birincisi, yapıdaki kütle dağılımının modellenmesi ile ilgilidir. Kütle dağılımı için tartışmasız en çok kullanılan yöntem; pratik kullanımı ve anlaşılması kolay olması nedeniyle yığılı kütle modelidir. Kütle temsili için kullanılan diğer bir yöntem ise, uyuşumlu kütle yaklaşımıdır. Bu yöntemde; rijitlik katsayılarının türetilmesine benzer şekilde kütle katsayıları elde edilmektedir. Uyuşumlu kütle matrisinde, yığılı kütle matrisinden farklı olarak, köşegen dışı katsayılar da bulunmaktadır ki bu katsayılar sistemdeki kütlelerin hareketlerinin birbirine bağımlı olduğunu ifade etmektedir. Örneğin, bir betonarme çekirdek perdenin sürekli bir yapıya sahip olduğu düşünüldüğünde, uyuşumlu kütle modelini kullanmak bu tip bir yapı için oldukça makul bir yöntem gibi gözükmektedir. Bu sebeple, bahsedilen kütle modellerinin yapının sismik tepkisine etkisi 50 katlı bir betonarme çekirdek perde yapısı analiz edilerek incelenmiştir.

İkinci özellik, belki de yapı dinamiğinin en karmaşık konularından biri olarak sayılabilecek olan sönüm parametresidir. Sönüm matrisini, elemanın mukavemet ve/veya malzeme özelliklerinden elde etmek mümkün olmadığından, genellikle "orantısal viskoz sönüm matrisi" kullanılmaktadır ki bu matris, belli iki frekansa atanılan modal sönüm oranına bağlı olarak tanımlanmaktadır. Ancak, viskoz sönüm modelinin enerji mekanizmasıyla ilişkili önemli bir eksiği vardır. Deneysel olarak elde edilen verilere

dayanan çalışmalar göstermektedir ki; titreşen bir sistemin bir çevriminde tüketilen enerji, viskoz sönüm modelinde ortaya çıkanın aksine, yükleme frekansından bağımsızdır. Yapıların gerçek sönüm davranışını modelleyebildiğimiz bu sönüm çeşidi "frekanstan bağımsız yapısal sönüm" olarak ifade edilmektedir ve ancak frekans düzleminde karmaşık sayılarla ifade edilebilen rijitlik matrisi ile uygun bir şekilde tanımlanabilir. Bu çalışmanın amaçlarından bir tanesi, bu alternatif sönüm modelinin yapıların doğrusal sismik tepkisi üzerine olan etkisini incelemektir. Aynı yapı bu amaç için de analiz edilmiş, göreli kat ötelemesi ve mutlak ivme tepkileri bir takım deprem kaydı kullanılarak Fourier dönüşümü yöntemi ile hesaplanmıştır.

Bu tez kapsamında incelenen son konu ise deprem yüklemesiyle ilişkili olup, muhtemelen bu tezin içerdiği en yenilikçi fikri kapsamaktadır. Yükleme ile ilgili olarak yaygın bir şekilde kullanılan yöntem; yer ivmelerinin sistem kütleleri ile çarpılarak doğrudan yük olarak yapıya etki edilmesi yaklaşımına dayanmaktadır. Bu şekilde elde edilen deprem yüklemesi ile diferansiyel denklemin çözümü sonucunda rölatif deplasmanlar elde edilmektedir. Bu yöntemin temelini oluşturan fikir "sözde-statik deplasman iletimi" varsayımına dayanmaktadır. Bu varsayım, herhangi bir andaki yer deplasmanının, aynı anda statik olarak yapının her noktasına iletildiği düşüncesini kabul etmektedir. Bu varsayımdan hareketle; sistem tümüyle ötelendiğinden, doğal olarak bu gibi bir hareket yapıda bir deformasyona sebep olmaz. Bu çalışmanın diğer bir amacı, bu varsayımın yüksek bir bina için gerçekten geçerli olup olmadığını test etmektir. Bu sebeple aynı yapı göreli ve mutlak yapı tepkileri hesaplanmak suretiyle analiz edilmiş ve karşılaştırılmalı sonuçlar verilmiştir.

TABLE OF CONTENTS

LIST OF FIGURES

LIST OF TABLES

LIST OF SYMBOLS / ABBREVIATIONS

α	Viscous damping proportionality constant for mass
β	Viscous damping proportionality constant for stiffness
γ	Structural damping coefficient
ξ	Viscous damping ratio
ξ_{eq}	Equivalent viscous damping ratio
ξ_n	n^{th} mode viscous damping ratio
ξ_i	i^{th} mode viscous damping ratio
ξ_j	j^{th} mode viscous damping ratio
Γ_n	n^{th} mode modal participation factor
θ	Phase lag
$\ddot{\theta}$	Unit rotational acceleration
ω_n	n^{th} mode natural angular frequency
ω	Natural angular frequency
$\bar{\omega}$	Forcing angular frequency
ω_i	i^{th} mode natural angular frequency
ω_j	j^{th} mode natural angular frequency
$\bar{\omega}_0$	Angular forcing frequency
$\bar{\omega}_{max}$	Nyquist (angular) frequency
$\{\phi\}$	Mode shape vector
$\{\phi_n\}$	n^{th} mode shape vector
$\{\phi_j\}$	j^{th} mode shape vector
ϑ	Poisson ratio
c	Damping coefficient
C_n^*	n^{th} mode modal damping
dt	Time increment
E	Elasticity modulus of concrete
E_D	Dissipated energy per one cycle
E_{So}	Maximum strain energy
f	Forcing frequency

$\bar{f}_{max}$	Nyquist (cyclic) frequency
f_D	Damping force
G	Shear modulus
I	Moment of inertia of section
k	Stiffness
K_n^*	nth mode modal stiffness
$\widetilde{K}_n^*$	nth mode modal impedance or modal dynamic stiffness
L	Length of element or story
L_n^*	nth mode modal coefficient
m	Mass
m_i^j	Mass of jth portion of ith element for lumped mass
$\bar{m}$	Mass per unit length
m_r	Mass moment of inertia
m_t^i	ith element translational mass
m_r^i	ith element rotational mass
M_n^*	nth mode modal mass
N	Number of discrete intervals
NM_i	Normalization factor of both horizontal components of the ith record
$NTH_{1,i}$	Normalized ith record, horizontal component 1
$PGV_{PEER,i}$	Peak ground velocity of the ith record
t_d	Duration of ground motion
t_s	Duration of silent region
T_0	Duration of ground motion plus silent region (total forcing period)
$TH_{1,i}$	Record i, horizontal component 1
$[C], [C_{ss}]$	Structure damping matrix
$[C_{sb}], [C_{bs}]$	Base-structure interaction damping matrix
$[C_{bb}]$	Base damping matrix
$[K], [K_{ss}]$	Structure stiffness matrix
$[K_{sb}], [K_{bs}]$	Base-structure interaction stiffness matrix
$[K_{bb}]$	Base stiffness matrix
$[\widetilde{K}], [\widetilde{K}_{ss}]$	Impedance or structure dynamic stiffness matrix

$[M], [M_{ss}]$	Structure mass matrix
$[M_{sb}], [M_{bs}]$	Base-structure interaction mass matrix
$[M_{bb}]$	Base mass matrix
$[\widetilde{M}_{ss}]$	Dynamic mass matrix
$[T_{sb}]$	Transformation matrix
$\ddot{d}_n(t)$	n^{th} mode equivalent SDOF system acceleration response in time domain
$\dot{d}_n(t)$	n^{th} mode equivalent SDOF system velocity response in time domain
$d_n(t)$	n^{th} mode equivalent SDOF system displacement response in time domain
$p(t)$	Loading vector in time domain
$p_m(t)$	Discretized loading vector
$\ddot{y}_n(t)$	n^{th} mode generalized acceleration in time domain
$\dot{y}_n(t)$	n^{th} mode generalized velocity in time domain
$y_n(t)$	n^{th} mode generalized displacement in time domain
$\ddot{u}(t), \ddot{u}$	Structure acceleration response in time domain
$\dot{u}(t), \dot{u}$	Structure velocity response in time domain
$u(t), u$	Structure displacement response in time domain
$P_j(i\overline{w})$	Complex loading amplitude coefficient in frequency domain
$P_n(i\overline{w})$	n^{th} mode complex loading amplitude coefficient
$\ddot{Y}_n(i\overline{w})$	n^{th} mode complex acceleration response amplitude coefficient in modal coordinates
$\dot{Y}_n(i\overline{w})$	n^{th} mode complex velocity response amplitude coefficient in modal coordinates
$Y_n(i\overline{w})$	n^{th} mode complex displacement response amplitude coefficient in modal coordinates
$\ddot{U}(i\overline{w})$	Structure acceleration response in frequency domain
$\dot{U}(i\overline{w})$	Structure velocity response in frequency domain
$U(i\overline{w})$	Structure displacement response in frequency domain
$\{\ddot{u}_s^t\}$	Structure total acceleration response in time domain
$\{\dot{u}_s^t\}$	Structure total velocity response in time domain
$\{u_s^t\}$	Structure total displacement response in time domain

$\{\ddot{u}_b\}$	Ground acceleration record in time domain
$\{\dot{u}_b\}$	Ground velocity record in time domain
$\{u_b\}$	Ground displacement record in time domain
$\{u_s^p\}$	Pseudo-static displacement
$\{I\}$	Influence vector

ASCE/SEI	American Society of Civil Engineers / Structural Engineering Institute
C40	Concrete Class with 40 MPa Compressive Strength
DFT	Discrete Fourier Transform
FEMA	Federal Emergency Management Agency
LL	Live Load
SDL	Superimposed Dead Load
MCE	Maximum Credible Earthquake
NEHRP	Natural Earthquake Hazards Reduction Program
FFT	Fast Fourier Transform
PEER	Pacific Earthquake Engineering Research Center
Std.Dev	Standard Deviation
LATBSDC	Los Angeles Tall Buildings Structural Design Council
SDOF	Single Degree of Freedom System
MDOF	Multi Degree of Freedom System

1. INTRODUCTION

Classical equation of motion consists of four terms, namely, inertial resistance, damping resistance, structural resistance and seismic loading. Damping part has some ambiguity due to its complex nature. Reliability of inertial resistance part is based on proper distribution of mass. Loading part is based on pseudo-static transmission concept, which may have some deficiencies in some cases. Therefore, this ambiguity and potential deficiencies due to assumptions have been motivations of this study. It is worth to note that issues mentioned above seem insignificant but we could have never known how significant the effects of them, without examining.

1.1. Objective

They say “old habits die hard.” This dissertation is a product of an idea challenging the statement mentioned above. The main objective is to investigate the effects of alternate representations of dynamic properties and loading on seismic response and to compare the results obtained by using ‘old habits’, that is to say, routine lumped mass approach, proportional viscous damping assumptions and broadly-accepted acceleration loading concept.

1.2. Scope of Work

Mechanical and cross sectional properties, modeling procedure, related drawings and mass calculations are presented in Chapter 2.

Current mass distribution assumptions for structures, as follows, lumped mass approach specified as translational, rotational inertia of structure and consistent mass approach related to mass influence coefficients are given in Chapter 3.

Extreme cases for proportional damping approaches, Rayleigh damping assumption and rate-independent (structural) damping concept are explained in Chapter 4.

Pseudo-static transmission and dynamically transmitted base loading assumptions, derivation of equilibrium equations for displacement and acceleration loading cases are given in Chapter 5.

Basics of response history analysis in time and frequency domain; modal analysis, arbitrary loading, silent region and discrete Fourier concepts are summarized in Chapter 6.

Ground motion selection and scaling procedure presented in FEMA P-695 document is explained and a set of far field ground motion records are listed in Chapter 7.

Combinations of dynamic properties and seismic loading are discussed extensively and equations are derived for all combinations in Chapter 8.

Drift ratio and total acceleration responses of combinations are compared and interpretations on results are given in Chapter 9.

In the last chapter, general results and effects of alternate representations are evaluated.

All modeling and analysis process have been executed in “MATLAB” numerical computing environment. All drawings except the ones indicated in Chapter 7 have been drawn in “AUTOCAD”.

2. STRUCTURAL SYSTEM: CORE WALL TALL BUILDING

For the implementation of issues investigated in this thesis, as a structural system, a 50 story realistic 200 meter-long building is pre-designed (Figure 2.1). C40 concrete class, of which properties are given below, is projected as material used for construction of the building.

Mechanical Properties C40 Concrete Class:

E : 34000000 KN/m^2

G : 14166667 KN/m^2

ν : 0.20

The system consists of a core wall in the middle, peripheral gravity columns and flat slabs (Figure 2.2). Cross section of core wall is reduced gradually by each ten story throughout the building. Height of the each story is constant along the building and it is 4 m. Whole system is rectangle in plan and perfectly symmetrical with respect to x and y axes, excluding core wall. Dimensions of structural elements are given in Table 2.1 below.

Table 2.1. Dimensions of structural elements.

Story	Slab Length and Width (mm)	Slab Thick. (mm)	Coupling Beam Length (mm)	Coupling Beam Height (mm)	Coupling Beam Width (mm)	Wall Length and Width (mm)	Wall Thick. (mm)
0 - 10	36000	250	2500	1750	1000	15000	1000
11 - 20	36000	250	2500	1750	900	14800	900
21 - 30	36000	250	2500	1750	800	14600	800
31 - 40	36000	250	2500	1750	700	14400	700
41 - 50	36000	250	2500	1750	600	14200	600

Since the building will be modeled as a stick, it is sufficient to present framework plan of only first ten stories of the building in here. Framework plan and corresponding A-A section drawing are illustrated in Figure 2.3 and Figure 2.4.

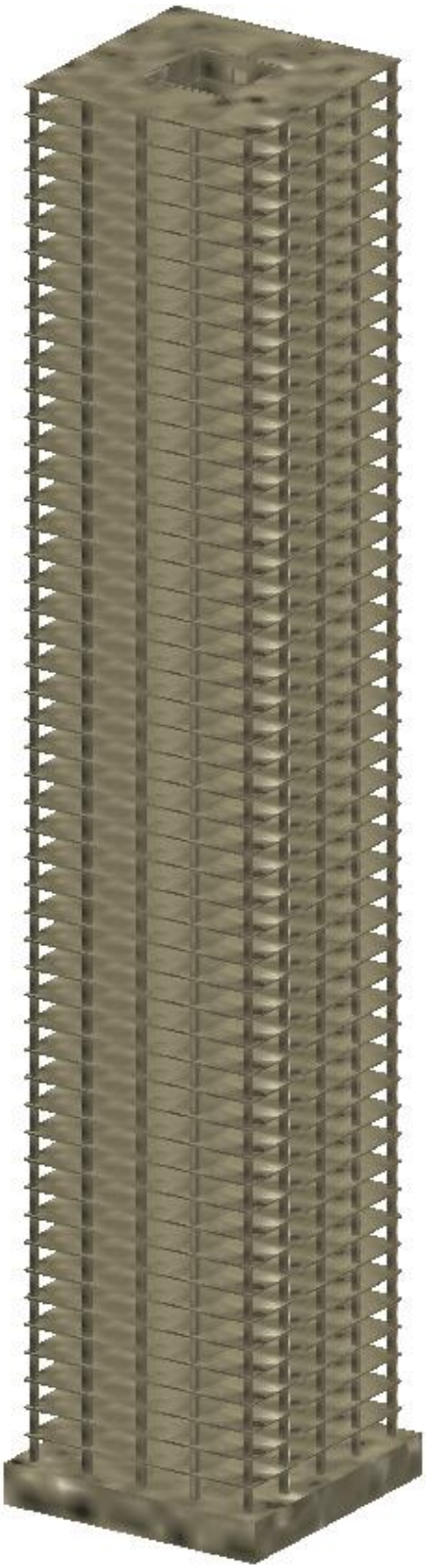

Figure 2.1. 3D Model of building.

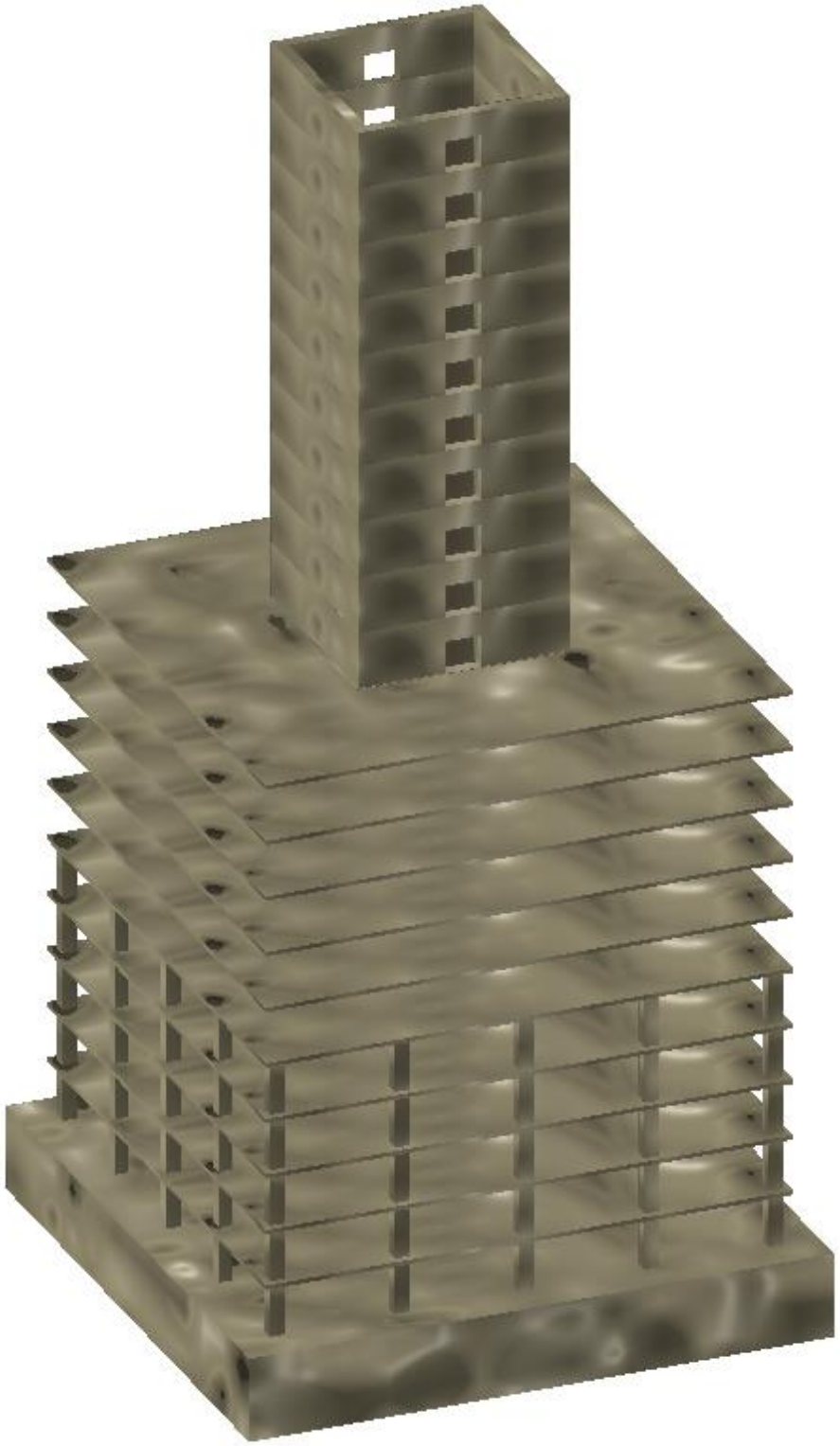

Figure 2.2. Parts of the buildings in 3D Model.

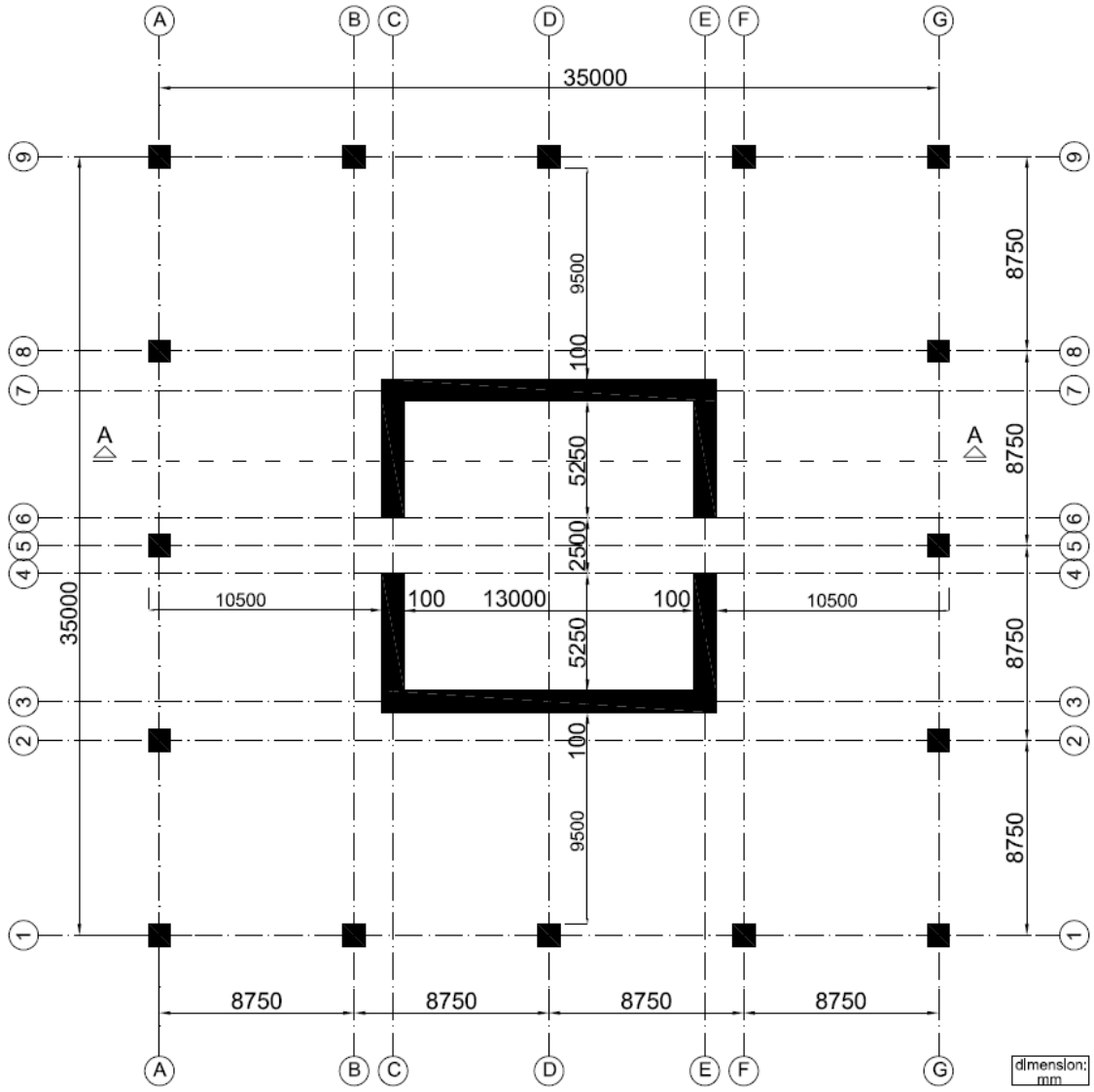

Figure 2.3. Framework plan of first ten stories.

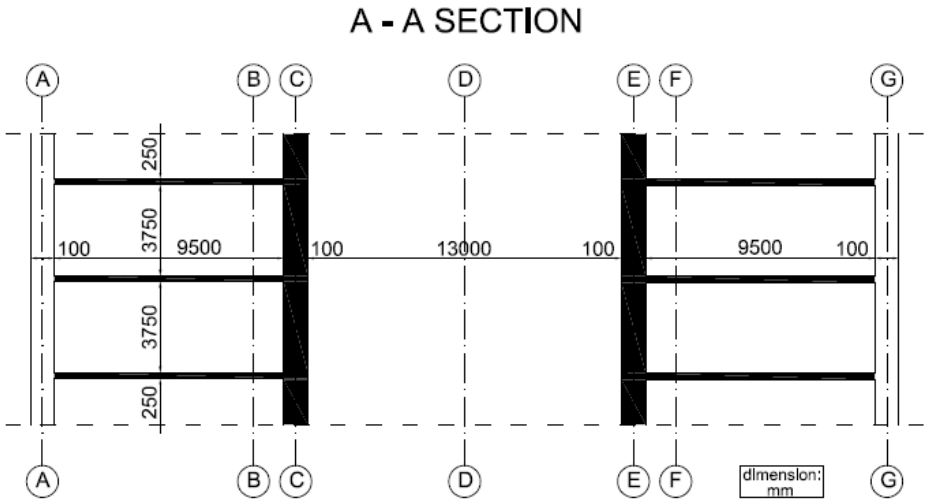

Figure 2.4. A-A Section drawing represented first ten stories.

2.1. Stick Model

Considering framework plan of the building, it can be assumed that stiff core wall in the middle of the structure governs dynamic behavior of whole building, that is to say, it is reasonable to model only core wall system in order to represent the entire system. Mathematical modeling of core wall system is generated by paying regard to finite element procedures given in "*Theory of Matrix Structural Analysis"* by J. S. Przemieniecki [1]. For the sake of the simplicity, core wall is represented as stick model for implementation of a set of response history analysis in frequency domain.

Based on the idea mentioned in the first paragraph, it can be claimed that whole floor mass will mobilize together with the core wall in the translational direction. Therefore, it is assumed that slab masses for each floor can be taken into account as if they are concentrated on the center of the floor levels. The loads on slabs, given below, are taken from ASCE 7-05 [2].

Loads on slab:

SDL: 2.0 KN/m^2

LL: 2.4 KN/m^2

Only 25% of masses coming from LL (Live Load) are included to concentrated slab masses according to directions of ASCE 7-05 [2].

Table 2.2. Mass calculation of structural elements.

Net Slab Area (m^2)	**Slab Mass (t)**	**Mass from SDL (t)**	**Mass from LL (25%) (t)**	**Total Slab Mass (t)**	**Mass of Coupling Beam (t)**	**Wall Mass (t)**	**Total Mass (t)**
1071	682	218	66	966	22	520	1508
1077	686	220	66	972	20	464	1456
1083	690	221	66	977	18	409	1404
1089	694	222	67	982	16	355	1353
1094	697	223	67	987	13	302	1303

Figure 2.5. 3D Model of core wall.

As it is mentioned in previous part, core wall thickness is reduced 100 mm by each ten floor along the building. Detailed sectional dimensions are given in Figure 2.3.

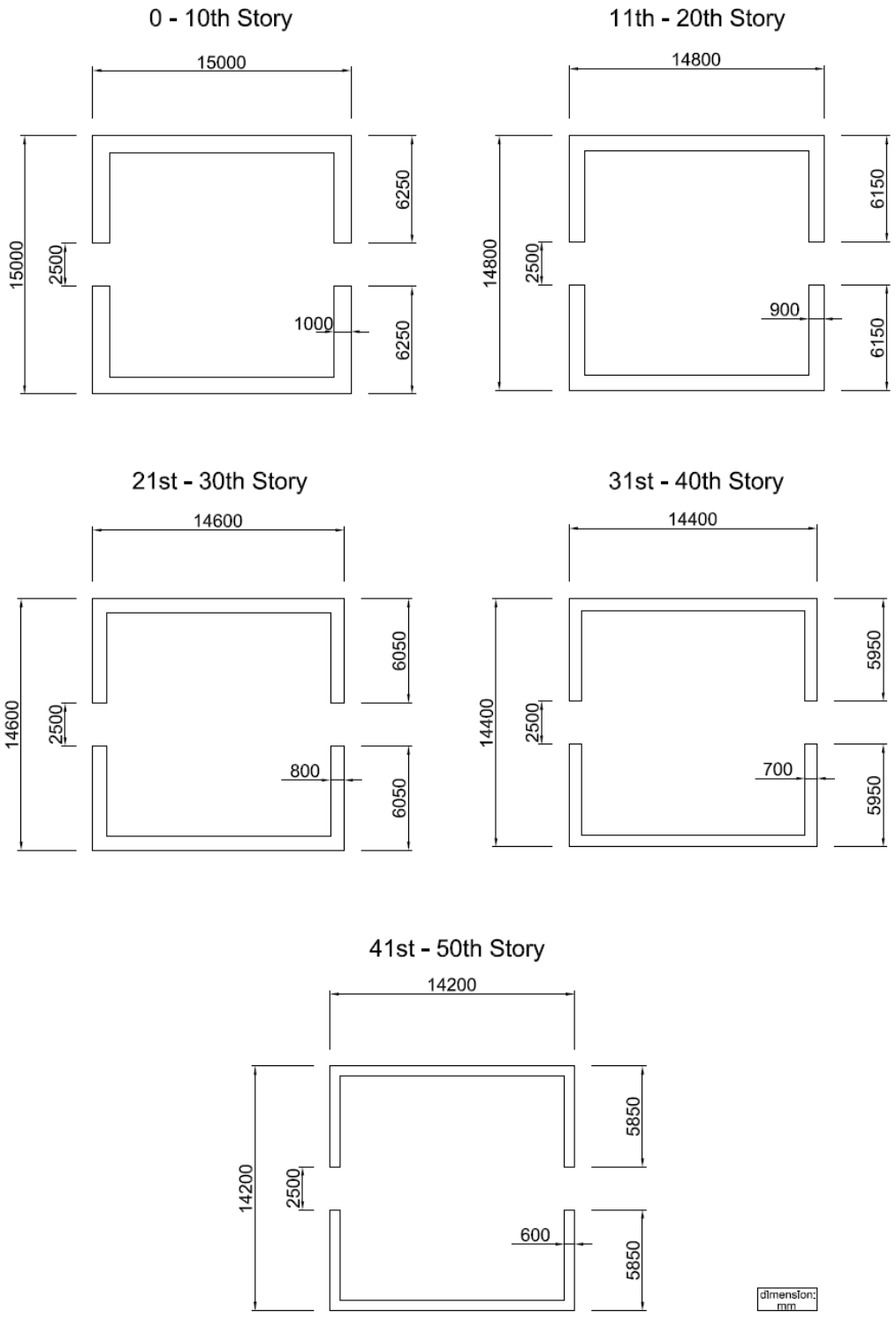

Figure 2.6. Core wall cross sections with respect to floor levels.

3. REPRESENTATION OF MASS

Undoubtedly, representation of mass property of a structure plays a vital role for performing of reasonable response history analysis. In this chapter, widely-accepted lumped mass and consistent mass approaches are presented. Mass representation of the building will be modeled in different ways using following approaches.

3.1. Lumped Mass Matrix Approach

Lumped mass assumption is the simplest way to model the mass of any structure. The underlying idea of this concept is that entire mass of a structural element or just a portion of that is assumed as concentrated at a point [3].

$m_i^{(j)}$: mass of j^{th} portion of i^{th} element

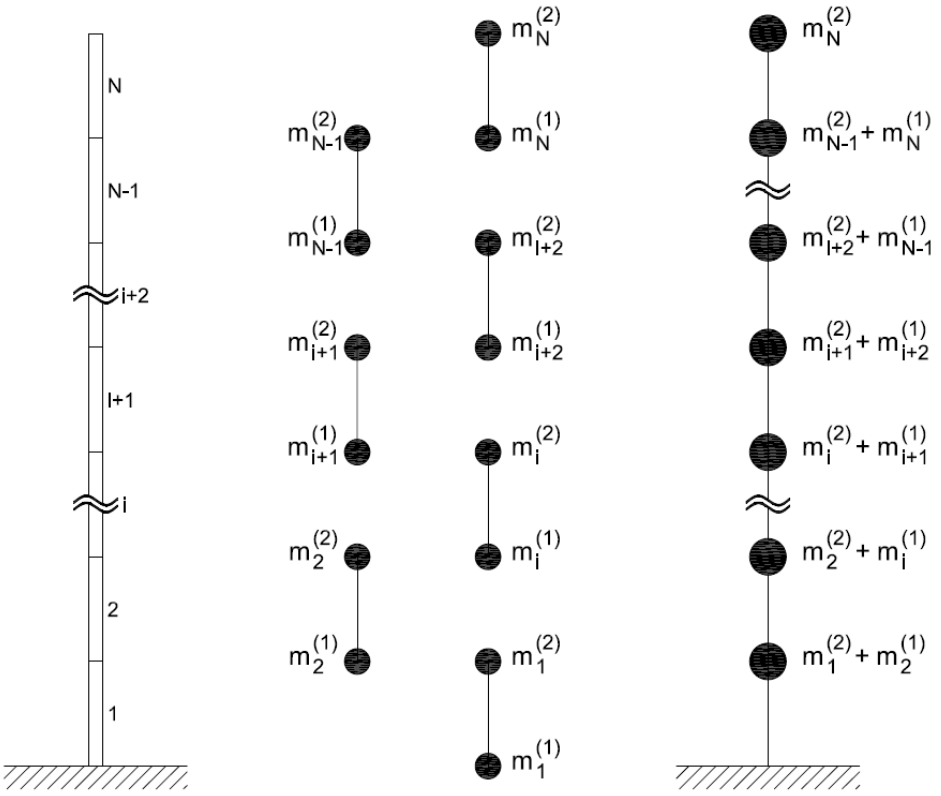

Figure 3.1. Calculation of lumped masses.

General simple procedure is illustrated in Figure 3.1. Elements are divided into two portions, mass of each portion is assumed that is concentrated on the ends of the element. Therefore, two lumped masses are occurred for each element, overlapping lumped masses on the connection points are summed and attached to nodes. Finally, lumped masses are obtained and they are depicted as in Figure 3.2.

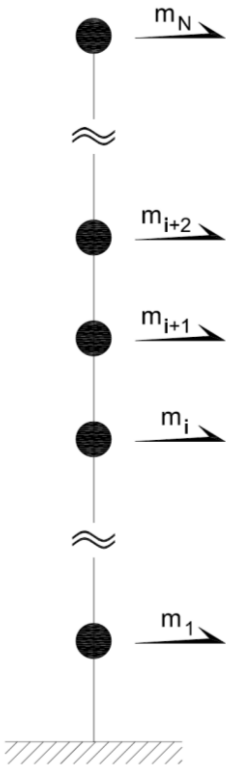

Figure 3.2. Representative drawing of lumped mass system.

Since acceleration of mass in any joint produces inertial force only in that joint there is no any coupling term, that is to say, off-diagonal terms of matrix vanish [3]. If just one translational degree of freedom is defined for each node, matrix representation of lumped masses will be like this:

$$M = \begin{bmatrix} m_1 & \vdots & 0 & 0 & 0 & \vdots & 0 \\ \cdots & \ddots & \cdots & \cdots & \cdots & \cdots & \cdots \\ 0 & \vdots & m_i & 0 & 0 & \vdots & 0 \\ 0 & \vdots & 0 & m_{i+1} & 0 & \vdots & 0 \\ 0 & \vdots & 0 & 0 & m_{i+2} & \vdots & 0 \\ \cdots & \vdots & \cdots & \cdots & \cdots & \ddots & \cdots \\ 0 & \vdots & 0 & 0 & 0 & \vdots & m_N \end{bmatrix} \tag{3.1}$$

Even if there is more than one degree of freedoms defined for each node, the same mass matrix can be used for the analyses by eliminating rotational degree of freedoms using static condensation procedure.

Not only translational mass but also rotational inertia terms can be defined and taken into account in the same manner. Mass moment of inertia of a rigid rod can be calculated as prescribed by Equation 3.2 [3]. Representative drawing of rotational inertia of a uniform rigid rod is illustrated in Figure 3.3.

$$m = \bar{m} * L \tag{3.2}$$

$$m_r = m * (L^2/12) \tag{3.3}$$

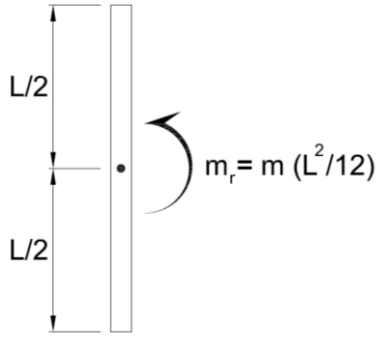

Figure 3.3. Calculation of mass moment of inertia.

For this case, mass matrix is diagonal again Equation 3.1, however, it will be double size of total node numbers since there are two mass terms defined for each node: translational, rotational lumped masses. Schematic drawing is presented in Figure 3.4.

$$M = \begin{bmatrix} m_t^{(1)} & 0 & \vdots & 0 & 0 & \vdots & 0 & 0 \\ 0 & m_r^{(1)} & \vdots & 0 & 0 & \vdots & 0 & 0 \\ \cdots & \cdots & \ddots & \cdots & \cdots & \vdots & \cdots & \cdots \\ 0 & 0 & \vdots & m_t^{(i)} & 0 & \vdots & 0 & 0 \\ 0 & 0 & \vdots & 0 & m_r^{(i)} & \vdots & 0 & 0 \\ \cdots & \cdots & \vdots & \cdots & \cdots & \ddots & \cdots & \cdots \\ 0 & 0 & \vdots & 0 & 0 & \vdots & m_t^{(N)} & 0 \\ 0 & 0 & \vdots & 0 & 0 & \vdots & 0 & m_r^{(N)} \end{bmatrix} \quad (3.4)$$

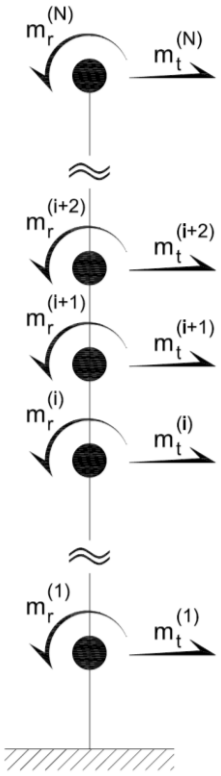

Figure 3.4. Representative drawing of translational and rotational lumped mass system.

3.2. Consistent Mass Matrix Approach

Another mass assumption used for mass representation is consistent mass approach, which is based on derivation of mass influence coefficient. These influence coefficients can be evaluated by considering same procedure used for derivation of stiffness coefficients of an element [3].

If unit acceleration sway is imposed to the beam, it will bend like this:

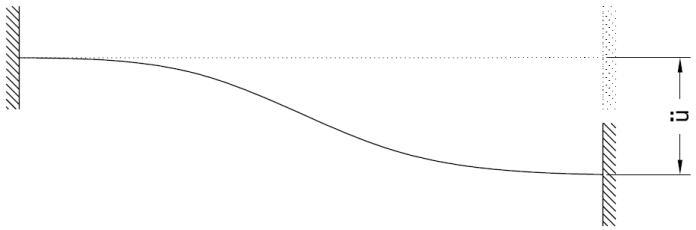

Figure 3.5. Representative drawing of unit acceleration excitation to a beam.

Similarly, if unit rotational acceleration is imposed to the beam, it will bend and deformed shape will be like this:

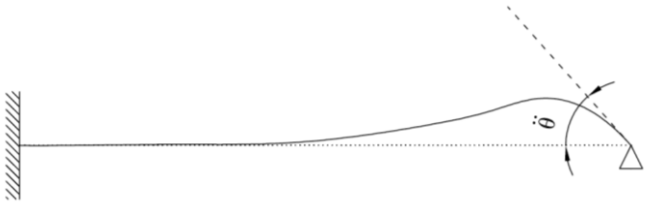

Figure 3.6. Representative drawing of unit rotational acceleration excitation to a beam.

By reason of these excitations, the reaction forces are obtained called mass coefficients similar to stiffness coefficients. This procedure is repeated for both two ends of this beam and also for coupling terms. Finally, 4 by 4 matrix is obtained for representation of consistent mass of the element:

$$M = {\bar{m}L}/{420}\begin{bmatrix} 156 & 22L & 54 & -13L \\ 22L & 4L^2 & 13L & -3L^2 \\ 54 & 13L & 156 & -22L \\ -13L & -3L^2 & -22L & 4L^2 \end{bmatrix} \tag{3.5}$$

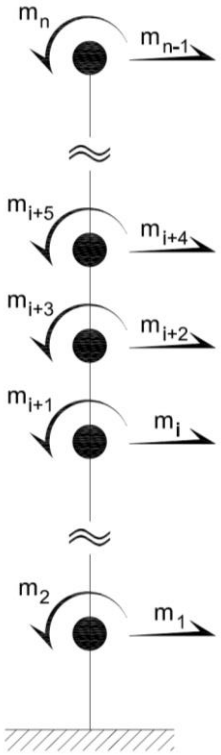

Figure 3.7. Representative drawing of consistent mass system.

4. REPRESENTATION OF DAMPING

Another dynamic property investigated, in this study, is damping, which has remained mystery since beginning of utilization for structural dynamic analysis. Due to the fact that it cannot be defined and formulated explicitly, it is not possible to derive a damping matrix from the elements size or cross section properties. Instead, we use generally proportional damping matrix and define it in terms of modal damping ratios because of its mathematical convenience. Viscous Rayleigh damping and its extreme cases; mass proportional and stiffness proportional damping properties have been investigated in this chapter.

On the other hand, there is one another damping property, discussed here, is rate-independent, so-called “structural damping” property which can only be defined in frequency domain because of its complex nature.

4.1. Mass Proportional Viscous Damping

First extreme case of Rayleigh damping is mass proportional damping, which is generally discussed in books just as a part of Rayleigh damping, is not evaluated as a distinct property. However, for the sake of better understanding, it has been dealt with in this study.

It is really hard to justify this formulation physically of course, because the air damping can be interpreted to model is negligibly small for most structures [4]. Figure 4.1 shows physical illustration of mass proportional damping phenomenon.

Equation 4.1 shows mathematical representation of it:

$$[C] = \alpha[M] \tag{4.1}$$

α is the proportionality constant, have a unit of sec^{-1}. This coefficient may be obtained by evaluating relationship between generalized modal mass and damping parameters for the n^{th} mode:

$$C_n^* = \alpha M_n^* \tag{4.2}$$

$$C_n^*/M_n^* = 2\xi_n\omega_n \tag{4.3}$$

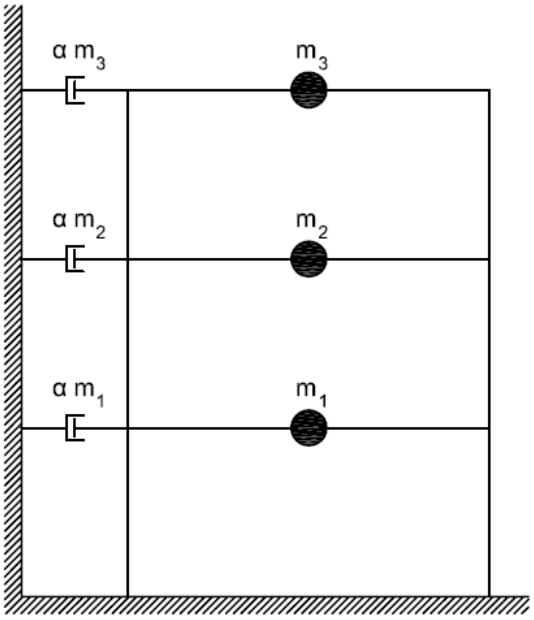

Figure 4.1. Physical representation of mass proportional damping.

Combining Equation 4.2 and Equation 4.3, proportionality constant α and damping ratio of n^{th} mode can be obtained:

$$\alpha = 2\xi_n\omega_n \tag{4.4}$$

$$\xi_n = \alpha/2\omega_n \tag{4.5}$$

Damping ratio of n^{th} mode is inversely proportional with corresponding vibration frequency. Vibration frequency and damping ratio relationship is given in Figure 4.2. This figure shows that damping ratios of corresponding vibration frequencies are getting smaller

as the number of mode increases. It means that response of higher modes cannot be diminished and effects of them will be significant unrealistically.

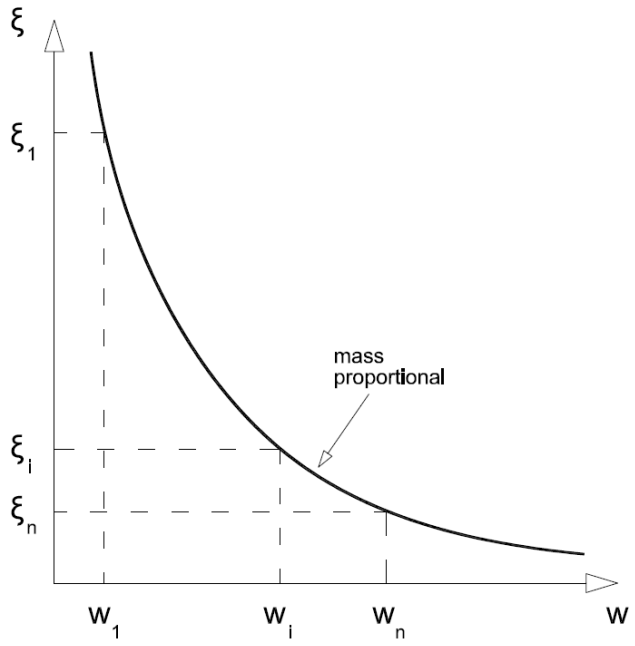

Figure 4.2. $\xi - \omega$ relationship for mass proportional viscous damping.

4.2. Stiffness Proportional Viscous Damping

Other extreme case of Rayleigh damping property is stiffness proportional viscous damping which formulation is given below:

$$[C] = \beta[K] \tag{4.6}$$

Physically, it can be interpreted to model energy dissipation due to story deformations Figure (4.3) [4]. Similarly, β proportionality constant for stiffness matrix can be obtained by evaluating relationship between generalized modal damping, mass and stiffness parameters:

$$C_n^* = \beta K_n^* \tag{4.7}$$

$$K_n^*/M_n^* = \omega_n^2 \tag{4.8}$$

$$C_n^*/M_n^* = 2\xi_n\omega_n \tag{4.9}$$

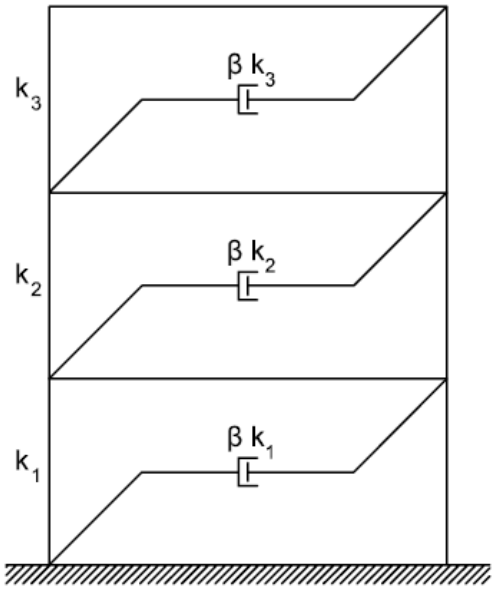

Figure 4.3. Physical representation of stiffness proportional damping.

Combining Equation 4.7 and Equation 4.8, relationship between generalized modal damping and stiffness parameters is achieved:

$$C_n^*/K_n^* = 2\xi_n/\omega_n \tag{4.10}$$

Hence, proportionality constant β and damping ratio of n^{th} mode becomes:

$$\beta = 2\xi_n/\omega_n \tag{4.11}$$

$$\xi_n = \beta\omega_n/2 \tag{4.12}$$

It is observed from Equation 4.12 that stiffness proportional damping is directly in proportion with vibration frequency of structure (Figure 4.4). This means that effects of structural response of higher modes will diminish because of the high damping ratios. It can be reasonable maybe for first mode dominant structures, however, for the other types of structures, it cannot be considered as true.

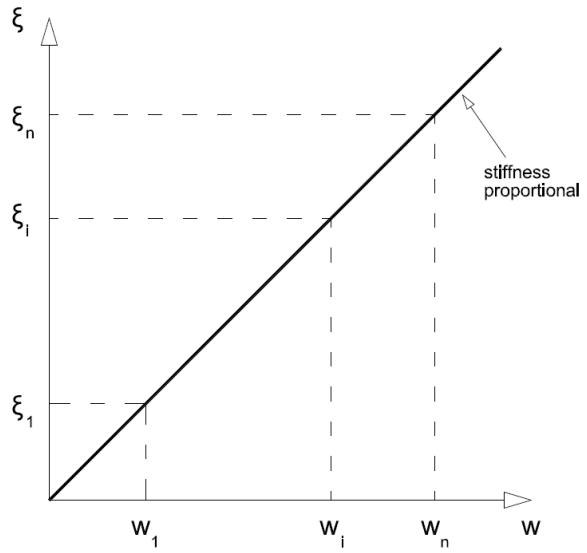

Figure 4.4. $\xi - \omega$ relationship for stiffness proportional damping.

4.3. Mass and Stiffness Proportional (Rayleigh) Viscous Damping

According to the definition of Rayleigh damping, it is assumed as both proportional with mass and stiffness properties of structures (Figure 4.5).

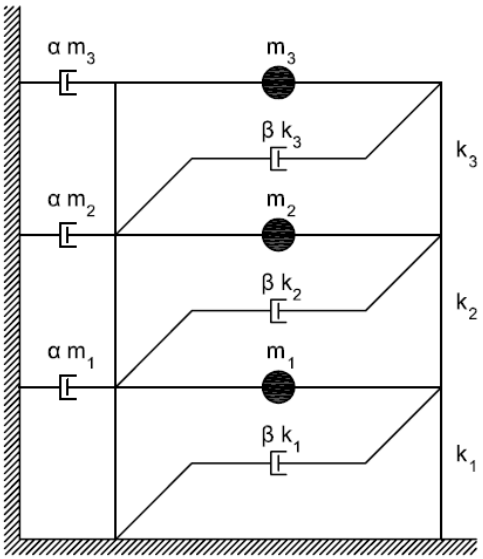

Figure 4.5. Physical representation of Rayleigh damping.

Mathematical representation of Rayleigh damping is combination of Equation 4.1 and Equation 4.6:

$$[C] = \alpha[M] + \beta[K] \tag{4.13}$$

The damping ratio for the nth mode of such system is:

$$\xi_n = \left({}^{\alpha}/_{2\omega_n}\right) + \left({}^{\beta\omega_n}/_{2}\right) \tag{4.14}$$

The proportionality constants can be derived from specified ξ_i and ξ_j represented ith and jth modes respectively. For these two modes, damping ratios can be determined by solving following matrix [3]:

$$\begin{Bmatrix}\xi_i \\ \xi_j\end{Bmatrix} = {}^{1}/_{2}\begin{bmatrix}{}^{1}/_{\omega_i} & \omega_i \\ {}^{1}/_{\omega_j} & \omega_j\end{bmatrix}\begin{Bmatrix}\alpha \\ \beta\end{Bmatrix} \tag{4.15}$$

Using an inverse matrix operation, proportionality constants can be derived [3]:

$$\begin{Bmatrix}\alpha\\ \beta\end{Bmatrix} = \left(2\omega_i\omega_j \Big/ \omega_j^2 - \omega_i^2\right) \begin{bmatrix}\omega_j & -\omega_i\\ -1/\omega_j & 1/\omega_i\end{bmatrix} \begin{Bmatrix}\xi_i\\ \xi_j\end{Bmatrix} \tag{4.16}$$

If these two modes have the same damping ratio (ξ), which gives reasonable results based on experimental data [4], proportionality constants become:

$$\alpha = 2\xi\left(\omega_i\omega_j \Big/ \omega_i+\omega_j\right) \tag{4.17}$$

$$\beta = 2\xi\left(1/\omega_i+\omega_j\right) \tag{4.18}$$

Now Equation 4.13 can be used and damping matrix of structure can be derived. After this point, damping ratio for n^{th} mode can be calculated by using Equation 4.14. Since the same damping ratio is chosen for ith and jth mode, any other n^{th} mode between these modes will have less damping ratio. It means that effects of n^{th} mode response may be remarkable. On the other hand, damping ratios of chosen mode frequencies after j^{th} mode will increase monotonically and effects of these modal responses will be diminished (Figure 4.6).

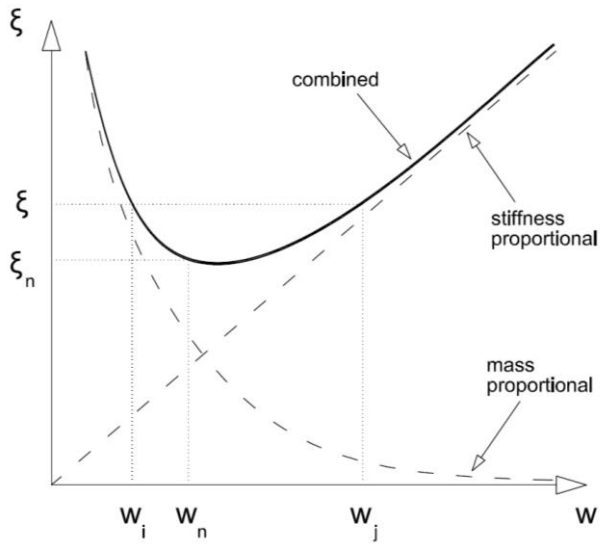

Figure 4.6. $\xi - \omega$ relationship for Rayleigh damping.

4.4. Structural (Rate-Independent) Damping

Broadly accepted viscous damping procedures are usually preferred for modeling of damping property of structures because of the mathematical convenience. However, viscous damping representation has a significant deficiency associated with the energy mechanism. Studies based on experimental data show that dissipated energy per cycle of an oscillating system is essentially independent of the excitation frequency (Figure 4.7) as opposed to dependency inherent in the viscous damping model [5]. Such damping model is called rate-independent or structural damping. It is convenient to express structural damping force during harmonic motion like that [4]:

$$f_D = \left(\gamma k / \overline{\omega}\right) \dot{u}(t) \tag{4.19}$$

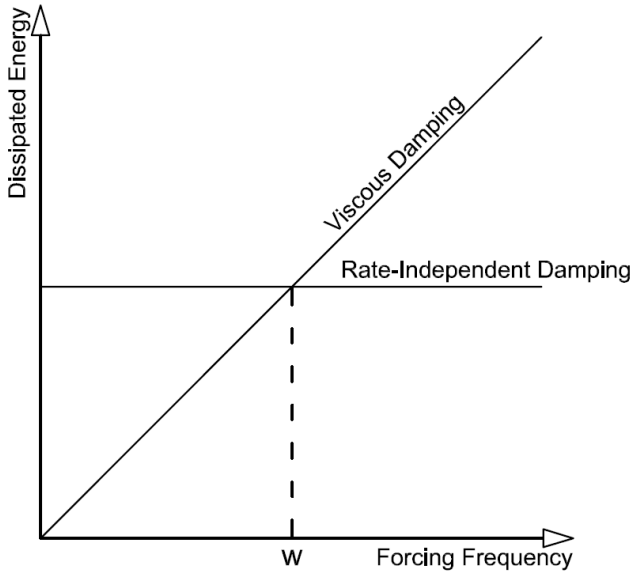

Figure 4.7. Forcing Frequency – Dissipated Energy relationship for different damping approaches.

If Equation 4.18 is written in classical equation of motion instead of viscous damping coefficient “c”, following equation is obtained:

$$m\ddot{u}(t) + \left(\gamma k/_{\bar{\omega}}\right)\dot{u}(t) + ku(t) = p(t) \tag{4.20}$$

Where, "γ" is structural damping coefficient, "$\bar{\omega}$" is forcing frequency. In order to remove frequency dependence of the system for the case of harmonic motion, structural damping may be defined as a damping force proportional to displacement but in phase with the velocity [3]. Note that because of the non-physical character of structural damping, it is only applicable in frequency domain [6]. It can be provided that writing the velocity in terms of the displacement:

$$\dot{U}(i\bar{\omega}) = i\bar{\omega}\, U(i\bar{\omega}) \tag{4.21}$$

$$\ddot{U}(i\bar{\omega}) = -\bar{\omega}^2\, U(i\bar{\omega}) \tag{4.22}$$

Equation 4.21 is substituted in Equation (4.20) and if it is written in simplified form:

$$m\ddot{U}(i\bar{\omega}) + k(\gamma i + 1)\, U(i\bar{\omega}) = P(i\bar{\omega}) \tag{4.23}$$

In here, only unknown term is structural damping coefficient, which can be derived in terms of equivalent viscous damping ratio by using dissipated energy relationship at resonance frequency. As it is seen from Figure 4.7 and Figure 4.8, energy dissipated per cycle of SDOF system with viscous damping, in the case of harmonic motion, is equal to actual dissipated energy at resonance frequency.

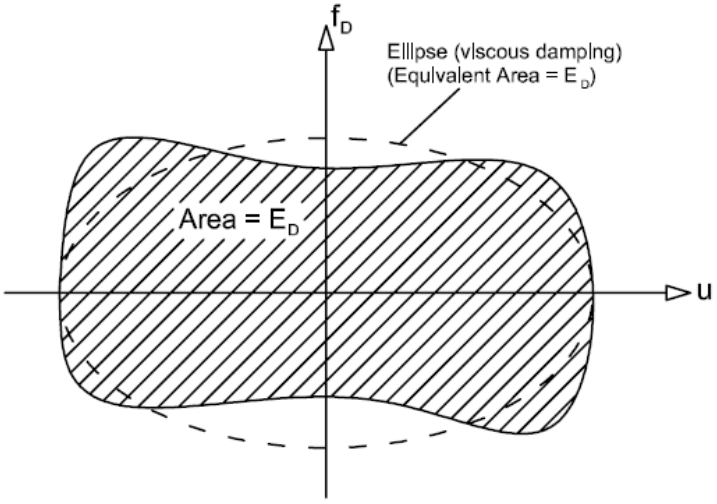

Figure 4.8. Actual and equivalent damping energy per cycle.

Equivalent damping ratio can be expressed as below, where E_{So} is maximum strain energy [4].

$$\xi_{eq} = \frac{1}{4\pi}\left(E_D/E_{So}\right) \tag{4.24}$$

Dissipated energy (independent from forcing frequency) in a cycle of harmonic motion at resonance frequency:

$$E_D = 2\pi\gamma E_{So} \tag{4.25}$$

If Equation 4.25 is substituted in Equation 4.24, structural damping coefficient is obtained in terms of equivalent viscous damping ratio:

$$\xi_{eq} = \gamma/2 \tag{4.26}$$

Hence, final form of structural damping becomes when Equation 4.26 is substituted in Equation 4.23:

$$m\ddot{U}(i\bar{\omega}) + k(2\xi i + 1)\, U(i\bar{\omega}) = P(i\bar{\omega}) \tag{4.27}$$

5. REPRESENTATION OF SEISMIC LOADING

Right hand side of classical equation of motion (Equation 5.18) shows that a structure is exposed to forces due to only ground acceleration (Figure 5.1a). This kind of thinking, which occupies our minds entirely, sometimes, does not let us think on other effects that may cause to deform structure during an earthquake. Such that, real action is not like the equation says. Seismic action does not apply forces to masses of a structure with fixed base in actual life, but it starts to excite at base and propagates throughout the structure (Figure 5.1b). Thus, base of the structure moves with ground, excitation is transferred to structure from the base.

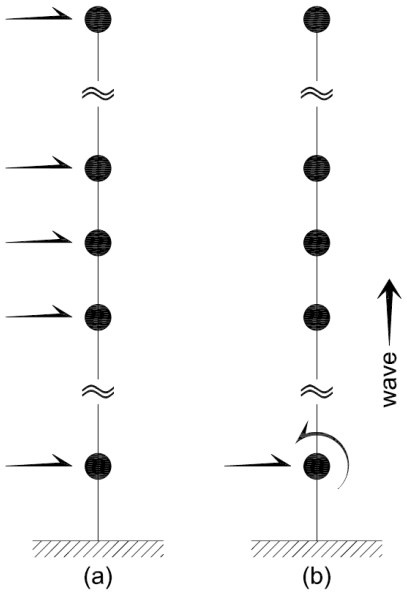

Figure 5.1. (a) Relative formulation - acceleration loading,
(b) Absolute formulation – displacement loading.

Starting point of acceleration loading with relative formulation is based on pseudo-static transmission concept. This assumption supposes that base displacement caused by seismic action, at any time, does not generate any structural deformation in any building (independent from the building height) since the same displacement excitation is transmitted to whole structure concurrently, as independent from time (Figure 5.2).

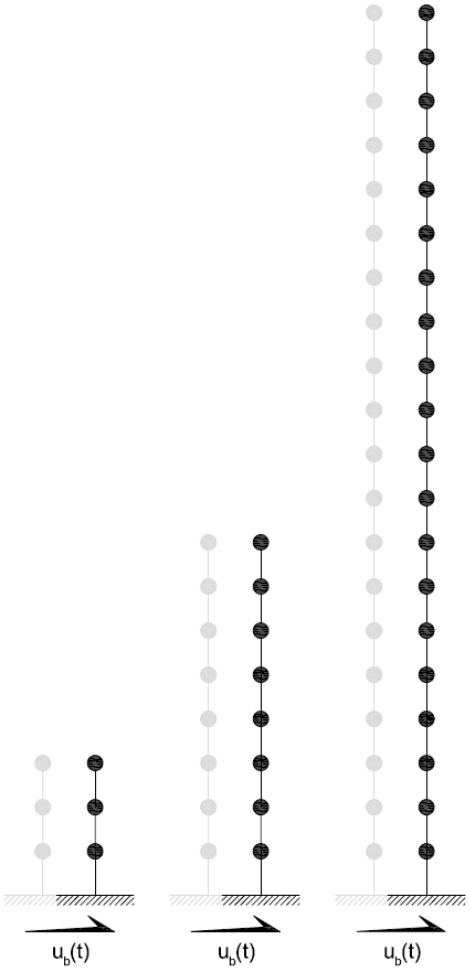

Figure 5.2. Physical representation of pseudo-static transmission for low-rise, mid-rise and high-rise model.

In other words, when the wave strikes the building at the base, the same impact will be seen at all floor levels at the same time. As a matter of fact, base displacement has a propagation velocity, thus it needs time to reach top of the building. The idea presented herein is that, if the building is tall enough, delay in displacement action transmission may cause structural deformation (Figure 5.3).

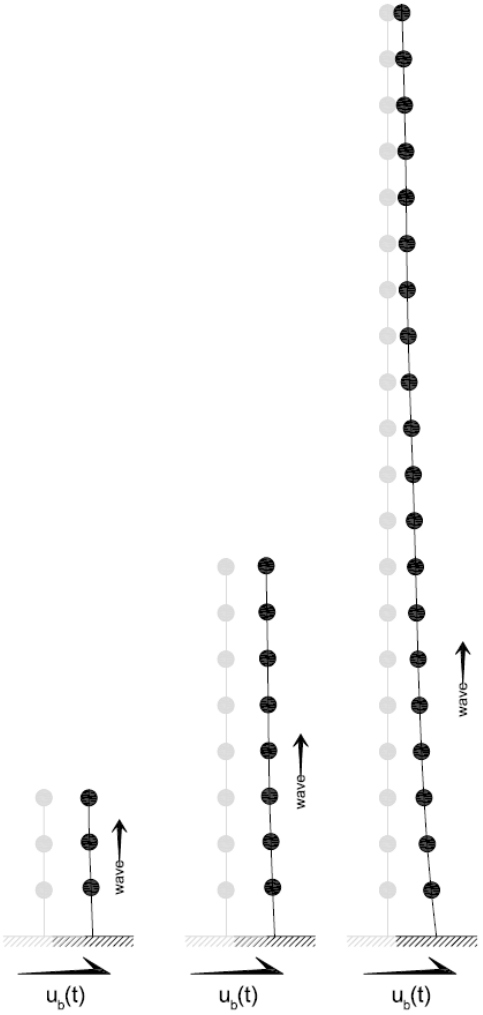

Figure 5.3. Physical representation of dynamic transmission for low-rise, mid-rise and high-rise model.

In this chapter, procedure devoted to investigation of this effect is presented via comparing displacement and acceleration loading methodologies.

5.1. Formulation Based on Total Response Quantities: Displacement Loading

Equation 5.1 shows general form of dynamic equilibrium equation in terms of absolute displacements, u_s^t indicates total displacement response of structure, u_b shows base displacement [7]. M_{ss}, C_{ss}, K_{ss} terms state structure mass, damping and stiffness

matrices, respectively. M_{sb}, C_{sb}, K_{sb} terms indicates base-structure interaction matrices, where “s” stands for structure, “b” stands for base.

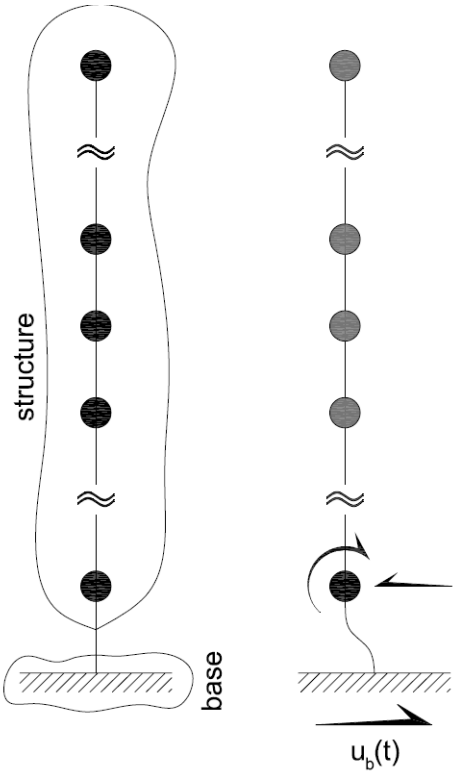

Figure 5.4. Base, structure, base-structure interaction representation.

$$\begin{bmatrix}[M_{ss}] & [M_{sb}]\\ [M_{bs}] & [M_{bb}]\end{bmatrix}\begin{Bmatrix}\{\ddot{u}_s^t\}\\ \{\ddot{u}_b\}\end{Bmatrix}+\begin{bmatrix}[C_{ss}] & [C_{sb}]\\ [C_{bs}] & [C_{bb}]\end{bmatrix}\begin{Bmatrix}\{\dot{u}_s^t\}\\ \{\dot{u}_b\}\end{Bmatrix}+\begin{bmatrix}[K_{ss}] & [K_{sb}]\\ [K_{bs}] & [K_{bb}]\end{bmatrix}\begin{Bmatrix}\{u_s^t\}\\ \{u_b\}\end{Bmatrix}=\begin{Bmatrix}0\\ 0\end{Bmatrix} \quad (5.1)$$

From Equation 5.1, equation associated to superstructure can be extracted:

$$[M_{ss}]\{\ddot{u}_s^t\}+[C_{ss}]\{\dot{u}_s^t\}+[K_{ss}]\{u_s^t\}=-[M_{sb}]\{\ddot{u}_b\}-[C_{sb}]\{\dot{u}_b\}-[K_{sb}]\{u_b\} \quad (5.2)$$

Right hand side of Equation 5.2 shows the forces acting on base joint of structure. For lumped mass representation of structure, since there would not be base-structure interaction term (M_{sb}), equation yields to this form:

$$[M_{ss}]\{\ddot{u}_s^t\}+[C_{ss}]\{\dot{u}_s^t\}+[K_{ss}]\{u_s^t\}=-[C_{sb}]\{\dot{u}_b\}-[K_{sb}]\{u_b\} \quad (5.3)$$

Damping matrix can be derived by numerical evaluation but normally it is not defined [7]. Thus, damping forces can be neglected and equation can be written in following final form:

$$[M_{ss}]\{\ddot{u}_s^t\} + [C_{ss}]\{\dot{u}_s^t\} + [K_{ss}]\{u_s^t\} = -[K_{sb}]\{u_b\} \tag{5.4}$$

Equation 5.4 shows that forces acting on base joint, are associated to base displacements and affect degree of freedoms of only first joint (Figure 5.4). It means that base displacements will be dynamically transmitted to the upper levels throughout the building.

5.2. Formulation Based on Relative Response Quantities: Acceleration Loading

Structural total displacement response can be divided into two parts, namely, base displacement and relative displacement response (Fig 5.5).

$$\{u_s^t\} = \{u_b\} + \{u_s\} \tag{5.5}$$

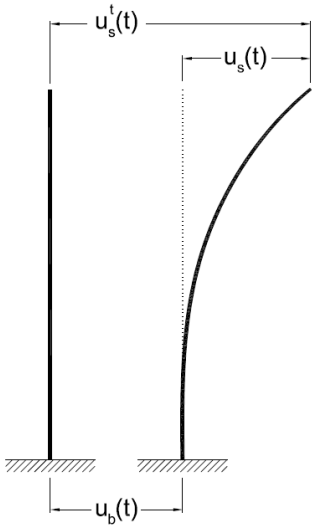

Figure 5.5. Base displacement, relative response, total response.

If total displacement is written as summation of pseudo-static displacements and relative displacements, Equation 5.6 is obtained.

$$\{u_s^t\} = \{\boldsymbol{u_s^p}\} + \{u_s\} \tag{5.6}$$

Using pseudo-static displacements and base-structure interaction matrix, static support excitation statement can be defined as below:

$$[K_{ss}]\{u_s^p\} = -[K_{sb}]\{u_b\} \tag{5.7}$$

$$\{u_s^p\} = -[K_{ss}]^{-1}[K_{sb}]\{u_b\} \tag{5.8}$$

Finally, pseudo-static displacements can be defined via using a transformation matrix:

$$[T_{sb}] = -[K_{ss}]^{-1}[K_{sb}] \tag{5.9}$$

$$\{u_s^p\} = [T_{sb}]\{u_b\} \tag{5.10}$$

In the same manner, following derived statements are:

$$\{\dot{u}_s^t\} = [T_{sb}]\{\dot{u}_b\} + \{\dot{u}_s\} \tag{5.11}$$

$$\{\ddot{u}_s^t\} = [T_{sb}]\{\ddot{u}_b\} + \{\ddot{u}_s\} \tag{5.12}$$

Substitution of Equation 5.6, Equation 5.11 and Equation 5.12 into Equation 5.2 yields statements below:

$$\begin{aligned}[M_{ss}]([T_{sb}]\{\ddot{u}_b\} + \{\ddot{u}_s\}) + [C_{ss}]([T_{sb}]\{\dot{u}_b\} + \{\dot{u}_s\}) + [K_{ss}]([T_{sb}]\{u_b\} + \{u_s\}) \\ = -[M_{sb}]\{\ddot{u}_b\} - [C_{sb}]\{\dot{u}_b\} - [K_{sb}]\{u_b\}\end{aligned} \tag{5.13}$$

$$[M_{ss}]\{\ddot{u}_s\} + [C_{ss}]\{\dot{u}_s\} + [K_{ss}]\{u_s\} = -[M_{sb}]\{\ddot{u}_b\} - [C_{sb}]\{\dot{u}_b\} - [K_{sb}]\{u_b\}$$

$$-[M_{ss}][T_{sb}]\{\ddot{u}_b\} - [C_{ss}][T_{sb}]\{\dot{u}_b\} - [K_{ss}][T_{sb}]\{u_b\} \quad (5.14)$$

If Equation 5.9 is substituted into last stiffness term at right hand side of Equation 5.14, it is easily seen that sum of stiffness terms is equal to zero. Thus, simplified form leads to following equation:

$$[M_{ss}]\{\ddot{u}_s\} + [C_{ss}]\{\dot{u}_s\} + [K_{ss}]\{u_s\}$$
$$= -[M_{sb}]\{\ddot{u}_b\} - [C_{sb}]\{\dot{u}_b\} - [M_{ss}][T_{sb}]\{\ddot{u}_b\} - [C_{ss}][T_{sb}]\{\dot{u}_b\} \quad (5.15)$$

In a similar way, damping terms can be neglected. (Effects of these terms on response will be discussed later.) Therefore, only acceleration terms are remained at the right hand side:

$$[M_{ss}]\{\ddot{u}_s\} + [C_{ss}]\{\dot{u}_s\} + [K_{ss}]\{u_s\} = -[M_{sb}]\{\ddot{u}_b\} - [M_{ss}][T_{sb}]\{\ddot{u}_b\} \quad (5.16)$$

For lumped mass assumption, conventional equation of motion is obtained:

$$[M_{ss}]\{\ddot{u}_s\} + [C_{ss}]\{\dot{u}_s\} + [K_{ss}]\{u_s\} = -[M_{ss}]\{I\}\{\ddot{u}_b\} \quad (5.17)$$

6. ANALYSIS IN TIME AND FREQUENCY DOMAIN

6.1. Time Domain Analysis

Indisputably, time history analysis is the most popular analysis method for evaluating dynamic response of structures. In the literature, several methods are available so as to perform dynamic analysis. The most powerful one of these methodologies is undoubtedly mode superposition procedure. In the first part of this chapter, this procedure is explained briefly.

6.1.1. Modal Analysis

Well-known mode superposition methodology based on the idea that combination of responses of generalized SDOF systems, which is derived by coordinate transformation procedure from coupled equations of MDOF system. To implement this procedure, firstly, mode shape (amount of degree of freedoms) functions are required. For this purpose, Equation 5.18 is converted into free vibration form omitting damping matrix and loading vector. (Subscripts of matrices are ignored for the sake of the brevity.)

$$[M]\{\ddot{u}_s(t)\} + [K]\{u_s(t)\} = 0 \tag{6.1}$$

It can be assumed that free vibration motion is simple harmonic [3]:

$$\{u_s(t)\} = \{\phi\}\sin(\omega t + \theta) \tag{6.2}$$

Where, $\{\phi\}$ is the shape vector, w is vibration frequency and θ is phase angle. If this Equation 6.2 is derived two times,

$$\{\ddot{u}_s(t)\} = -\omega^2\{\phi\}\sin(wt + \theta) \tag{6.3}$$

$$\{\ddot{u}_s(t)\} = -\omega^2\{\phi\}\{u_s(t)\} \tag{6.4}$$

If Equation 6.2 and Equation 6.4 are substituted into Equation 6.1, formulation becomes so-called eigenvalue problem:

$$[K]\{\phi\} - \omega^2[M]\{\phi\} = \{0\} \tag{6.5}$$

Eigenvalue problem is solved by expanding determinant:

$$\|[K] - \omega^2[M]\| = 0 \tag{6.6}$$

This solution gives N mode vibration frequencies and then mode shape functions for corresponding vibration frequencies are obtained via Equation 6.5.

$$\omega = \begin{Bmatrix} \omega_1 \\ \omega_2 \\ \omega_3 \\ \vdots \\ \omega_N \end{Bmatrix} \tag{6.7}$$

$$\{\phi_1\} = \begin{Bmatrix} \phi_1^1 \\ \phi_1^2 \\ \phi_1^3 \\ \vdots \\ \phi_1^n \end{Bmatrix} \quad \{\phi_2\} = \begin{Bmatrix} \phi_2^1 \\ \phi_2^2 \\ \phi_2^3 \\ \vdots \\ \phi_2^n \end{Bmatrix} \quad \{\phi_3\} = \begin{Bmatrix} \phi_3^1 \\ \phi_3^2 \\ \phi_3^3 \\ \vdots \\ \phi_3^n \end{Bmatrix} \quad \dots \quad \{\phi_N\} = \begin{Bmatrix} \phi_N^1 \\ \phi_N^2 \\ \phi_N^3 \\ \vdots \\ \phi_N^n \end{Bmatrix} \tag{6.8}$$

After this point, in order to determine the displaced positions of the system, we need modal amplitudes:

$$\{u_s(t)\} = \sum_{j=1}^{N} \{\phi_j\} y_j(t) \tag{6.9}$$

Calculation of modal amplitudes is based on the coordinate transformation procedure which is explained briefly here:

Coordinate Transformation:

Equation 5.18 can be written in following form without subscripts of matrices:

$$[M]\{\ddot{u}_s(t)\} + [C]\{\dot{u}_s(t)\} + [K]\{u_s(t)\} = -[M]\{I\}\ddot{u}_b(t) \quad (6.10)$$

Equation 6.9 and its derivatives are substituted into Equation 6.10:

$$[M]\left(\sum_{j=1}^{N}\{\phi_j\}\ddot{y}_j(t)\right) + [C]\left(\sum_{j=1}^{N}\{\phi_j\}\dot{y}_j(t)\right) + [K]\left(\sum_{j=1}^{N}\{\phi_j\}y_j(t)\right) = -[M]\{I\}\ddot{u}_b(t) \quad (6.11)$$

If all terms are pre-multiplied by transpose of n^{th} mode shape, Equation 6.12 will become in following form:

$$\{\boldsymbol{\phi_n^T}\}\,[M]\left(\sum_{j=1}^{N}\{\phi_j\}\ddot{y}_j(t)\right) + \{\boldsymbol{\phi_n^T}\}\,[C]\left(\sum_{j=1}^{N}\{\phi_j\}\dot{y}_j(t)\right) + \{\boldsymbol{\phi_n^T}\}\,[K]\left(\sum_{j=1}^{N}\{\phi_j\}y_j(t)\right) = -\{\boldsymbol{\phi_n^T}\}\,[M]\{I\}\ddot{u}_b(t) \quad (6.12)$$

Mode shapes are orthogonal with respect to both mass and stiffness matrices [3]. The same property is valid for damping matrix because it is constructed by proportional with mass matrix and stiffness matrix or combination of them. By nature of orthogonality property of these mode shapes, these terms will be zero:

$$\{\phi_n^T\}[M_{ss}]\{\phi_m\} = 0 \quad (6.13)$$

$$\{\phi_n^T\}[K_{ss}]\{\phi_m\} = 0 \quad (6.14)$$

$$\{\phi_n^T\}[C_{ss}]\{\phi_m\} = 0 \quad (6.15)$$

Products for the same mode are called modal mass, modal stiffness and modal damping respectively:

$$\{\phi_n^T\}[M_{ss}]\{\phi_n\} = M_n^* \quad (6.16)$$

$$\{\phi_n^T\}\,[K_{ss}]\,\{\phi_n\} = K_n^* \quad (6.17)$$

$$\{\phi_n^T\}\,[C_{ss}]\,\{\phi_n\} = C_n^* \quad (6.18)$$

And if the loading term is defined as like this:

$$L_n^* = \{\phi_n^T\}\,[M]\,\{I\} \tag{6.19}$$

Following equation will become:

$$M_n^*\ddot{y}_n(t) + C_n^*\dot{y}_n(t) + K_n^* y_n(t) = -L_n^*\ddot{u}_b(t) \tag{6.20}$$

If each term in Equation (6.20) is divided by modal mass and then term in loading part is substituted by Equation 6.21 called modal participation factor, Equation 6.22 is obtained.

$$\Gamma_n = {}^{L_n^*}\!/_{M_n^*} \tag{6.21}$$

$$\ddot{y}_n(t) + 2\xi_n\omega_n\dot{y}_n(t) + \omega_n^2 y_n(t) = -\Gamma_n\,\ddot{u}_b(t) \tag{6.22}$$

This equation resembles equation of SDOF system but with a little difference. Thus, following statement is required to get perfect match with SDOF system.

$$y_n(t) = \Gamma_n\,d_n(t) \tag{6.23}$$

$$\ddot{d}_n(t) + 2\xi_n\omega_n\dot{d}_n(t) + \omega_n^2 d_n(t) = -\,\ddot{u}_b(t) \tag{6.24}$$

Finally, we get a bunch of equivalent SDOF systems, which can be solved by probably the best tool named piecewise exact methodology [8]. Therefore, structural responses in modal coordinates are obtained. Then, by using modal participation factors mode shapes, response amplitudes in modal coordinates, and structural response in normal coordinates is achieved.

6.2. Frequency Domain Analysis

Although Fourier analysis in frequency domain has been known as early as time domain analysis, frequency domain analysis could not have been used for earthquake response analysis of structures until such time as powerful FFT (Fast Fourier Transform) algorithm was developed in the middle of 1960s by Cooley-Tukey [11]. After this milestone, frequency domain analysis has become popular. Today, it is known that frequency domain analysis is much superior since the equation of motion contains frequency dependent parameters such as stiffness or damping [3]. Purpose of this chapter is to give discrete integral formulations of frequency domain approach and to establish procedures for evaluating structural response in both modal and normal coordinates under arbitrary loading conditions.

The general frequency domain approach is similar to periodic loading analysis procedure; however, to apply this approach to arbitrary loading, Fourier series concept is required. Aim of the Fourier series expansion is to discretize the raw data to sine functions. In other words, it is assumed that a non-periodic signal is combination of a bunch of harmonic signal (Figure 6.2).

Figure 6.1 shows the excitation pattern p(t) during t_d, and t_s indicates duration of silent region. In frequency domain analysis, silent region should be placed after ground motion data in order to represent the free vibration response of structure. The length of the silent region depends on the response amplitudes of structure and damping ratio. For example, if damping ratio is chosen small like 1%, due to fact that diminishing of free vibration response will take long, silent region length must be extended. Otherwise, some additional spurious response onset of structural response history will be seen. Moreover, if response amplitudes of structure is major due to its long natural vibration period maybe, again, diminishing of free vibration response will take long time. Thus, in such cases, length of silent region should be chosen carefully. Investigations in this study show that length of the silent region should be chosen 2 times larger of excitation data (ground motion) for 5% damping ratio. For 2.5% damping ratio, 4 times larger silent region and for 1% damping ratio, 9 times larger silent region is required respectively. It should not be forgotten that these values are valid for the building investigated in this study, thus, length

of silent region may be less than specified here for low and mid-rise buildings. Justification of perfect matching with the results obtained in time domain is achieved by the analyses performed in SAP2000.

$$T_0 = t_d + t_s \tag{6.25}$$

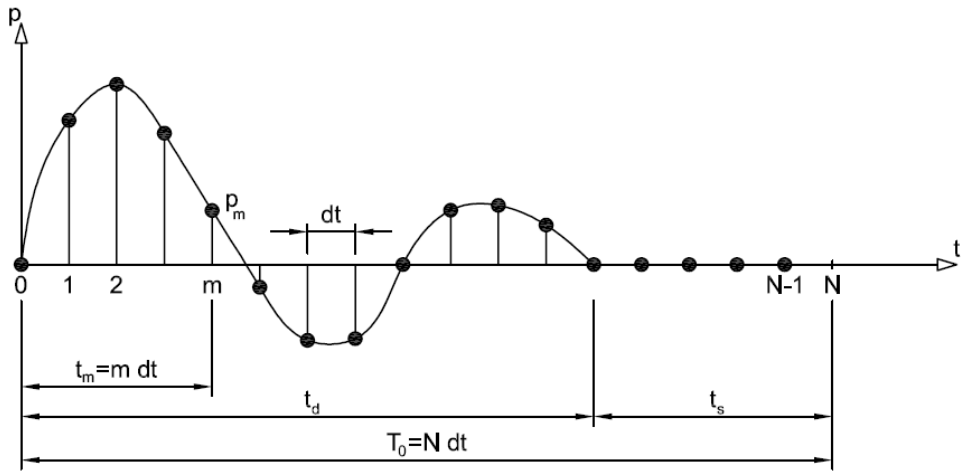

Figure 6.1. Digitization of excitation.

T_0 is sampled at N equally spaced time instants, thus, the sampling interval is denoted by dt [4]:

$$T_0 = N\ dt \tag{6.26}$$

$$T_0 = {}^{2\pi}/_{\bar{\omega}_0} \tag{6.27}$$

p_m indicates discretized excitation function in Equation 6.28, it is stated as superposition of N harmonic functions. Complex amplitude coefficients (P_j) defines the phase and amplitude of j[th] harmonic. Parseval's Equality [11] also known as Discrete Fourier transform pair [4] is given below:

$$p_m(t) = \sum_{j=0}^{N-1} P_j(i\bar{\omega})\, e^{i(\,j\,\bar{\omega}_0\,t_m\,)} \tag{6.28}$$

$$P_j(i\bar{\omega}) = \frac{1}{T_0}\sum_{m=0}^{N-1} p_m(t)\, e^{-i(\, j\, \bar{\omega}_0\, t_m\,)} \tag{6.29}$$

It should be observed from Equation 6.28 that only positive frequencies are considered. This is called one-sided Fourier Transform. Two-sided Fourier Transform contains negative frequencies as well [4]. It means that half of the frequencies are negative, but these have no physical meaning, therefore, highest harmonic frequency will be:

$$\bar{\omega}_{max} = \left({}^{N}/_{2}\right)\bar{\omega}_0 \tag{6.30}$$

$$\bar{f}_{max} = {}^{\bar{\omega}_{max}}/_{2\pi} \tag{6.31}$$

It is called Nyquist frequency or folding frequency. It is observed that forcing frequency is over at N/2+1 in Figure 6.2.

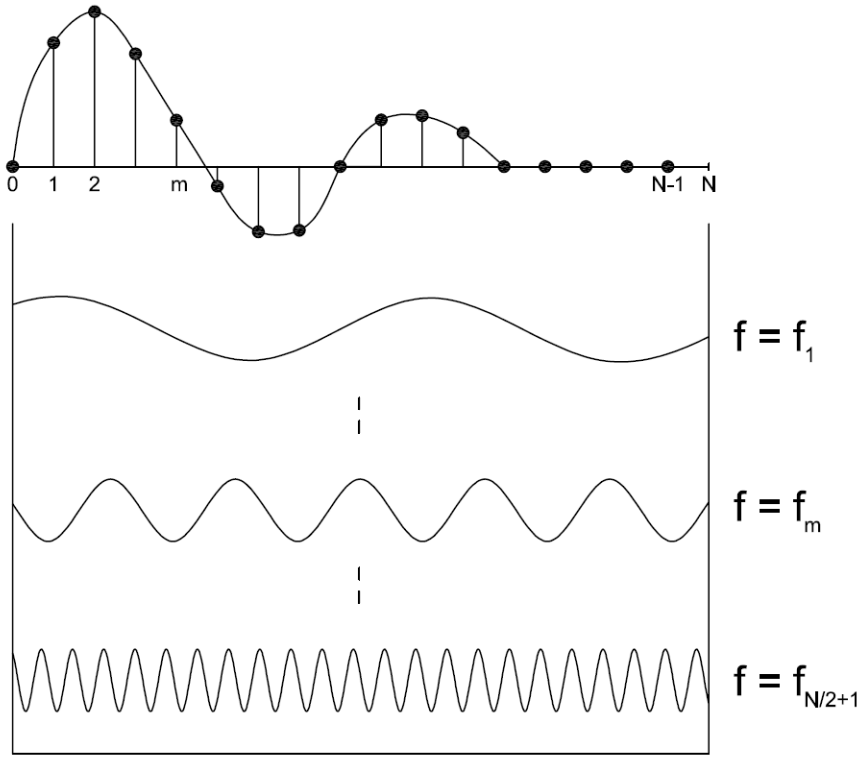

Figure 6.2. Discretization of non-periodic signal to sine functions.

Table 6.1 shows that complex amplitude coefficients after Nyquist frequency are complex conjugate of those before Nyquist frequency.

Table 6.1. Discrete time and Fourier series.

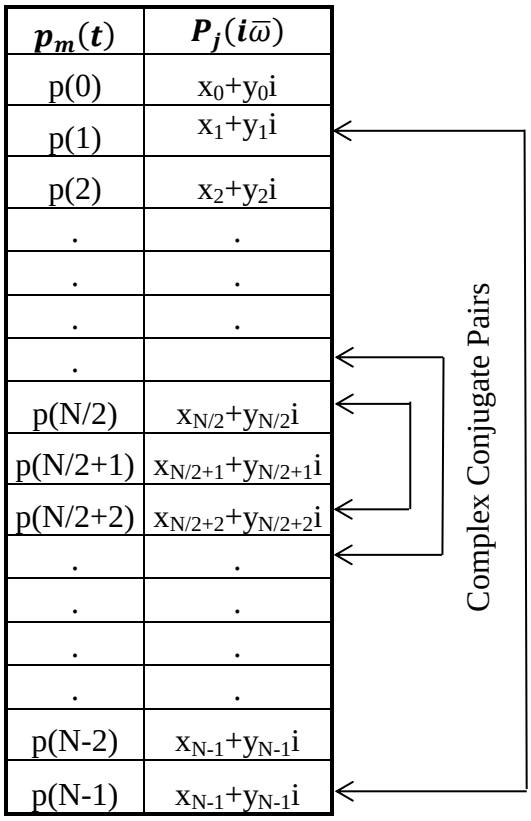

It should be mentioned that all of the DFT procedure is not so meaningful without Fast Fourier Transform (FFT) because of its cumbersomeness. By means of the discovery of FFT algorithm, computational effort required is drastically reduced. Besides, almost the same procedure is valid for FFT with an only difference which based on determination of N. There are N sums, each of which requires N complex products, or there are N^2 products required for the original FFT algorithm is given by $(N/2)\log_2 N$ [4]. For example, if the signal length is 970, it rounds to closest 2^m, therefore, $N=2^{10}=1024$.

6.2.1. In Modal Coordinates

Equation 6.20 can be written in frequency domain as below:

$$M_n^*\ddot{Y}_n(i\bar{\omega}) + C_n^*\dot{Y}_n(i\bar{\omega}) + K_n^*Y_n(i\bar{\omega}) = P_n(i\bar{\omega}) \tag{6.32}$$

Similar approaching to Equation 4.20 and Equation 4.21, displacement response quantities in modal coordinates can be written in terms of velocity and acceleration:

$$\dot{Y}_n(i\bar{\omega}) = i\bar{\omega}\, Y_n(i\bar{\omega}) \tag{6.33}$$

$$\ddot{Y}_n(i\bar{\omega}) = -\bar{\omega}^2 Y_n(i\bar{\omega}) \tag{6.34}$$

And Equation (6.30) is reduced to a simple linear equation form:

$$(-\bar{w}^2 M_n^* + i\bar{\omega}C_n^* + K_n^*)\, Y_n(i\bar{\omega}) = P_n(i\bar{\omega}) \tag{6.35}$$

Terms between brackets at the left hand side is called impedance or dynamic stiffness [3] since it changes with each forcing frequency:

$$\widetilde{K}_n^* = -\bar{w}^2 M_n^* + i\bar{\omega}C_n^* + K_n^* \tag{6.36}$$

Therefore, complex displacement amplitude coefficients can be obtained by following equation:

$$\widetilde{K}_n^*\, Y_n(i\bar{\omega}) = P_n(i\bar{\omega}) \tag{6.37}$$

Complex displacement amplitude coefficients are superposed by using equation Equation 6.28 and converted back to time domain. Once all procedure is applied for all modes in the same manner, response quantities in modal coordinates are achieved. They are combined by Equation 6.9 and eventually, response quantities are obtained in normal coordinates.

6.2.1.1. In Modal Coordinates with Structural Damping. Equation 4.26 can be written in terms of response quantities in modal coordinates:

$$M_n^*\ddot{Y}_n(i\bar{\omega}) + K_n^*(2\xi i + 1)Y_n(i\bar{\omega}) = P_n(i\bar{\omega}) \tag{6.38}$$

Substituting Equation 6.31 and Equation 6.32 into Equation 6.36, Equation 6.37 is derived:

$$(-\bar{\omega}^2 M_n^* + K_n^*(2\xi i + 1))\, Y_n(i\bar{\omega}) = P_n(i\bar{\omega}) \tag{6.39}$$

Terms between brackets at the left hand side is called impedance or dynamic stiffness [3] since it changes with each forcing frequency:

$$\widetilde{K}_n^* = -\bar{\omega}^2 M_n^* + K_n^*(2\xi i + 1) \tag{6.40}$$

Hence, complex displacement amplitude coefficients can be obtained by following equation:

$$\widetilde{K}_n^*\, Y_n(i\bar{\omega}) = P_n(i\bar{\omega}) \tag{6.41}$$

Response quantities in normal coordinates are obtained by applying exactly the same procedure prescribed in last paragraph of Chapter 6.2.1.

6.2.2. In Normal Coordinates

Second and more practical solution for obtaining response quantities is to get directly in normal coordinates. It can be possible just in frequency domain because response quantities can be written in terms of each other Equation 6.31 and 6.32. Thus, the equation of motion yields simple linear form and it can be solved without needing coordinate transformation procedure. Equation 6.10 can be written in following form and in frequency domain respectively:

$$[M]\{\ddot{u}_s(t)\} + [C]\{\dot{u}_s(t)\} + [K]\{u_s(t)\} = p(t) \tag{6.42}$$

$$[M]\{\ddot{U}_s(i\bar{\omega})\} + [C]\{\dot{U}_s(i\bar{\omega})\} + [K]\{U_s(i\bar{\omega})\} = P(i\bar{\omega}) \tag{6.43}$$

By substituting Equation 4.20 and Equation 4.21 into Equation 6.41, following equation is derived:

$$(-\bar{\omega}^2[M] + i\bar{\omega}[C] + [K])\{U_s(i\bar{\omega})\} = P(i\bar{\omega}) \tag{6.44}$$

Terms between brackets at the left hand side of Equation 6.42 is called impedance or dynamic stiffness matrix [3] since it changes with each forcing frequency:

$$\left[\widetilde{K}\right] = -\bar{\omega}^2[M] + i\bar{\omega}[C] + [K] \tag{6.45}$$

The complex displacement amplitude coefficients are obtained by following equation directly in normal coordinates:

$$\left[\widetilde{K}\right]\{U_s(i\bar{\omega})\} = P(i\bar{\omega}) \tag{6.46}$$

Finally, complex displacement amplitude coefficients are converted back to time domain by Equation 6.28 and eventually, displacement response quantities are achieved.

6.2.2.1. In Normal Coordinates with Structural Damping. Equation 4.26 can be written directly for MDOF systems:

$$[M]\left\{\ddot{U}_s(i\bar{\omega})\right\} + [K](2\xi i + 1)\{U_s(i\bar{\omega})\} = P(i\bar{\omega}) \tag{6.47}$$

By substituting Equation 4.20 and Equation 4.21 into Equation 6.41, following equation is derived:

$$(-\bar{\omega}^2[M] + [K](2\xi i + 1))\{U_s(i\bar{\omega})\} = P(i\bar{\omega}) \tag{6.48}$$

Terms between brackets at the left hand side of Equation 6.46 is called impedance or dynamic stiffness matrix [3] since it changes with each forcing frequency:

$$\left[\widetilde{K}\right] = -\bar{w}^2[M] + [K](2\xi i + 1) \tag{6.49}$$

The complex displacement amplitude coefficients are obtained by following equation directly in normal coordinates:

$$\left[\widetilde{K}\right]\{U_s(i\bar{\omega})\} = P(i\bar{\omega}) \tag{6.50}$$

Eventually, response quantities in normal coordinates are obtained by using Equation 6.28.

7. GROUND MOTION SELECTION AND SCALING PROCEDURE

Attractiveness of response history analysis is based on the capability of showing response of structures at each instant of an earthquake. By using several ground motion records, time history analyses are realized. However, it is explicit that these earthquakes will not be occurred again, thus it is really difficult to decide which earthquakes will be used in the analyses.

In this part, major part of far field record list presented in the FEMA-695 document is used for the analyses of the building. Totally, 20 records (40 individual components) selected from this document. Event magnitudes range from M6.5 to M7.6 with an average magnitude of M7.0 for far-field record set [11]. Records are obtained regions of which site classes C and D according to NEHRP site classification. In terms of source mechanism, fault types are predominantly consist of strike slip fault and several thrust faults are available. Peak ground acceleration values vary from 0.21g to 0.82g with an average PGA of 0.43g [11].

Normalization of Records:

Normalization procedure is done to provide the same overall ground motion strength of record set. This is the one of the simplest procedures to remove unwarranted variability between records due to inherent differences in magnitude, distance to source, source type and site conditions [11].

Firstly, geometric mean of two individual components of a record, which is called $PGV_{PEER,}$ is calculated. After this procedure is applied for all record set, median of all PGV_{PEER} values is divided by each record PGV_{PEER} value Equation 7.1. Therefore, normalization factor of each record is computed. Then, each component of any record is multiplied by NM values respectively to get normalized ground motion records (Equation 7.1 and Equation 7.2).

$$NM_i = Median(PGV_{PEER,i})/PGV_{PEER,i} \quad (7.1)$$

$$NTH_{1,i} = NM_i * TH_{1,i} \tag{7.2}$$

$$NTH_{2,i} = NM_i * TH_{2,i} \tag{7.3}$$

Scaling of Records:

Scaling procedure is done to a MCE level of ground motion according to ground motion scaling requirements of ASCE/SEI 7.05 [11]. Scaling process is starts with the calculation of median spectrum of record set (Figure 7.1).

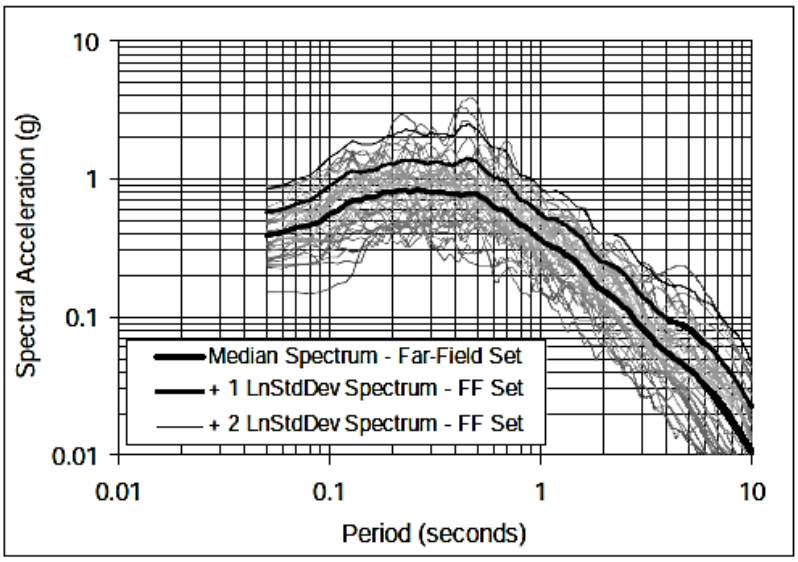

Figure 7.1. Derivation of median spectrum from response spectra of record set [11].

Then, this median spectrum is matched with MCE design spectra specified in ASCE/SEI 7.05 [2] anchoring associated fundamental period and site classification (Figure 7.2).

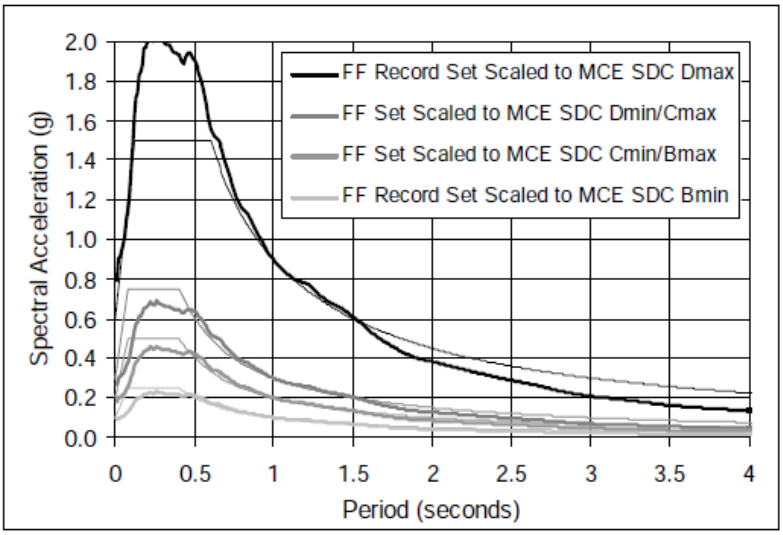

Figure 7.2. Example anchoring of median spectrum of records to MCE spectral acceleration at 1 second for B, C, D site classes according to NEHRP [11].

For wide range of fundamental period (T = 0.25 to 5 sec), this procedure is repeated according to site classification in NEHRP and results are presented as a table (Table 7.1) in FEMA document.

Table 7.1. Scaling factors with respect to fundamental periods and site classifications [11].

Period $T = C_u T_a$ (sec.)	Median Value of Normalized Record Set $\hat{S}_{NRT}$ (g)		Scaling Factors for Anchoring Far-Field Record Set to MCE Spectral Demand			
	Near-Field Set	Far-Field Set	SDC D_{max}	SDC C_{max} / SDC D_{min}	SDC B_{max} / SDC C_{min}	SDC B_{min}
2.0	0.284	0.148	3.05	1.02	0.68	0.34
2.2	0.258	0.133	3.08	1.03	0.68	0.34
2.4	0.230	0.118	3.18	1.06	0.71	0.35
2.6	0.210	0.106	3.28	1.09	0.73	0.36
2.8	0.190	0.091	3.53	1.18	0.79	0.39
3.0	0.172	0.080	3.75	1.25	0.83	0.42
3.5	0.132	0.063	4.10	1.37	0.91	0.46
4.0	0.104	0.052	4.29	1.43	0.95	0.48
4.5	0.086	0.046	4.34	1.45	0.96	0.48
5.0	0.072	0.041	4.43	1.48	0.98	0.49

As it is seen from highlighted bottom line in Table 7.1, the list is over with 5 sec at most. However, fundamental period of our building is approximately 6 seconds and site class is assumed as $B_{max} - C_{min}$ level. Under these conditions, the closest scaling factor is 0.98. For the sake of the undisturbed ground motion set, scale factor is assumed as **1**. In other words, in whole normalization and scaling procedure, each data is only multiplied by corresponding normalization factor. Lastly, ground motion records with normalization factors are given in Table 7.2 below.

Table 7.2. Ground motion record set.

ID No	M	Year	Earthquake Name	Station Name	Normalization Factor
1	6.7	1994	Northridge	Beverly Hills - Mulhol	0.65
2	6.7	1994	Northridge	Canyon Country - WLC	0.83
3	7.1	1999	Duzce	Bolu	0.63
4	7.1	1999	Hector Mine	Hector	1.09
5	6.5	1979	Imperial Valley	Delta	1.31
6	6.5	1979	Imperial Valley	El Centro Array #11	1.01
7	6.9	1995	Kobe	Nishi-Akashi	1.03
8	6.9	1995	Kobe	Shin-Osaka	1.10
9	7.5	1999	Kocaeli	Duzce	0.69
10	7.5	1999	Kocaeli	Arcelik	1.36
11	7.3	1992	Landers	Yermo Fire Station	0.99
12	7.3	1992	Landers	Coolwater	1.15
13	6.9	1989	Loma Prieta	Capitola	1.09
14	6.9	1989	Loma Prieta	Gilroy Array #3	0.88
15	6.5	1987	Superstition Hills	El Centro Imp. Co.	0.87
16	6.5	1987	Superstition Hills	Poe Road (temp)	1.17
17	7.6	1999	Chi-Chi	CHY101	0.41
18	7.6	1999	Chi-Chi	TCU045	0.96
19	6.6	1971	San Fernando	LA - Hollywood Stor	2.10
20	6.5	1976	Friuli	Tolmezzo	1.44

8. DYNAMIC PROPERTY AND SEISMIC LOADING COMBINATIONS

In this chapter, different mass, damping and seismic loading representations are combined as listed below, equation of motion for each combination is derived respectively.

Table 8.1. Combinations with respect to dynamic properties and loading.

Comb No	Mass Type	Damping Type	Loading Type
Comb#1	Translational Lumped	Mass Prop. Viscous	Acceleration
Comb#2	Trans. + Rot. Lumped	Mass Prop. Viscous	Acceleration
Comb#3	Translational Lumped	Stiffness Prop. Viscous	Acceleration
Comb#4	Trans. + Rot. Lumped	Stiffness Prop. Viscous	Acceleration
Comb#5a*	Translational Lumped	Rayleigh	Acceleration
Comb#5b**	Translational Lumped	Rayleigh	Acceleration
Comb#6a*	Trans. + Rot. Lumped	Rayleigh	Acceleration
Comb#6b**	Trans. + Rot. Lumped	Rayleigh	Acceleration
Comb#7	Translational Lumped	Structural	Acceleration
Comb#8	Trans. + Rot. Lumped	Structural	Acceleration
Comb#9	Consistent	Mass Prop. Viscous	Acceleration
Comb#10	Consistent	Stiffness Prop. Viscous	Acceleration
Comb#11	Consistent	Rayleigh	Acceleration
Comb#12	Consistent	Structural	Acceleration
Comb#13	Translational Lumped	Mass Prop. Viscous	Displacement
Comb#14	Trans. + Rot. Lumped	Mass Prop. Viscous	Displacement
Comb#15	Translational Lumped	Stiffness Prop. Viscous	Displacement
Comb#16	Trans. + Rot. Lumped	Stiffness Prop. Viscous	Displacement
Comb#17	Translational Lumped	Rayleigh	Displacement
Comb#18	Trans. + Rot. Lumped	Rayleigh	Displacement
Comb#19	Translational Lumped	Structural	Displacement
Comb#20	Trans. + Rot. Lumped	Structural	Displacement
Comb#21	Consistent	Mass Prop. Viscous	Displacement
Comb#22	Consistent	Stiffness Prop. Viscous	Displacement
Comb#23	Consistent	Rayleigh	Displacement
Comb#24	Consistent	Structural	Displacement

* Theoretically correct version (detailed explanation is given below.)
** Theoretically wrong version (detailed explanation is given below.)

8.1. Comb#1: Translational Lumped Mass, Mass Proportional Viscous Damping, Acceleration Loading

First two terms at the right hand side in Equation 8.1 vanishes because of the fact that M_{sb} term is not available in lumped mass system. Since the system has mass proportional damping property (Equation 8.2 and Equation 8.3), C_{sb} term is proportional with M_{sb} term, thus it also disappears:

$$\begin{aligned}&[M_{ss}]\{\ddot{u}_s\} + [C_{ss}]\{\dot{u}_s\} + [K_{ss}]\{u_s\} \\ &= -[\boldsymbol{M_{sb}}]\{\boldsymbol{\ddot{u}_b}\} - [\boldsymbol{C_{sb}}]\{\boldsymbol{\dot{u}_b}\} - [M_{ss}][T_{sb}]\{\ddot{u}_b\} - [C_{ss}]\{T_{sb}\}\{\dot{u}_b\}\end{aligned} \tag{8.1}$$

$$[C_{ss}] = \alpha[M_{ss}] \tag{8.2}$$

$$[\boldsymbol{C_{sb}}] = \boldsymbol{\alpha}[\boldsymbol{M_{sb}}] \tag{8.3}$$

$$[M_{ss}]\{\ddot{u}_s(t)\} + [C_{ss}]\{\dot{u}_s(t)\} + [K_{ss}]\{u_s(t)\} = -[M_{ss}]\{I\}\{\ddot{u}_b(t)\} - [C_{ss}]\{T_{sb}\}\{\dot{u}_b(t)\} \tag{8.4}$$

If displacement, velocity and acceleration terms are substituted with corresponding frequency domain terms,

$$\begin{aligned}&[M_{ss}]\{\ddot{U}_s(i\bar{\omega})\} + [C_{ss}]\{\dot{U}_s(i\bar{\omega})\} + [K_{ss}]\{U_s(i\bar{\omega})\} = \\ &-[M_{ss}]\{I\}\{\ddot{U}_b(i\bar{\omega})\} - [C_{ss}]\{T_{sb}\}\{\dot{U}_b(i\bar{\omega})\}\end{aligned} \tag{8.5}$$

Terms in frequency domain can be converted the other one easily divided or multiplied by $i\bar{w}$. Therefore, Equation 8.5 is become linear equation form:

$$(-\bar{\omega}^2[M_{ss}] + i\bar{\omega}[C_{ss}] + [K_{ss}])\{U_s(i\bar{\omega})\} = -([M_{ss}]\{I\} + \frac{[C_{ss}]\{T_{sb}\}}{i\bar{w}})\{\ddot{U}_b(i\bar{\omega})\} \tag{8.6}$$

Finally, Equation 8.6 can be written in simplified form:

$$[\tilde{K}_{ss}]\{U_s(i\bar{\omega})\} = -[\tilde{M}_{ss}]\{\ddot{U}_b(i\bar{\omega})\} \tag{8.7}$$

8.2. Comb#2: Translational + Rotational Lumped Mass, Mass Proportional Viscous Damping, Acceleration Loading

The same procedure is valid until Equation 8.6 for Comb#2. Instead of Equation 8.6, Equation 8.8 should be used to define transmission well. Difference between the Equation 8.6 and Equation 8.8 is transformation matrix (T_{sb}) in the first term at right hand side. This indicates that only translational base forces are transmitted to upper levels of structure.

$$(-\bar{\omega}^2[M_{ss}] + i\bar{\omega}[C_{ss}] + [K_{ss}])\{U_s(i\bar{\omega})\} = -([M_{ss}]\{T_{sb}\} + \frac{[C_{ss}]\{T_{sb}\}}{i\bar{\omega}})\{\ddot{U}_b(i\bar{\omega})\} \quad (8.8)$$

$$[\widetilde{K}_{ss}]\{U_s(i\bar{\omega})\} = -[\widetilde{M}_{ss}]\{\ddot{U}_b(i\bar{\omega})\} \quad (8.9)$$

8.3. Comb#3: Translational Lumped Mass, Stiffness Proportional Viscous Damping, Acceleration Loading

First forcing term vanishes since the system has lumped mass matrix. Sum of the second and fourth terms are equal to zero since system damping is proportional with stiffness. (Because of the same reason specified in Equation 5.13 and Equation 5.16)

$$\begin{aligned}&[M_{ss}]\{\ddot{u}_s\} + [C_{ss}]\{\dot{u}_s\} + [K_{ss}]\{u_s\} \\ &= -[\boldsymbol{M_{sb}}]\{\ddot{\boldsymbol{u}}_{\boldsymbol{b}}\} - [\boldsymbol{C_{sb}}]\{\dot{\boldsymbol{u}}_{\boldsymbol{b}}\} - [M_{ss}]\{T_{sb}\}\{\ddot{u}_b\} - [\boldsymbol{C_{ss}}]\{\boldsymbol{T_{sb}}\}\{\dot{\boldsymbol{u}}_{\boldsymbol{b}}\}\end{aligned} \quad (8.10)$$

$$[\boldsymbol{C_{ss}}] = \boldsymbol{\beta}[\boldsymbol{K_{ss}}] \quad (8.11)$$

$$[\boldsymbol{C_{sb}}] = \boldsymbol{\beta}[\boldsymbol{K_{sb}}] \quad (8.12)$$

Final form of the statement is classical equation of motion for MDOF system:

$$[M_{ss}]\{\ddot{u}_s(t)\} + [C_{ss}]\{\dot{u}_s(t)\} + [K_{ss}]\{u_s(t)\} = -[M_{ss}]\{I\}\{\ddot{u}_b(t)\} \quad (8.13)$$

If the statement is written in frequency domain and simplified linear equation form respectively:

$$[M_{ss}]\{\ddot{U}_s(i\omega)\} + [C_{ss}]\{\dot{U}_s(i\bar{\omega})\} + [K_{ss}]\{U_s(i\bar{\omega})\} = -[M_{ss}]\{I\}\{\ddot{U}_b(i\bar{\omega})\} \quad (8.14)$$

$$(-\bar{\omega}^2[M_{ss}] + i\bar{\omega}[C_{ss}] + [K_{ss}])\{U_s(i\bar{\omega})\} = -[M_{ss}]\{I\}\{\ddot{U}_b(i\bar{\omega})\} \quad (8.15)$$

$$[\tilde{K}_{ss}]\{U_s(i\bar{\omega})\} = -[M_{ss}]\{I\}\{\ddot{U}_b(i\bar{\omega})\} \quad (8.16)$$

8.4. Comb#4: Translational + Rotational Lumped Mass, Stiffness Proportional Viscous Damping, Acceleration Loading

The same procedure defined in Comb#3 is valid for Comb#4. Note that only last equation will be like this:

$$[\tilde{K}_{ss}]\{U_s(i\bar{\omega})\} = -[M_{ss}]\{T_{sb}\}\{\ddot{U}_b(i\bar{\omega})\} \quad (8.17)$$

8.5. Comb#5a: Translational Lumped Mass, Mass and Stiffness Proportional (Rayleigh) Viscous Damping, Acceleration Loading

Comb#5a is the actual version of the classical equation of motion (Equation 5.18) with Rayleigh damping. Normally, some terms are neglected by reason of ease of applicability and Equation 5.18 is used. In this case, actual procedure will be given for the calculation of the system with Rayleigh damping.

Only first forcing term of Equation 8.18 vanishes because system mass matrix is lumped, accordingly diagonal.

$$\begin{aligned}&[M_{ss}]\{\ddot{u}_s\} + [C_{ss}]\{\dot{u}_s\} + [K_{ss}]\{u_s\}\\ &= -[\boldsymbol{M_{sb}}]\{\boldsymbol{\ddot{u}_b}\} - [C_{sb}]\{\dot{u}_b\} - [M_{ss}]\{T_{sb}\}\{\ddot{u}_b\} - [C_{ss}]\{T_{sb}\}\{\dot{u}_b\}\end{aligned} \quad (8.18)$$

Due to the same reason, C_{sb} term is proportional with only stiffness term (Equation 8.20). This can cause incompatibility between upper levels of structure and base.

$$[C_{ss}] = \alpha[M_{ss}] + \beta[K_{ss}] \quad (8.19)$$

$$[C_{sb}] = \boldsymbol{\alpha}[\boldsymbol{M_{sb}}] + \beta[K_{sb}] \quad (8.20)$$

$$\begin{aligned}&[M_{ss}]\{\ddot{u}_s(t)\} + [C_{ss}]\{\dot{u}_s(t)\} + [K_{ss}]\{u_s(t)\}\\ &= -[M_{ss}]\{I\}\{\ddot{u}_b(t)\} - [C_{ss}]\{T_{sb}\}\{\dot{u}_b(t)\} - [C_{sb}]\{\dot{u}_b(t)\}\end{aligned} \quad (8.21)$$

If the statement is written in frequency domain and simplified linear equation form respectively:

$$[M_{ss}]\{\ddot{U}_s(i\bar{\omega})\} + [C_{ss}]\{\dot{U}_s(i\bar{\omega})\} + [K_{ss}]\{U_s(i\bar{\omega})\} = -[M_{ss}]\{I\}\{\ddot{U}_b(i\bar{\omega})\} - [C_{ss}]\{T_{sb}\}\{\dot{U}_b(i\bar{\omega})\} - [C_{sb}]\{\dot{U}_b(i\bar{\omega})\} \quad (8.22)$$

$$(-\bar{\omega}^2[M_{ss}] + i\bar{\omega}[C_{ss}] + [K_{ss}])\{U_s(i\bar{\omega})\} = -([M_{ss}]\{I\} + \frac{[C_{ss}]\{T_{sb}\}+[C_{sb}]}{i\bar{\omega}})\{\ddot{U}_b(i\bar{\omega})\} \quad (8.23)$$

$$[\tilde{K}_{ss}]\{U_s(i\bar{\omega})\} = -[\tilde{M}_{ss}]\{\ddot{U}_b(i\bar{\omega})\} \quad (8.24)$$

8.6. Comb#5b: Translational Lumped Mass, Mass and Stiffness Proportional (Rayleigh) Viscous Damping, Acceleration Loading (Common Usage, Theoretically Wrong)

Comb#5b indicates the conventional usage of equation of motion for Rayleigh damping. However, in order to reduce the equation to ordinary form (Equation 8.13), damping property must be proportional only stiffness matrix. Otherwise, equation becomes like Equation 8.21. In this combination, for the sake of the simplicity, sum of the second and third terms in the loading part of Equation 8.21 is assumed that equals to zero. Hence, equation will be as specified below:

$$[M_{ss}]\{\ddot{u}_s(t)\} + [C_{ss}]\{\dot{u}_s(t)\} + [K_{ss}]\{u_s(t)\} = -[M_{ss}]\{I\}\{\ddot{u}_b(t)\} \quad (8.25)$$

Equation 8.25 can be written in terms of frequency domain:

$$[M_{ss}]\{\ddot{U}_s(i\bar{\omega})\} + [C_{ss}]\{\dot{U}_s(i\bar{\omega})\} + [K_{ss}]\{U_s(i\bar{\omega})\} = -[M_{ss}]\{I\}\{\ddot{U}_b(i\bar{\omega})\} \quad (8.26)$$

The statement is reduced to linear equation form:

$$(-\bar{\omega}^2[M_{ss}] + i\bar{\omega}[C_{ss}] + [K_{ss}])\{U_s(i\bar{\omega})\} = -[M_{ss}]\{I\}\{\ddot{U}_b(i\bar{\omega})\} \quad (8.27)$$

$$\left[\widetilde{K}_{ss}\right]\{U_s(i\bar{\omega})\} = -[M_{ss}]\{I\}\left\{\ddot{U}_b(i\bar{\omega})\right\} \tag{8.28}$$

8.7. Comb#6a: Translational + Rotational Lumped Mass, Mass and Stiffness Proportional (Rayleigh) Viscous Damping, Acceleration Loading

Comb#6a has exactly the same form of Comb#5a. Additionally, it includes rotational lumped mass terms but it does not change the form of equation. Only difference is that Equation 8.29 includes transformation matrix instead of influence vector.

$$(-\bar{\omega}^2[M_{ss}] + i\bar{\omega}[C_{ss}] + [K_{ss}])\{U_s(i\bar{\omega})\} = -([M_{ss}]\{T_{sb}\} + \frac{[C_{ss}]\{T_{sb}\} + [C_{sb}]}{i\bar{w}})\left\{\ddot{U}_b(i\bar{\omega})\right\} \tag{8.29}$$

$$\left[\widetilde{K}_{ss}\right]\{U_s(i\bar{\omega})\} = -\left[\widetilde{M}_{ss}\right]\left\{\ddot{U}_b(i\bar{\omega})\right\} \tag{8.30}$$

8.8. Comb#6b: Translational + Rotational Lumped Mass, Mass and Stiffness Proportional (Rayleigh) Viscous Damping, Acceleration Loading (Common Usage, Theoretically Wrong)

Equation 8.28 derived in Comb#5b can be used for analyzing of this combination, with a difference that influence vector $\{I\}$ must be substituted by transformation matrix $\{T_{sb}\}$.

$$\left[\widetilde{K}_{ss}\right]\{U_s(i\bar{\omega})\} = -[M_{ss}]\{T_{sb}\}\left\{\ddot{U}_b(i\bar{\omega})\right\} \tag{8.31}$$

8.9. Comb#7: Translational Lumped Mass, Structural Damping, Acceleration Loading

Due to fact that Comb#7 includes complex term, it is only defined in frequency domain. Having stiffness proportional damping cancels out the damping terms, therefore, following formulations are obtained:

$$[M_{ss}]\{\ddot{U}_s(i\bar{\omega})\} + (2\xi i + 1)[K_{ss}]\{U_s(i\bar{\omega})\} = -[M_{ss}]\{T_{sb}\}\{\ddot{U}_b(i\bar{\omega})\} \quad (8.32)$$

$$(-\bar{\omega}^2[M_{ss}] + (2\xi i + 1)[K_{ss}])\{U_s(i\bar{\omega})\} = -[M_{ss}]\{T_{sb}\}\{\ddot{U}_b(i\bar{\omega})\} \quad (8.33)$$

$$[\widetilde{K}_{ss}]\{U_s(i\bar{\omega})\} = -[M_{ss}]\{I\}\{\ddot{U}_b(i\bar{\omega})\} \quad (8.34)$$

8.10. Comb#8: Translational + Rotational Lumped Mass, Structural Damping, Acceleration Loading

Equation 8.34 can be used for performing analysis of Comb#8 by substituting influence vector with transformation matrix:

$$[\widetilde{K}_{ss}]\{U_s(i\bar{\omega})\} = -[M_{ss}]\{T_{sb}\}\{\ddot{U}_b(i\bar{\omega})\} \quad (8.35)$$

8.11. Comb#9: Consistent Wall Mass + Translational Slab Lumped Mass, Mass Proportional Viscous Damping, Acceleration Loading

In consistent mass system, no terms are canceled; Equation 8.36 will be remained:

$$\begin{aligned}&[M_{ss}]\{\ddot{u}_s\} + [C_{ss}]\{\dot{u}_s\} + [K_{ss}]\{u_s\}\\ &= -[M_{sb}]\{\ddot{u}_b\} - [C_{sb}]\{\dot{u}_b\} - [M_{ss}]\{T_{sb}\}\{\ddot{u}_b\} - [C_{ss}]\{T_{sb}\}\{\dot{u}_b\}\end{aligned} \quad (8.36)$$

$$[C_{ss}] = \alpha[M_{ss}] \quad (8.37)$$

$$[C_{sb}] = \alpha[M_{sb}] \quad (8.38)$$

If Equation 8.36 is written in frequency domain:

$$\begin{aligned}&[M_{ss}]\{\ddot{U}_s(i\bar{\omega})\} + [C_{ss}]\{\dot{U}_s(i\bar{\omega})\} + [K_{ss}]\{U_s(i\bar{\omega})\}\\ &= -[M_{sb}]\{\ddot{U}_b(i\bar{\omega})\} - [C_{sb}]\{\dot{U}_b(i\bar{\omega})\} - [M_{ss}]\{T_{sb}\}\{\ddot{U}_b(i\bar{\omega})\} - [C_{ss}]\{T_{sb}\}\{\dot{U}_b(i\bar{\omega})\}\end{aligned} \quad (8.39)$$

And it becomes linear equation form:

$$(-\bar{\omega}^2[M_{ss}] + i\bar{\omega}[C_{ss}] + [K_{ss}])\{U_s(i\bar{\omega})\}$$
$$= -(\,[M_{sb}] + [M_{ss}]\{T_{sb}\} + \frac{[C_{sb}]+[C_{ss}]\{T_{sb}\}}{i\bar{w}}\,)\{\ddot{U}_b(i\bar{\omega})\} \quad (8.40)$$

$$[\widetilde{K}_{ss}]\{U_s(i\bar{\omega})\} = -[\widetilde{M}_{ss}]\{\ddot{U}_b(i\bar{\omega})\} \quad (8.41)$$

8.12. Comb#10: Consistent Wall Mass + Translational Slab Lumped Mass, Stiffness Proportional Viscous Damping, Acceleration Loading

Due to stiffness proportionality, damping terms are cancelled out:

$$[M_{ss}]\{\ddot{u}_s\} + [C_{ss}]\{\dot{u}_s\} + [K_{ss}]\{u_s\}$$
$$= -[M_{sb}]\{\ddot{u}_b\} - [\boldsymbol{C_{sb}}]\{\boldsymbol{\dot{u}_b}\} - [M_{ss}]\{T_{sb}\}\{\ddot{u}_b\} - [\boldsymbol{C_{ss}}]\{\boldsymbol{T_{sb}}\}\{\boldsymbol{\dot{u}_b}\} \quad (8.42)$$

$$[\boldsymbol{C_{ss}}] = \boldsymbol{\beta}[\boldsymbol{K_{ss}}] \quad (8.43)$$

$$[\boldsymbol{C_{sb}}] = \boldsymbol{\beta}[\boldsymbol{K_{sb}}] \quad (8.44)$$

$$[M_{ss}]\{\ddot{u}_s(t)\} + [C_{ss}]\{\dot{u}_s(t)\} + [K_{ss}]\{u_s(t)\} = -[M_{sb}]\{\ddot{u}_b(t)\} - [M_{ss}]\{T_{sb}\}\{\ddot{u}_b(t)\} \quad (8.45)$$

If Equation 8.45 is defined in frequency domain:

$$[M_{ss}]\{\ddot{U}_s(i\bar{\omega})\} + [C_{ss}]\{\dot{U}_s(i\bar{\omega})\} + [K_{ss}]\{U_s(i\bar{\omega})\} =$$
$$-[M_{sb}]\{\ddot{U}_b(i\bar{\omega})\} - [M_{ss}]\{T_{sb}\}\{\ddot{U}_b(i\bar{\omega})\} \quad (8.46)$$

Equation 8.47 can be written as linear equation:

$$(-\bar{\omega}^2[M_{ss}] + i\bar{\omega}[C_{ss}] + [K_{ss}])\{U_s(i\bar{\omega})\} = -(\,[M_{sb}] + [M_{ss}]\{T_{sb}\}\,)\{\ddot{U}_b(i\bar{\omega})\} \quad (8.47)$$

$$[\widetilde{K}_{ss}]\{U_s(i\bar{\omega})\} = -(\,[M_{sb}] + [M_{ss}]\{T_{sb}\}\,)\{\ddot{U}_b(i\bar{\omega})\} \quad (8.48)$$

8.13. Comb#11: Consistent Wall Mass + Translational Slab Lumped Mass, Mass and Stiffness Proportional (Rayleigh) Viscous Damping, Acceleration Loading

Equation 8.35 can be used for analyzing of Comb#11, but damping matrix should be defined as Rayleigh damping:

$$[C_{ss}] = \alpha[M_{ss}] + \beta[K_{ss}] \tag{8.49}$$

$$[C_{sb}] = \alpha[M_{sb}] + \beta[K_{sb}] \tag{8.50}$$

Frequency domain representation:

$$\begin{aligned}&[M_{ss}]\{\ddot{U}_s(i\bar{\omega})\} + [C_{ss}]\{\dot{U}_s(i\bar{\omega})\} + [K_{ss}]\{U_s(i\bar{\omega})\} \\ &= -[M_{sb}]\{\ddot{U}_b(i\bar{\omega})\} - [C_{sb}]\{\dot{U}_b(i\bar{\omega})\} - [M_{ss}]\{T_{sb}\}\{\ddot{U}_b(i\bar{\omega})\} - [C_{ss}]\{T_{sb}\}\{\dot{U}_b(i\bar{\omega})\}\end{aligned} \tag{8.51}$$

Converted into linear equation form and dynamic stiffness matrix representation respectively:

$$\begin{aligned}&(-\bar{\omega}^2[M_{ss}] + i\bar{\omega}[C_{ss}] + [K_{ss}])\{U_s(i\bar{\omega})\} \\ &= -([M_{sb}] + [M_{ss}]\{T_{sb}\} + \tfrac{[C_{sb}]+[C_{ss}]\{T_{sb}\}}{i\bar{\omega}})\{\ddot{U}_b(i\bar{\omega})\}\end{aligned} \tag{8.52}$$

$$[\widetilde{K}_{ss}]\{U_s(i\bar{\omega})\} = -[\widetilde{M}_{ss}]\{\ddot{U}_b(i\bar{\omega})\} \tag{8.53}$$

8.14. Comb#12: Consistent Wall Mass + Translational Slab Lumped Mass, Structural Damping, Acceleration Loading

Structural (Rate-independent) damping is only defined in frequency domain and its mathematical representation will be as below:

$$[M_{ss}]\{\ddot{U}_s(i\bar{\omega})\} + (2\xi i + 1)[K_{ss}]\{U_s(i\bar{\omega})\} = -[M_{sb}]\{\ddot{U}_b(i\bar{\omega})\} - [M_{ss}]\{T_{sb}\}\{\ddot{U}_b(i\bar{\omega})\} \tag{8.54}$$

All terms can be stated in terms of complex displacement amplitude, thus the equation yields:

$$(-\overline{w}^2[M_{ss}] + (2\xi i + 1)[K_{ss}])\{U_s(i\overline{\omega})\} = -(\,[M_{sb}] + [M_{ss}]\{T_{sb}\}\,)\{\ddot{U}_b(i\overline{\omega})\} \quad (8.55)$$

The terms in brackets at left hand side can be represented as one term called dynamic stiffness matrix and its representation:

$$[\widetilde{K}_{ss}]\{U_s(i\overline{\omega})\} = -(\,[M_{sb}] + [M_{ss}]\{T_{sb}\}\,)\{\ddot{U}_b(i\overline{\omega})\} \quad (8.56)$$

8.15. Comb#13: Translational Lumped Mass, Mass Proportional Viscous Damping, Displacement Loading

Beginning from this combination, the equations are derived for calculation of absolute response quantities. M_{sb} term is not available because of lumped mass assumption, C_{sb} term is not available since it is assumed that damping is proportional with mass:

$$[M_{ss}]\{\ddot{u}_s^t\} + [C_{ss}]\{\dot{u}_s^t\} + [K_{ss}]\{u_s^t\} = -[\boldsymbol{M_{sb}}]\{\boldsymbol{\ddot{u}_b}\} - [\boldsymbol{C_{sb}}]\{\boldsymbol{\dot{u}_b}\} - [K_{sb}]\{u_b\} \quad (8.57)$$

$$[C_{ss}] = \alpha[M_{ss}] \quad (8.58)$$

$$[\boldsymbol{C_{sb}}] = \boldsymbol{\alpha}[\boldsymbol{M_{sb}}] \quad (8.59)$$

$$[M_{ss}]\{\ddot{u}_s^t(t)\} + [C_{ss}]\{\dot{u}_s^t(t)\} + [K_{ss}]\{u_s^t(t)\} = -[K_{sb}]\{u_b(t)\} \quad (8.60)$$

If Equation 8.60 is stated in frequency domain:

$$[M_{ss}]\{\ddot{U}_s^t(i\overline{\omega})\} + [C_{ss}]\{\dot{U}_s^t(i\overline{\omega})\} + [K_{ss}]\{U_s^t(i\overline{\omega})\} = -[K_{sb}]\{U_b(i\overline{\omega})\} \quad (8.61)$$

All terms can be expressed in terms of complex displacement amplitudes, thus Equation 8.61 yields:

$$(-\overline{\omega}^2[M_{ss}] + i\overline{\omega}[C_{ss}] + [K_{ss}])\{U_s^t(i\overline{\omega})\} = -[K_{sb}]\{U_b(i\overline{\omega})\} \quad (8.62)$$

$$[\widetilde{K}_{ss}]\{U_s^t(i\overline{\omega})\} = -[K_{sb}]\{U_b(i\overline{\omega})\} \quad (8.63)$$

8.16. Comb#14: Translational + Rotational Lumped Mass, Mass Proportional Viscous Damping, Displacement Loading

Exactly the same formulation procedure is followed in Comb#13 is valid for Comb#14.

8.17. Comb#15: Translational Lumped Mass, Stiffness Proportional Viscous Damping, Displacement Loading

Only mass interaction term is not available due to lumped mass assumption, other two terms are remained:

$$[M_{ss}]\{\ddot{u}_s^t\} + [C_{ss}]\{\dot{u}_s^t\} + [K_{ss}]\{u_s^t\} = -[\boldsymbol{M_{sb}}]\{\boldsymbol{\ddot{u}_b}\} - [C_{sb}]\{\dot{u}_b\} - [K_{sb}]\{u_b\} \quad (8.64)$$

$$[C_{ss}] = \beta[K_{ss}] \quad (8.65)$$

$$[C_{sb}] = \beta[K_{sb}] \quad (8.66)$$

$$[M_{ss}]\{\ddot{u}_s^t(t)\} + [C_{ss}]\{\dot{u}_s^t(t)\} + [K_{ss}]\{u_s^t(t)\} = -[C_{sb}]\{\dot{u}_b(t)\} - [K_{sb}]\{u_b(t)\} \quad (8.67)$$

If the statement is written in frequency domain:

$$\begin{aligned}[M_{ss}]\{\ddot{U}_s^t(i\bar{\omega})\} + [C_{ss}]\{\dot{U}_s^t(i\bar{\omega})\} + [K_{ss}]\{U_s^t(i\bar{\omega})\} \\ = -[C_{sb}]\{\dot{U}_b(i\bar{\omega})\} - [K_{sb}]\{U_b(i\bar{\omega})\}\end{aligned} \quad (8.68)$$

If the terms left hand side in Equation 8.68 are written in terms of complex displacement amplitudes, equation yields linear form:

$$(-\bar{\omega}^2[M_{ss}] + i\bar{\omega}[C_{ss}] + [K_{ss}])\{U_s^t(i\bar{\omega})\} = -(i\bar{\omega}[C_{sb}] + [K_{sb}])\{U_b(i\bar{\omega})\} \quad (8.69)$$

$$[\tilde{K}_{ss}]\{U_s^t(i\bar{\omega})\} = -[\tilde{K}_{sb}]\{U_b(i\bar{\omega})\} \quad (8.70)$$

8.18. Comb#16: Translational + Rotational Lumped Mass, Stiffness Proportional Viscous Damping, Displacement Loading

Exactly the same formulation procedure is followed in Comb#15 is valid for Comb#16.

8.19. Comb#17: Translational Lumped Mass, Mass and Stiffness Proportional (Rayleigh) Viscous Damping, Displacement Loading

Due to lumped mass assumption, M_{sb} term is not available, thus, C_{sb} term is only proportional with base-structure interaction term (K_{sb}). Inconsistent behavior is expected similar to Comb#5a.

$$[C_{ss}] = \alpha[M_{ss}] + \beta[K_{ss}] \tag{8.71}$$

$$[C_{sb}] = \boldsymbol{\alpha}[\boldsymbol{M_{sb}}] + \beta[K_{sb}] \tag{8.72}$$

$$[M_{ss}]\{\ddot{u}_s^t(t)\} + [C_{ss}]\{\dot{u}_s^t(t)\} + [K_{ss}]\{u_s^t(t)\} = -[C_{sb}]\{\dot{u}_b(t)\} - [K_{sb}]\{u_b(t)\} \tag{8.73}$$

Frequency domain representation:

$$\begin{aligned}&[M_{ss}]\{\ddot{U}_s^t(i\bar{\omega})\} + [C_{ss}]\{\dot{U}_s^t(i\bar{\omega})\} + [K_{ss}]\{U_s^t(i\bar{\omega})\}\\ &\quad = -[C_{sb}]\{\dot{U}_b(i\bar{\omega})\} - [K_{sb}]\{U_b(i\bar{\omega})\}\end{aligned} \tag{8.74}$$

All terms can be stated in terms of complex displacement amplitudes, thus the equation yields:

$$(-\bar{\omega}^2[M_{ss}] + i\bar{\omega}[C_{ss}] + [K_{ss}])\{U_s^t(i\bar{\omega})\} = -(i\bar{\omega}[C_{sb}] + [K_{sb}])\{U_b(i\bar{\omega})\} \tag{8.75}$$

$$[\widetilde{K}_{ss}]\{U_s^t(i\bar{\omega})\} = -[\widetilde{K}_{sb}]\{U_b(i\bar{\omega})\} \tag{8.76}$$

8.20. Comb#18: Translational + Rotational Lumped Mass, Mass and Stiffness Proportional (Rayleigh) Viscous Damping, Displacement Loading

Exactly the same formulation procedure used in Comb#17 is valid for Comb#18.

8.21. Comb#19: Translational Lumped Mass, Structural Damping, Displacement Loading

Structural damping has complex valued term, thus, it can be only defined in frequency domain. M_{sb} term is not available due to lumped mass assumption:

$$[M_{ss}]\{\ddot{U}_s^t(i\bar{\omega})\} + (2\xi i + 1)[K_{ss}]\{U_s^t(i\bar{\omega})\} = -[\boldsymbol{M_{sb}}]\{\boldsymbol{\ddot{U}_b(i\bar{\omega})}\} - (2\xi i + 1)[K_{sb}]\{U_b(i\bar{\omega})\} \quad (8.77)$$

All terms can be expressed in terms of complex displacement amplitudes, thus equation yields:

$$(-\bar{\omega}^2[M_{ss}] + (2\xi i + 1)[K_{ss}])\{U_s^t(i\bar{\omega})\} = -(2\xi i + 1)[K_{sb}]\{U_b(i\bar{\omega})\} \quad (8.78)$$

$$\left[\widetilde{K}_{ss}\right]\{U_s^t(i\bar{\omega})\} = -(2\xi i + 1)[K_{sb}]\{U_b(i\bar{\omega})\} \quad (8.79)$$

8.22. Comb#20: Translational + Rotational Lumped Mass, Structural Damping, Displacement Loading

Exactly the same formulation procedure used in Comb#19 is valid for Comb#20.

8.23. Comb#21: Consistent Wall Mass + Translational Slab Lumped Mass, Mass Proportional Viscous Damping, Displacement Loading

Consistent mass system contains all loading terms.

$$[M_{ss}]\{\ddot{u}_s^t\} + [C_{ss}]\{\dot{u}_s^t\} + [K_{ss}]\{u_s^t\} = -[M_{sb}]\{\ddot{u}_b\} - [C_{sb}]\{\dot{u}_b\} - [K_{sb}]\{u_b\} \quad (8.80)$$

$$[C_{ss}] = \alpha[M_{ss}] \quad (8.81)$$

$$[C_{sb}] = \alpha[M_{sb}] \tag{8.82}$$

Frequency domain representation and linear equation form of it will become respectively:

$$\begin{aligned}&[M_{ss}]\{\ddot{U}_s^t(i\bar{\omega})\} + [C_{ss}]\{\dot{U}_s^t(i\bar{\omega})\} + [K_{ss}]\{U_s^t(i\bar{\omega})\}\\ &= -[M_{sb}]\{\ddot{U}_b(i\bar{\omega})\} - [C_{sb}]\{\dot{U}_b(i\bar{\omega})\} - [K_{sb}]\{U_b(i\bar{\omega})\}\end{aligned} \tag{8.83}$$

$$\begin{aligned}&(-\bar{\omega}^2[M_{ss}] + i\bar{\omega}[C_{ss}] + [K_{ss}])\{U_s^t(i\bar{\omega})\}\\ &= -(-\bar{\omega}^2[M_{sb}] + i\bar{\omega}[C_{sb}] + [K_{sb}])\{U_b(i\bar{\omega})\}\end{aligned} \tag{8.84}$$

$$[\tilde{K}_{ss}]\{U_s^t(i\bar{\omega})\} = -[\tilde{K}_{sb}]\{U_b(i\bar{\omega})\} \tag{8.85}$$

8.24. Comb#22: Consistent Wall Mass + Translational Slab Lumped Mass, Stiffness Proportional Viscous Damping, Displacement Loading

The same formulation procedure specified in Comb#21 is valid for analyzing of Comb#22, but system damping matrix is proportional with stiffness:

$$[C_{ss}] = \beta[K_{ss}] \tag{8.86}$$

$$[C_{sb}] = \beta[K_{sb}] \tag{8.87}$$

8.25. Comb#23: Consistent Wall Mass + Translational Slab Lumped Mass, Mass and Stiffness (Rayleigh) Proportional Viscous Damping, Displacement Loading

The same formulation procedure specified in Comb#21 is valid for analyzing of Comb#23, but system damping matrix must be established as Rayleigh damping.

$$[C_{ss}] = \alpha[M_{ss}] + \beta[K_{ss}] \tag{8.88}$$

$$[C_{sb}] = \alpha[M_{sb}] + \beta[K_{sb}] \tag{8.89}$$

8.26. Comb#24: Consistent Wall Mass + Translational Slab Lumped Mass, Structural Damping, Displacement Loading

The last combination is formulated in frequency domain because of the fact that it has complex valued terms:

$$[M_{ss}]\{\ddot{U}_s^t(i\bar{\omega})\} + (2\xi i + 1)[K_{ss}]\{U_s^t(i\bar{\omega})\} = -[M_{sb}]\{\ddot{U}_b(i\bar{\omega})\} - (2\xi i + 1)[K_{sb}]\{U_b(i\bar{\omega})\} \quad (8.90)$$

All terms can be stated in terms of complex displacement amplitude, thus the equation yields:

$$(-\bar{\omega}^2[M_{ss}] + (2\xi i + 1)[K_{ss}])\{U_s^t(i\bar{\omega})\} = -(-\bar{\omega}^2[M_{sb}] + (2\xi i + 1)[K_{sb}])\{U_b(i\bar{\omega})\} \quad (8.91)$$

The terms in brackets both at left and right hand side can be represented as one term called dynamic stiffness matrix and its representation:

$$[\tilde{K}_{ss}]\{U_s^t(i\bar{\omega})\} = -[\tilde{K}_{sb}]\{U_b(i\bar{\omega})\} \quad (8.92)$$

9. COMPARATIVE RESULTS

In this chapter, comparative results are given and discussed in terms of drift ratios and total acceleration response. 40 individual components of 20 earthquake record set (mentioned in Chapter 7) are used for response history analysis. Analysis results presentation is based on comparison of mean values obtained by absolute-maximum response of each analysis result. Explicitly, one of the combinations is chosen, solved for an earthquake record, absolute-maximum response for each story is calculated. Blue curves indicate these absolute-maximum responses in Figure 9.1 and Figure 9.2 for all records. After this process is repeated for all individual records as in Figure 9.1 and Figure 9.2, mean of them is calculated (red curves in Figure 9.1 and Figure 9.2). Then, this process is repeated for each combination. Comparisons are done by using just mean values of each combination.

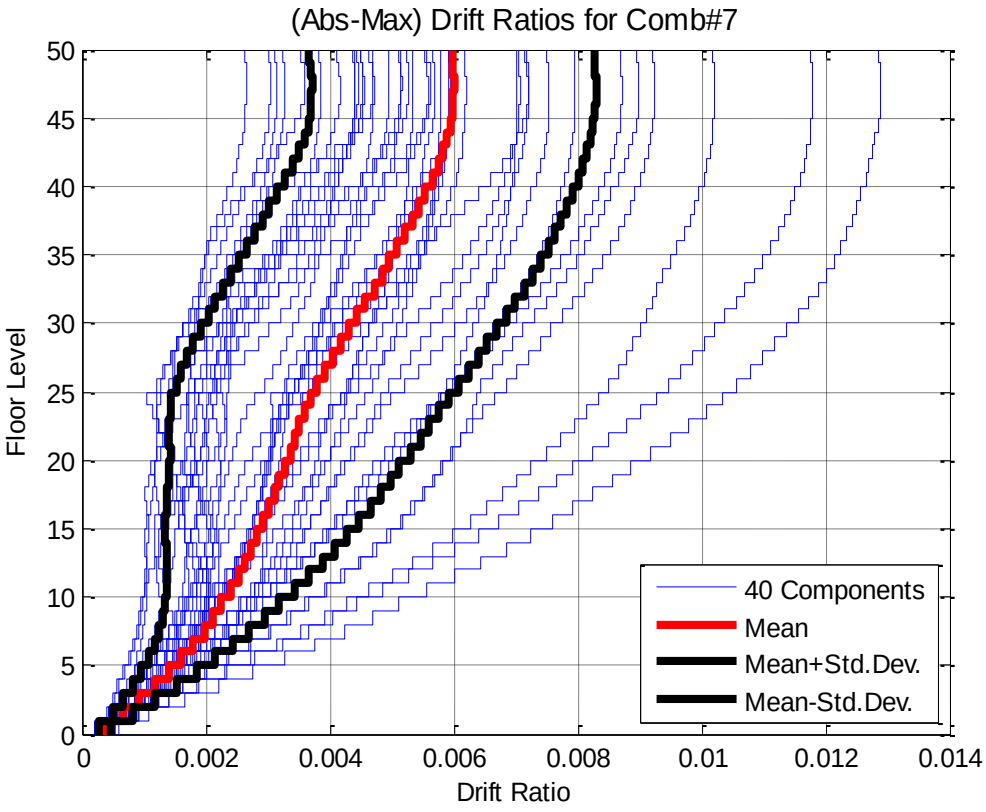

Figure 9.1. Absolute-maximum and mean drift ratios for any combination.

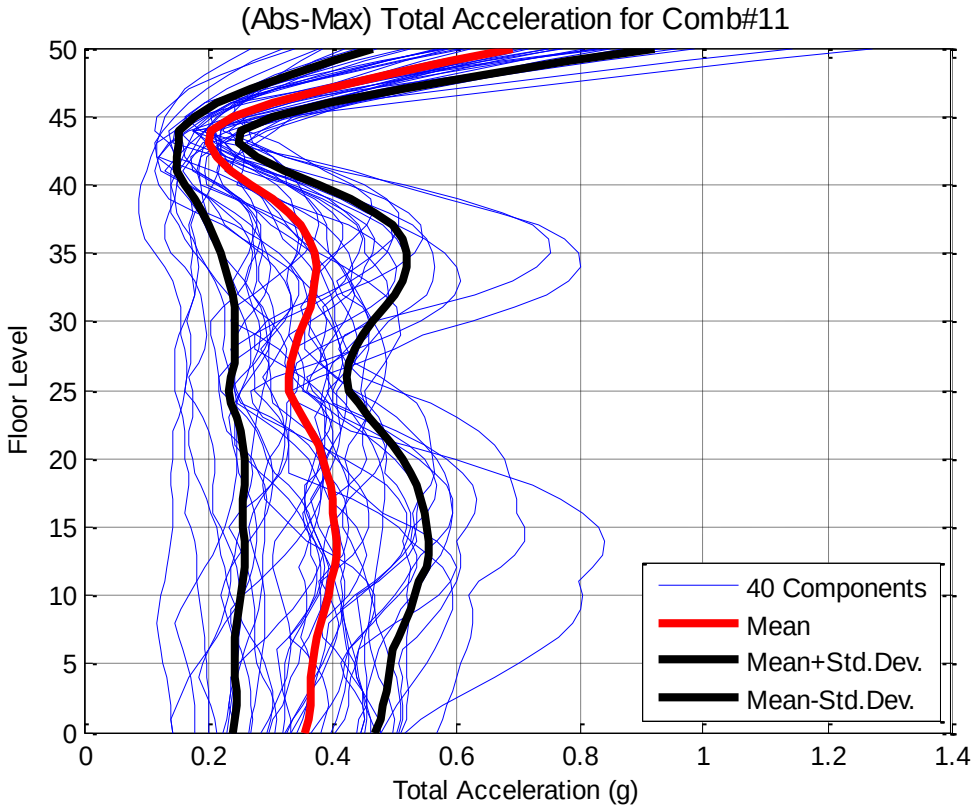

Figure 9.2. Absolute-maximum and mean total acceleration response for any combination.

According to regulations in LATBSDC consensus document [12], damping ratio is taken as 2.5% for all analysis unless otherwise specified.

Note that, analysis results in terms of drift and total acceleration in this chapter is mostly essential for non-structural elements. Obviously, drift response is not a good deformation indicator especially for cantilever structures. It is reasonable to give this explanation in order to express this claim that rotations at the nodes will be getting increase towards the higher levels for such cantilever structures. This means that the building will place inclined position without deforming because just the nodes rotate drastically. Drift ratio will look great in magnitude but it does not represent structural deformation well.

Total acceleration response also serves the purpose of anchorage design for non-structural elements in tall buildings. Briefly, it is more reasonable approximation to evaluate the results in terms of non-structural components.

9.1. Comparisons of Damping Properties for Mass Representations with Acceleration Loading

9.1.1. Comb#1 - Comb#3 - Comb#5b Comparison

In this case, different damping representations (ξ=2.5%) are compared for translational lumped mass system with acceleration loading.

9.1.1.1. Drift Ratio Comparison. Figure 9.3 shows drift ratios of lumped mass system for different proportional damping representations. One of these viscous damping properties is well-accepted Rayleigh damping assumption; other two ones indicate extreme cases, namely, mass proportional and stiffness proportional damping representations.

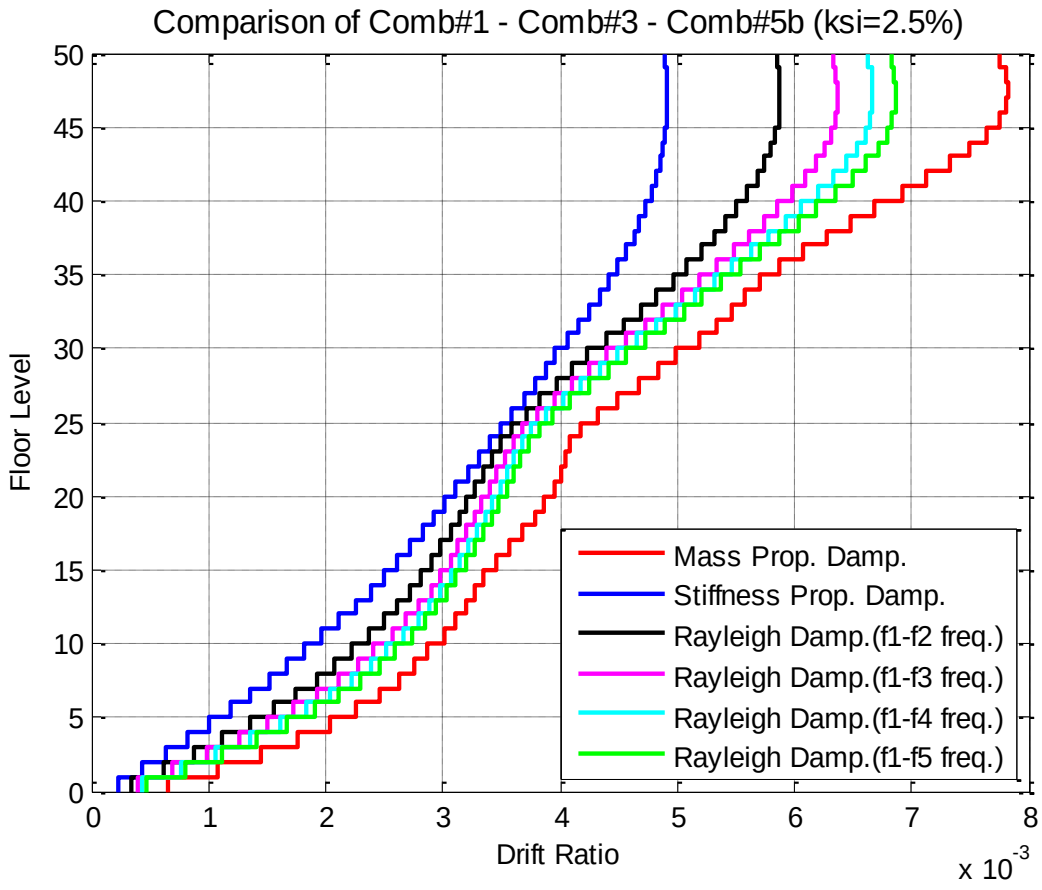

Figure 9.3. Drift ratio comparison Comb#1 – Comb#3 – Comb#5b.

Extreme cases position at two ends while Rayleigh damping representations for different frequencies chosen locate at the middle region of the graph respectively. It is reasonable, if it is thought that Rayleigh damping is somehow proportion with these cases. When the maximum responses of Rayleigh damping with f1-f2 and f1-f5 frequencies are evaluated, ratio of the maximum drift responses is approximately 85%.

9.1.1.2. Total Acceleration Response Comparison. Considering acceleration responses of combinations, identical trend can be observed from Figure 9.4. However, extreme cases look so far from Rayleigh damping cases as compared with drift ratios. When we look at these maximum responses, the ratio between Rayleigh f1-f2 and Rayleigh f1-f5 is approximately 63%. This means that choosing of Rayleigh damping frequencies play crucial role for determination of acceleration response of structure.

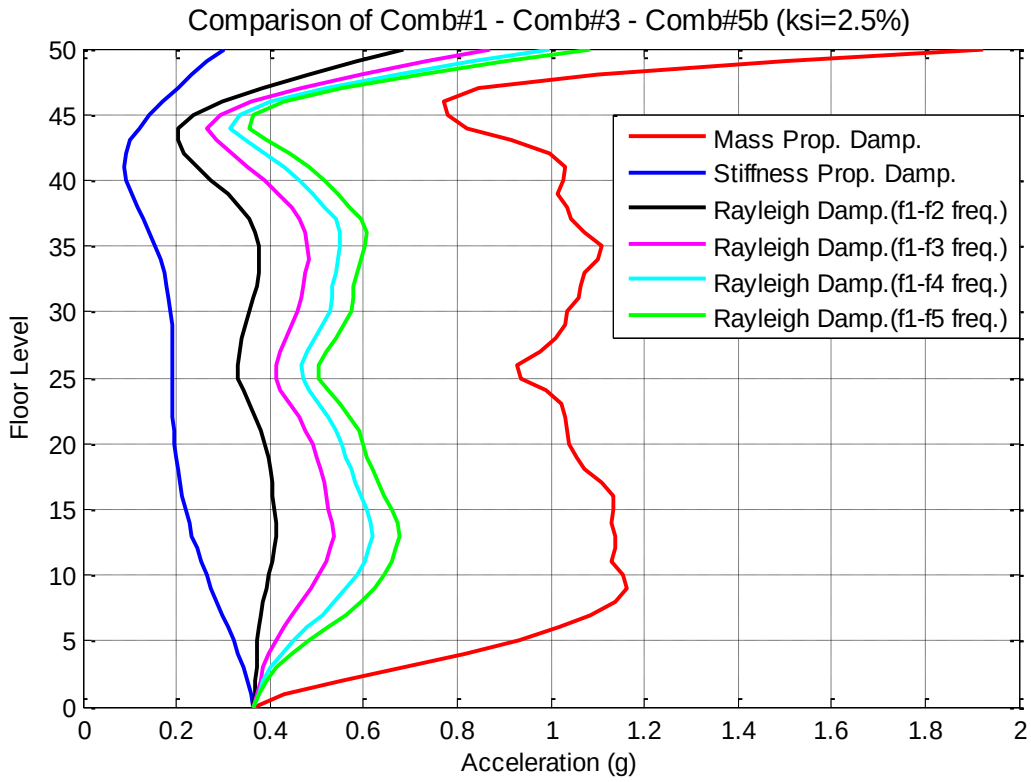

Figure 9.4. Total acceleration response comparison Comb#1 – Comb#3 – Comb#5b.

9.1.2. Comb#3 - Comb#7 Comparison

In this case, stiffness proportional damping and structural damping (rate-independent) are compared for lumped mass system with acceleration loading.

9.1.2.1. Drift Ratio Comparison. As it is mentioned in Chapter 4, structural damping is also named as complex stiffness damping. It is called like that because actually it is proportional with stiffness of structure and it shifts the phases of displacement amplitudes. Therefore, it is convenient to compare these two cases since the both of them are proportional with stiffness. Ratio of maximum drift ratios for two cases is approximately 82%.

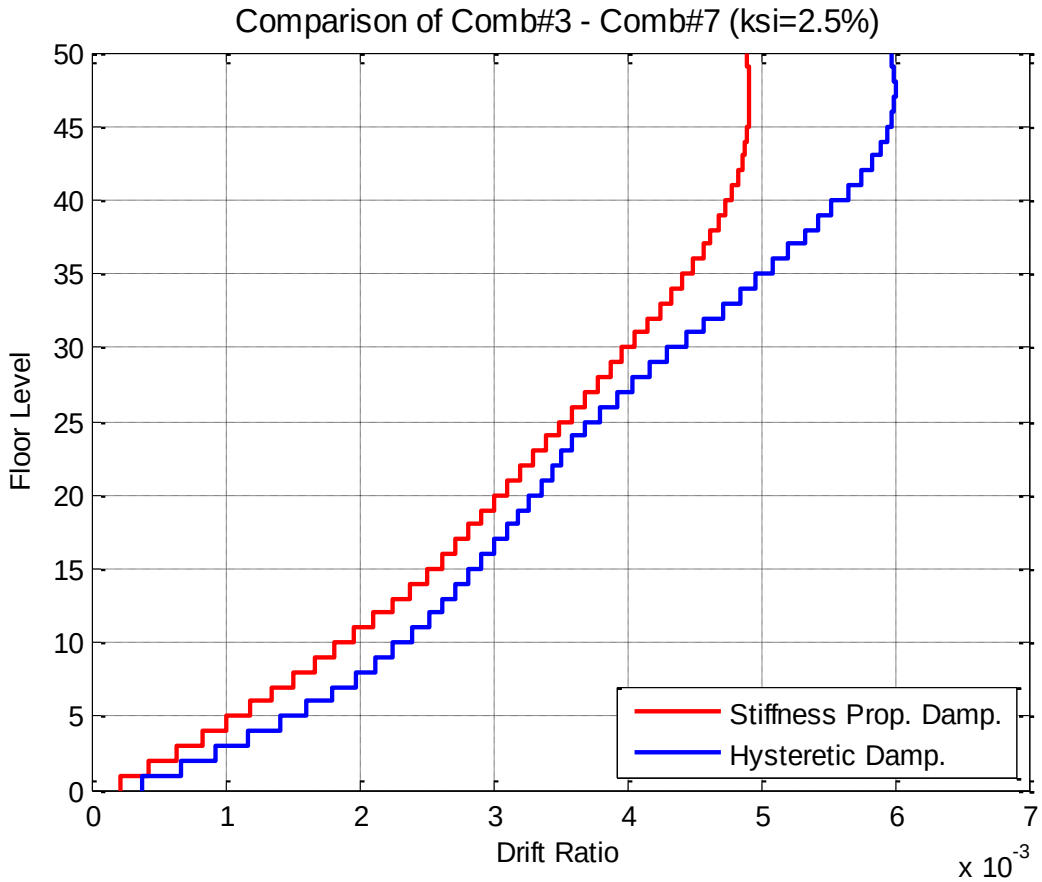

Figure 9.5. Drift ratio comparison Comb#3 – Comb#7.

9.1.2.2. Total Acceleration Response Comparison. Looking through total acceleration responses, drastic change can be observed easily due to just phase shifting. It is a proof that stiffness proportional damping should not be used for such structures.

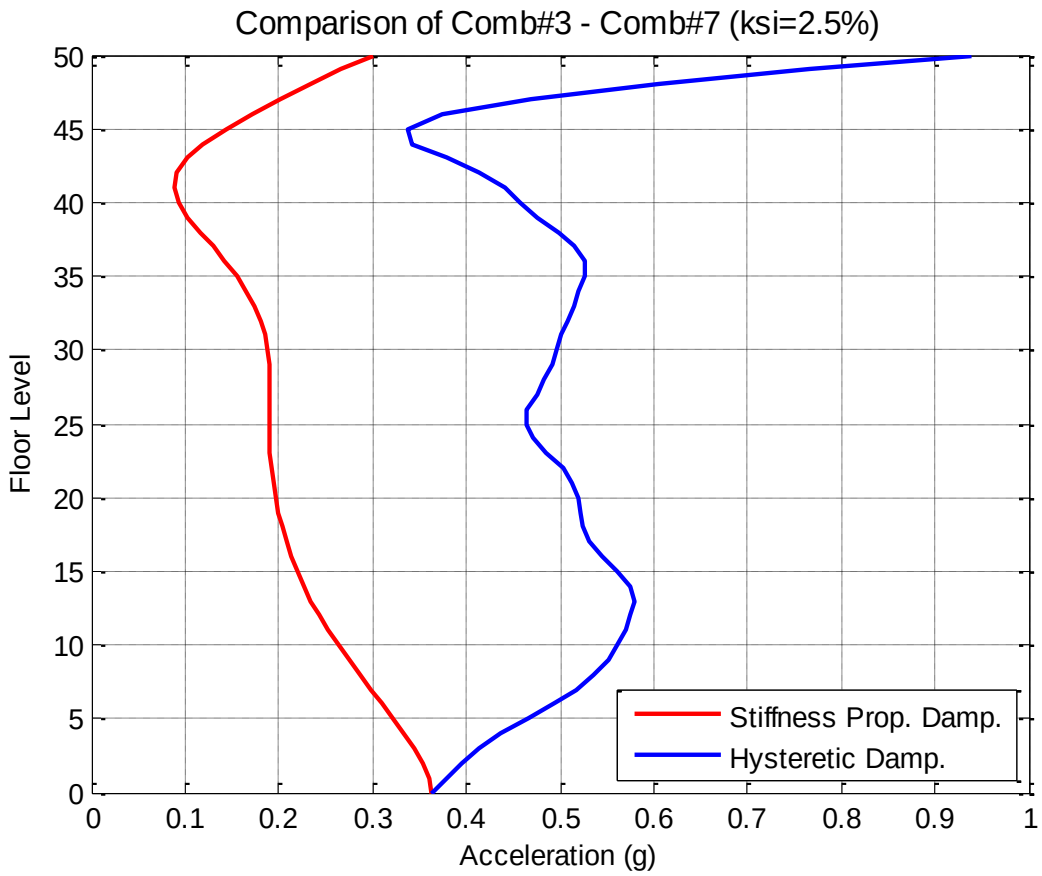

Figure 9.6. Total acceleration response comparison Comb#3 – Comb#7.

9.1.3. Comb#5b - Comb#7 Comparison

In this case, Rayleigh damping for different vibration frequencies and structural damping (rate-independent) are compared for lumped mass system with acceleration loading.

9.1.3.1. Drift Ratio Comparison. Another important comparison for this study, undoubtedly, is this case. It gives an idea about choosing of frequencies for Rayleigh damping. It can be observed from Figure 9.7, choosing of f1-f2 frequencies provides quite good correlation between structural damping.

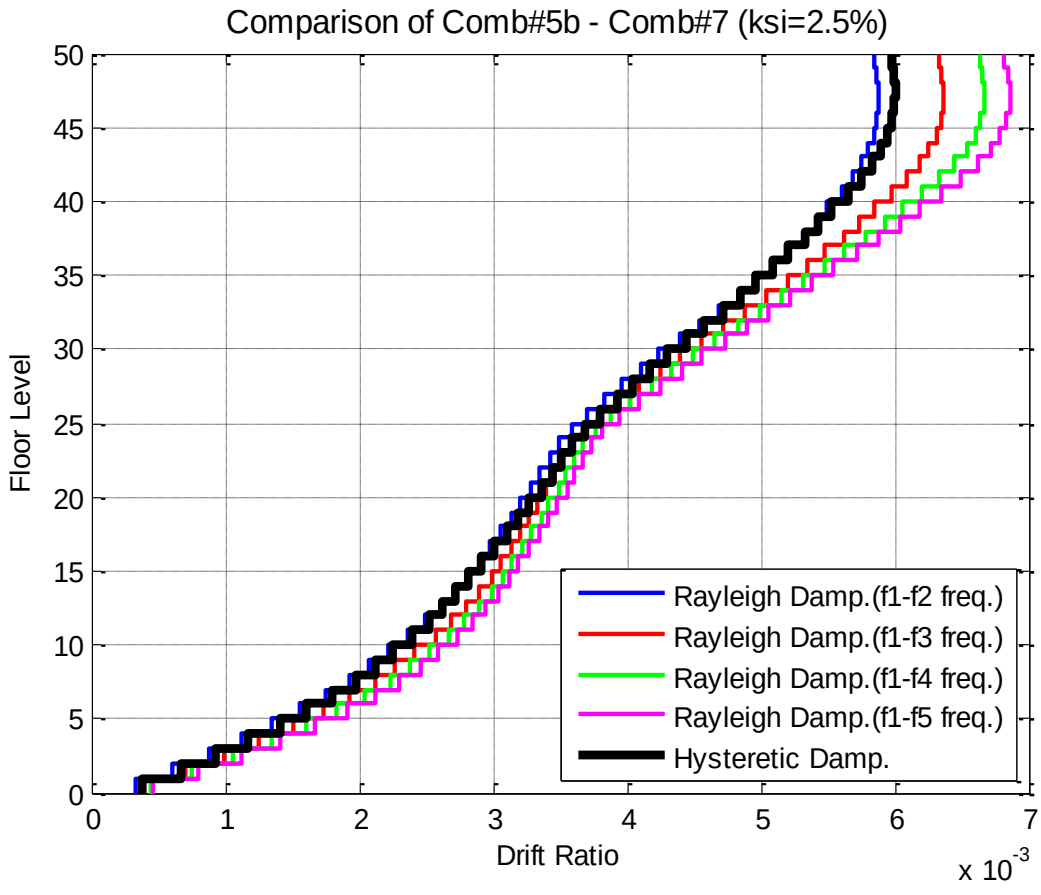

Figure 9.7. Drift ratio comparison Comb#5b – Comb#7.

9.1.3.2. Total Acceleration Response Comparison. Once we look at Figure 9.8, we can see that the same frequencies do not provide good matching with structural damping. Even though it is different for floor levels, for the sake of the security, f1-f4 frequencies should be chosen for Rayleigh damping.

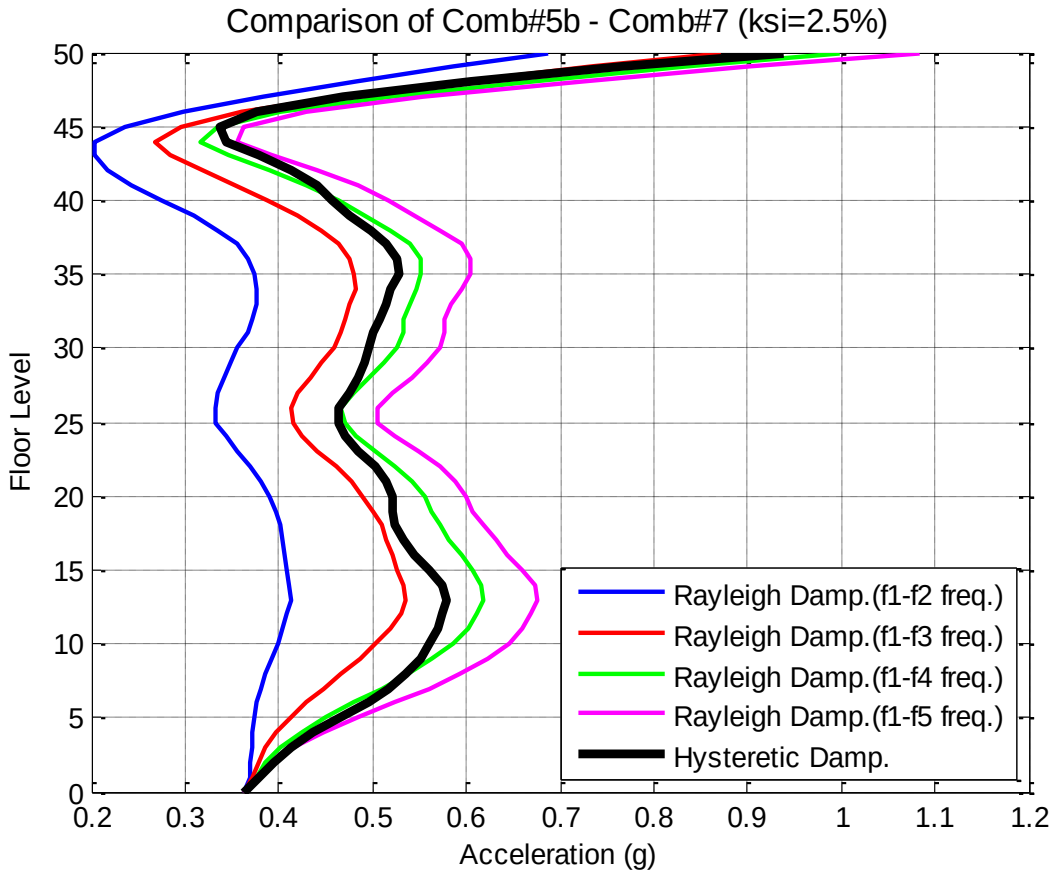

Figure 9.8. Total acceleration response comparison Comb#5b – Comb#7.

9.1.4. Comb#9 - Comb#10 - Comb#11 Comparison

In this case, different damping representations (ξ=2.5%) are compared for consistent mass system with acceleration loading.

9.1.4.1. Drift Ratio Comparison. More or less both the same trend and values are valid for consistent mass system. It will be observed obviously in mass comparisons.

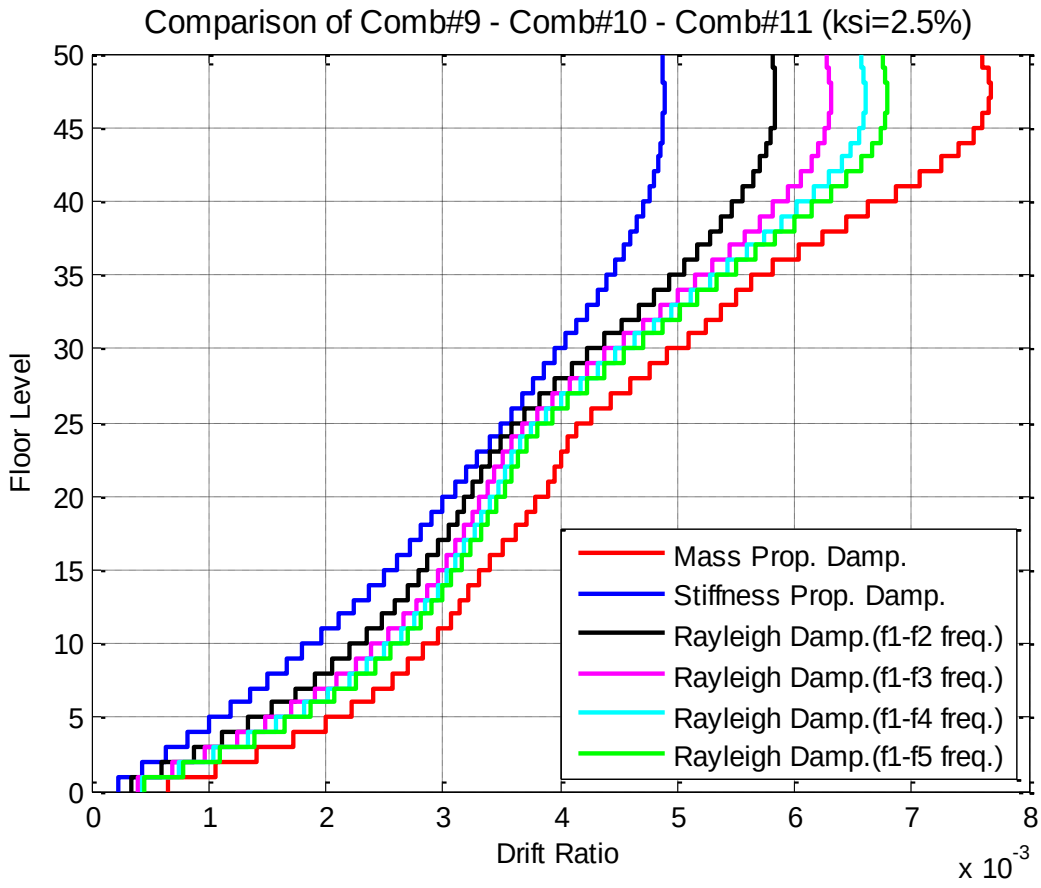

Figure 9.9. Drift ratio comparison Comb#9 – Comb#10 – Comb#11.

9.1.4.2. Total Acceleration Response Comparison. Approaching something from a different standpoint, it can be said that effects of higher modes can be observed from here also. Stiffness proportional damping, as it is mentioned in Chapter 4.2, sweeps away the effects of higher modes (Figure 4.4). Contrarily, mass proportional damping includes effects of higher modes (Figure 4.2). When they are combined, effects of higher modes still attract the attention especially for top levels of the building.

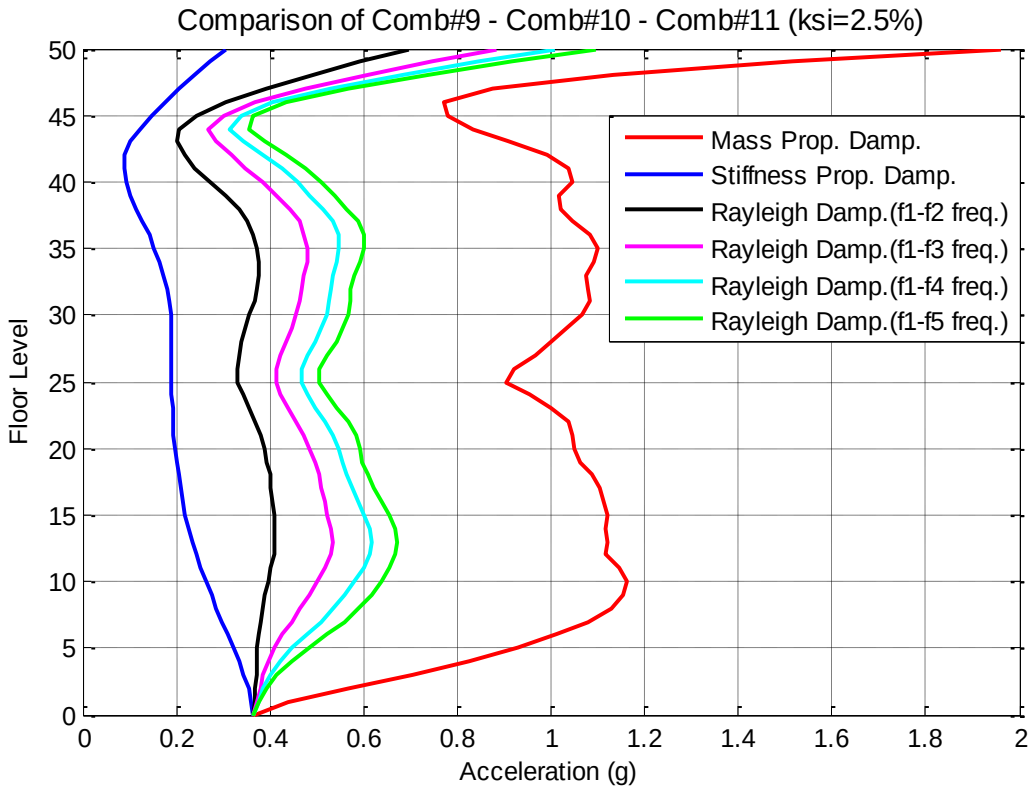

Figure 9.10. Total acceleration response comparison Comb#9 – Comb#10 – Comb#11.

9.1.5. Comb#10 - Comb#12 Comparison

In this case, stiffness proportional damping and structural damping are compared for consistent mass system with acceleration loading.

9.1.5.1. Drift Ratio Comparison. Figure 9.11 shows comparison of stiffness proportional damping cases for consistent mass, which is almost the same with lumped mass system.

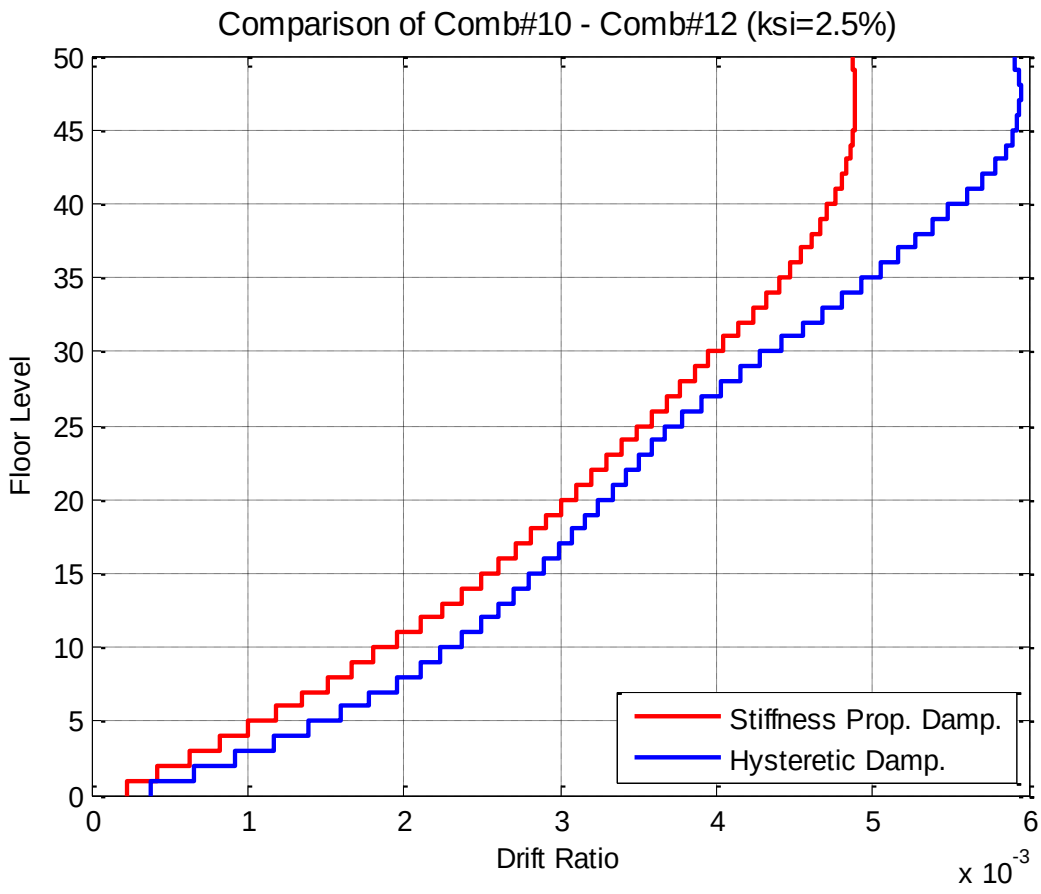

Figure 9.11. Drift ratio comparison Comb#10 – Comb#12.

9.1.5.2. Total Acceleration Response Comparison. As in the case of lumped mass system, drastic change leaps to the eye for consistent mass system as well.

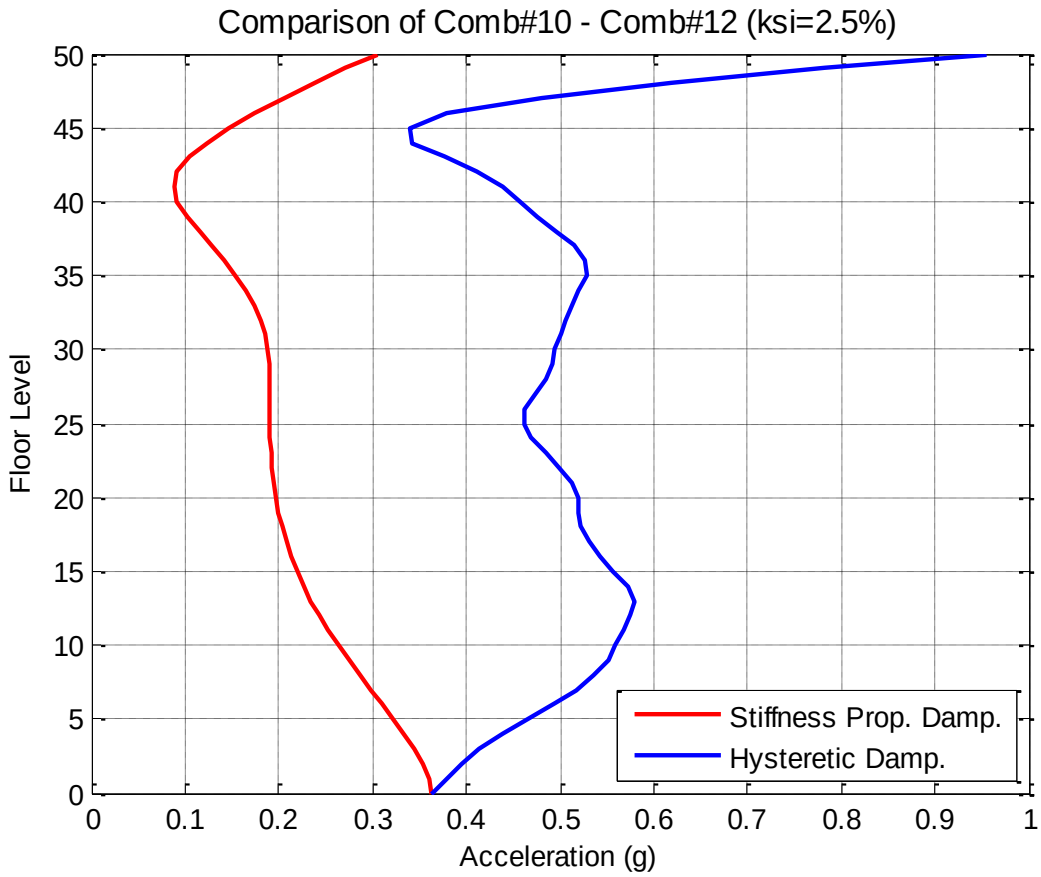

Figure 9.12. Total acceleration response comparison Comb#10 – Comb#12.

9.1.6. Comb#11 - Comb#12 Comparison

In this case, Rayleigh damping for different vibration frequencies and structural damping (rate-independent) are compared for consistent mass system with acceleration loading.

9.1.6.1. Drift Ratio Comparison. At the top level, rate between drift ratios for Rayleigh f1-f2 and structural damping case is 98%. For Rayleigh f1-f2 and structural damping case, the rate is 89%.

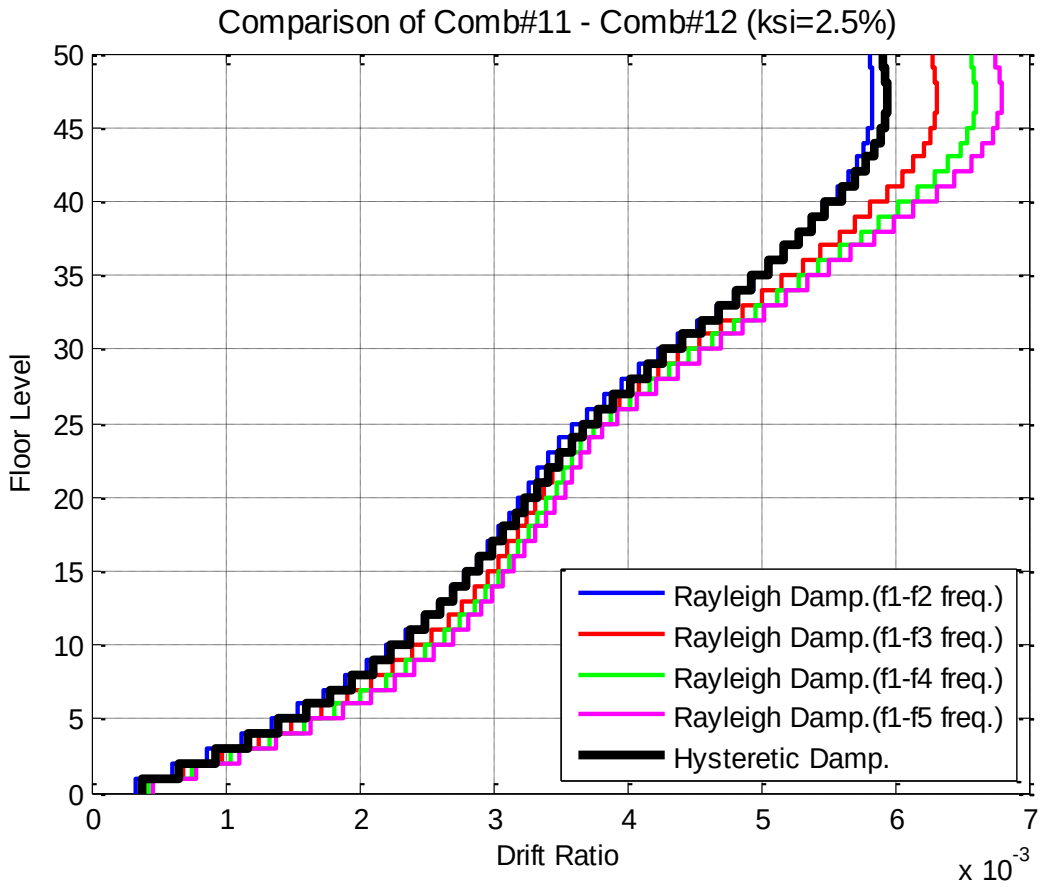

Figure 9.13. Drift ratio comparison Comb#11 – Comb#12.

9.1.6.2. Total Acceleration Response Comparison. Similar behavior both for drift and total acceleration responses are observed from Figure 9.14 and Figure 9.15. At the top level, rate of acceleration response for Rayleigh f1-f2 and structural case 73%. For Rayleigh f1-f4 and structural case, the rate is 95%.

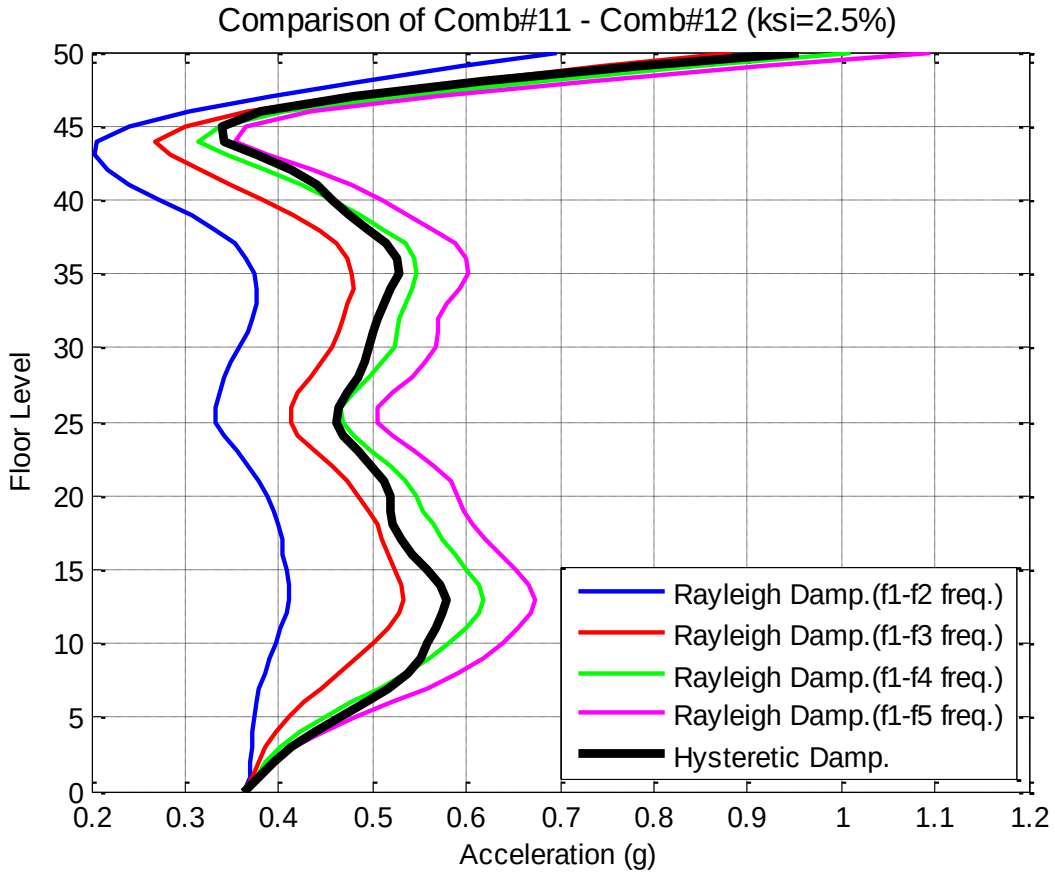

Figure 9.14. Total acceleration response comparison Comb#11 – Comb#12.

9.2. Comparisons of Mass Representations for Damping Properties with Acceleration Loading

9.2.1. Comb#11 - Comb#12 Comparison

In this case, different mass representations are compared for the mass proportional viscous damping (ξ=2.5%) with acceleration loading.

9.2.1.1. Drift Ratio Comparison. As it is seen in Figure 9.15, there is almost no difference between translational lumped mass and translational – rotational lumped mass systems. Consistent mass system slightly differs from the other two systems.

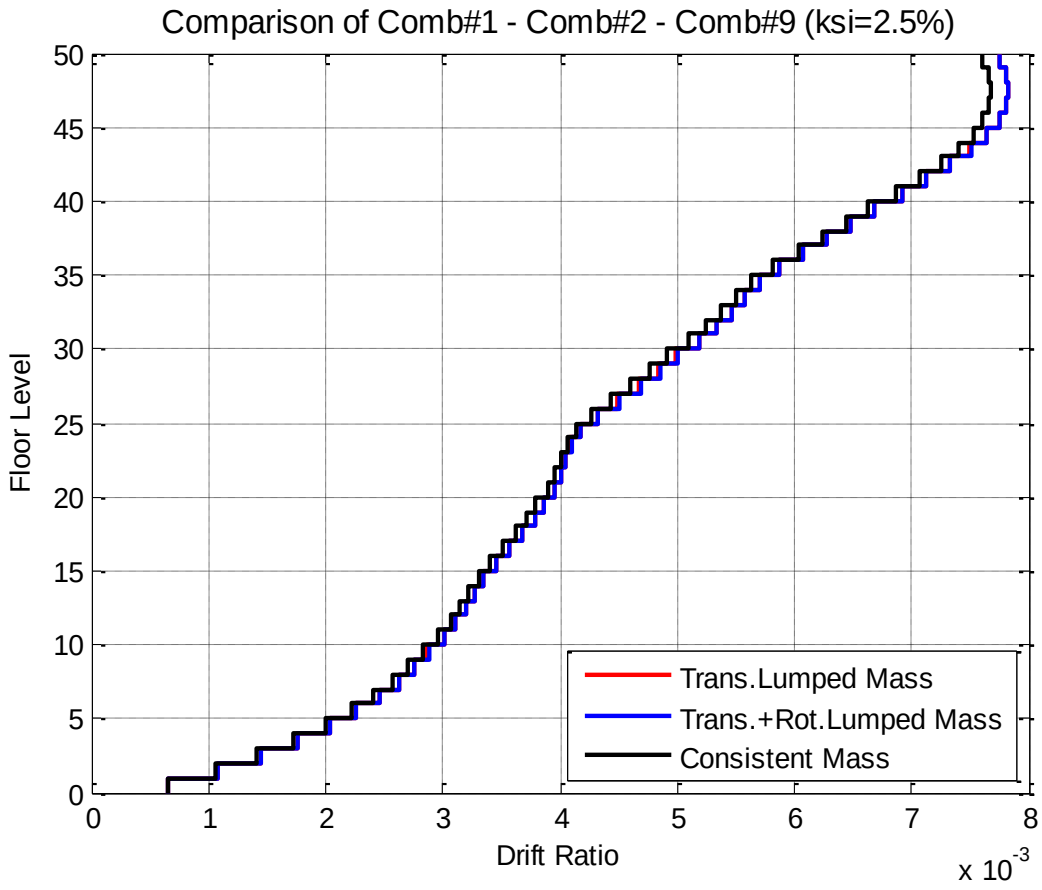

Figure 9.15. Drift ratio comparison of Comb#1 – Comb#2 – Comb#9.

9.2.1.2. Total Acceleration Response Comparison. In terms of total acceleration responses, results are almost in the same way with drift ratios. However, system including rotational lumped mass terms can be seen more apparently as compared with drift ratios but it is so small.

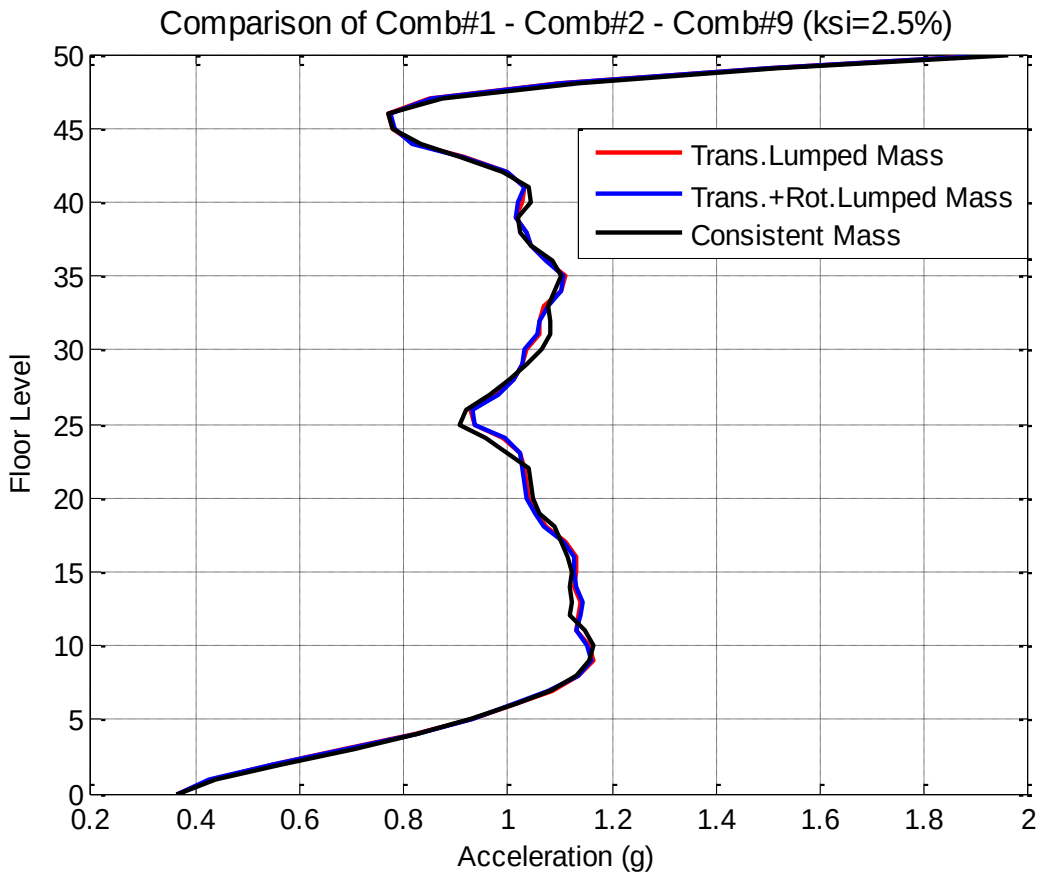

Figure 9.16. Total acceleration response comparison of Comb#1 – Comb#2 – Comb#9.

9.2.2. Comb#3 - Comb#4 - Comb#10 Comparison

In this case, different mass representations are compared for the stiffness proportional viscous damping (ξ=2.5%) with acceleration loading.

9.2.2.1. Drift Ratio Comparison. Consistent mass system slightly differs from the other mass systems in terms of drift ratios again. It can be said that differences for different mass systems, in this case, are less with respect to mass proportional damping system.

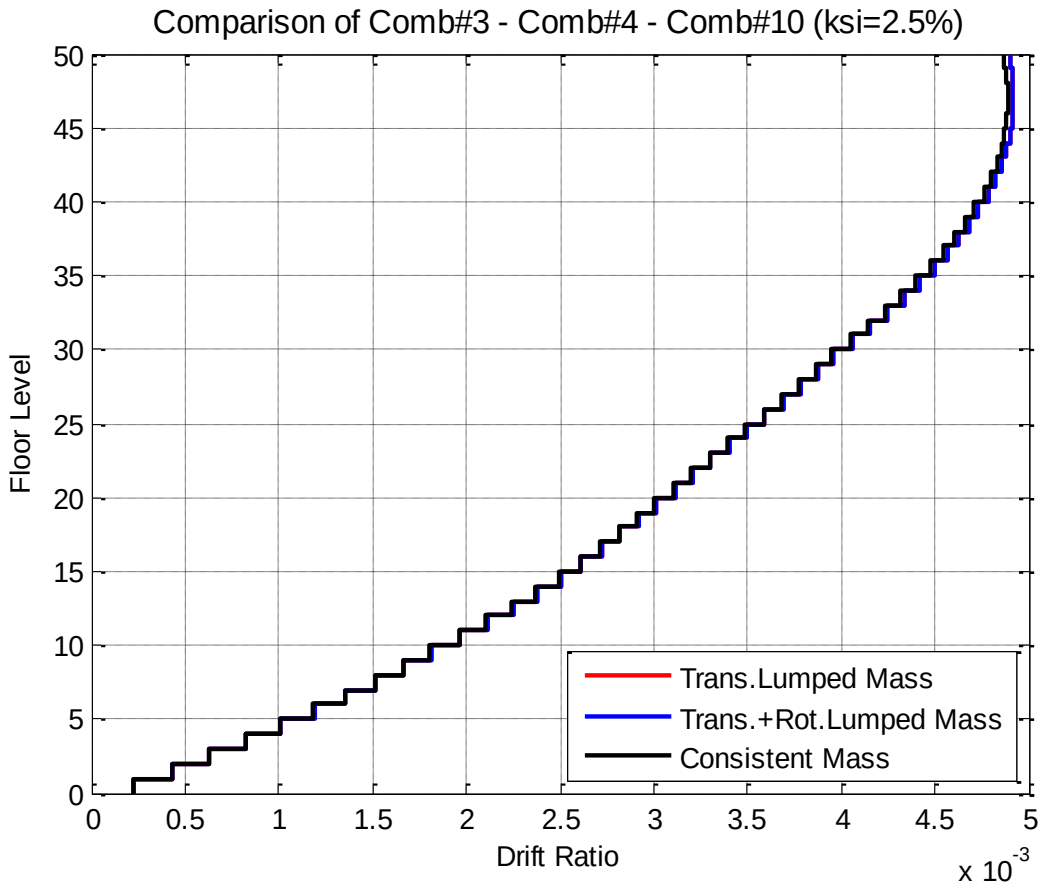

Figure 9.17. Drift ratio comparison Comb#3 – Comb#4 – Comb#10.

9.2.2.2. Total Acceleration Response Comparison. In terms of the acceleration response, this case differs from previous case (mass proportional damping case) in which difference can be observed between the mass systems but it is so small. However, in this case difference is almost zero both in terms of drift ratio and acceleration.

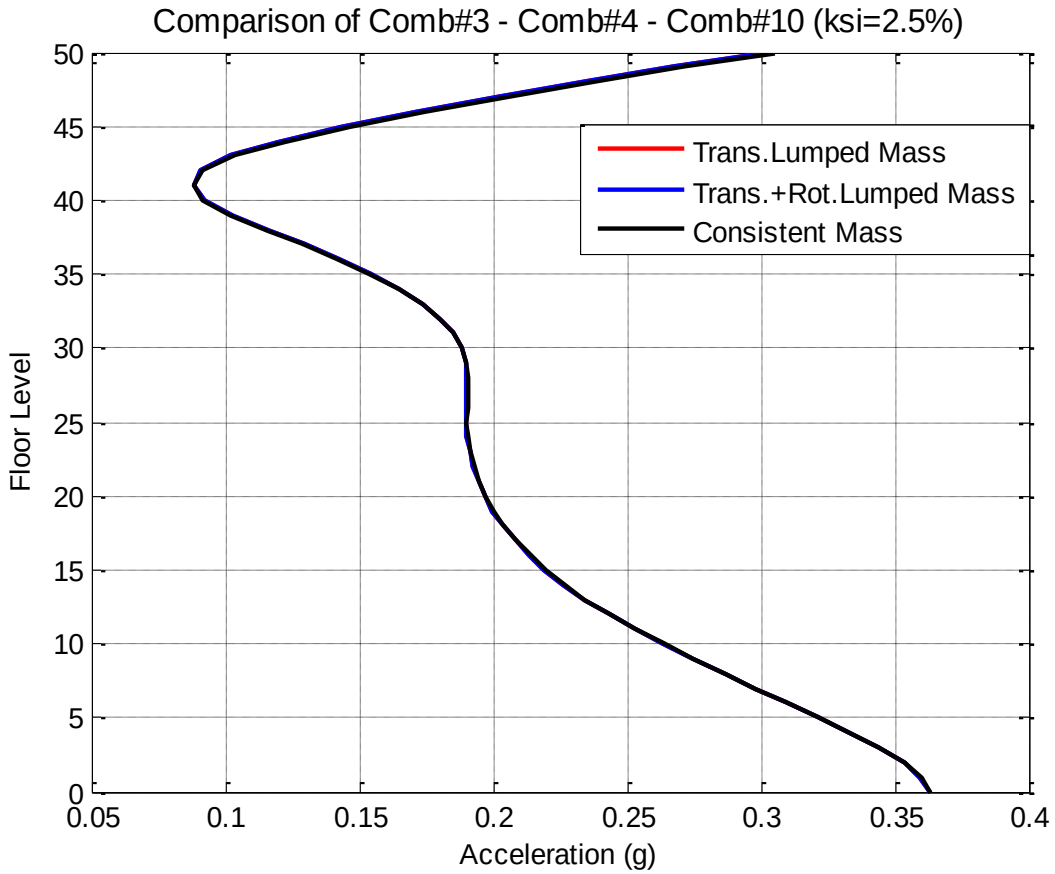

Figure 9.18. Total acceleration response comparison of Comb#3 – Comb#4 – Comb#10.

Due to fact that mass proportional viscous damping system is inversely proportional with natural vibration frequency, damping ratios of higher modes are quite small (Figure 4.1) and vibrations cannot diminish. Therefore, higher mode effects can be realized obviously in such structures rather than those with stiffness proportional damping. This is the reason of why amount of response difference in mass proportional systems is little bit larger than that of stiffness proportional systems. Sure that difference, in terms of drift ratio and acceleration response, between mass proportional and stiffness proportional systems are negligible.

9.2.3. Comb#5b - Comb#6b - Comb#11 Comparison

In this case, different mass representations are compared for mass and stiffness proportional (Rayleigh) viscous damping (ξ=2.5% for different natural vibration frequencies) with acceleration loading.

9.2.3.1. Drift Ratio Comparison. Due to fact that Rayleigh damping case is combination of mass and stiffness proportional damping cases (Figure 4.3), effects of that on different mass systems is based on natural vibration frequencies chosen obviously.

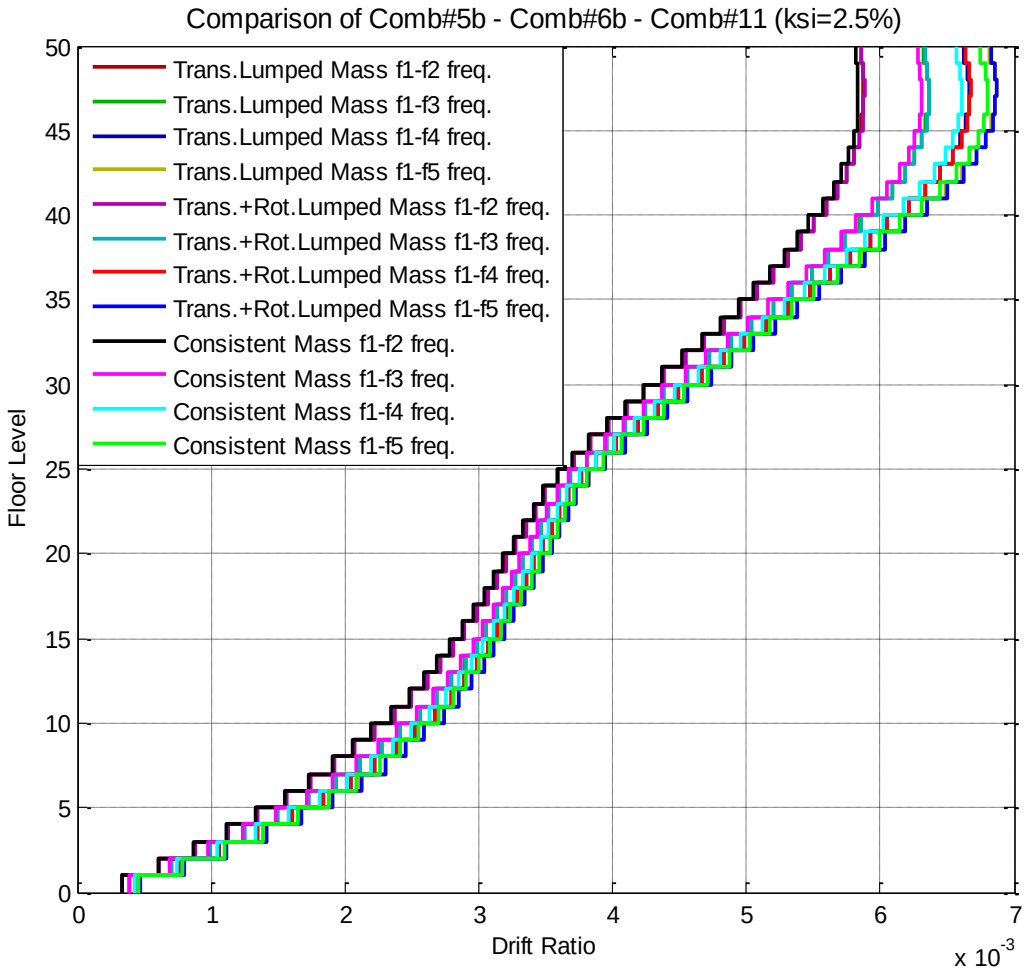

Figure 9.19. Drift ratio comparison Comb#5b – Comb#6b – Comb#11.

9.2.3.2. Total Acceleration Response Comparison. The same reason mentioned in previous discussions, both drift and total acceleration responses are almost the same. It is comprehensible that differences between lumped mass and consistent mass system increases slightly with increasing second frequency chosen for Rayleigh damping.

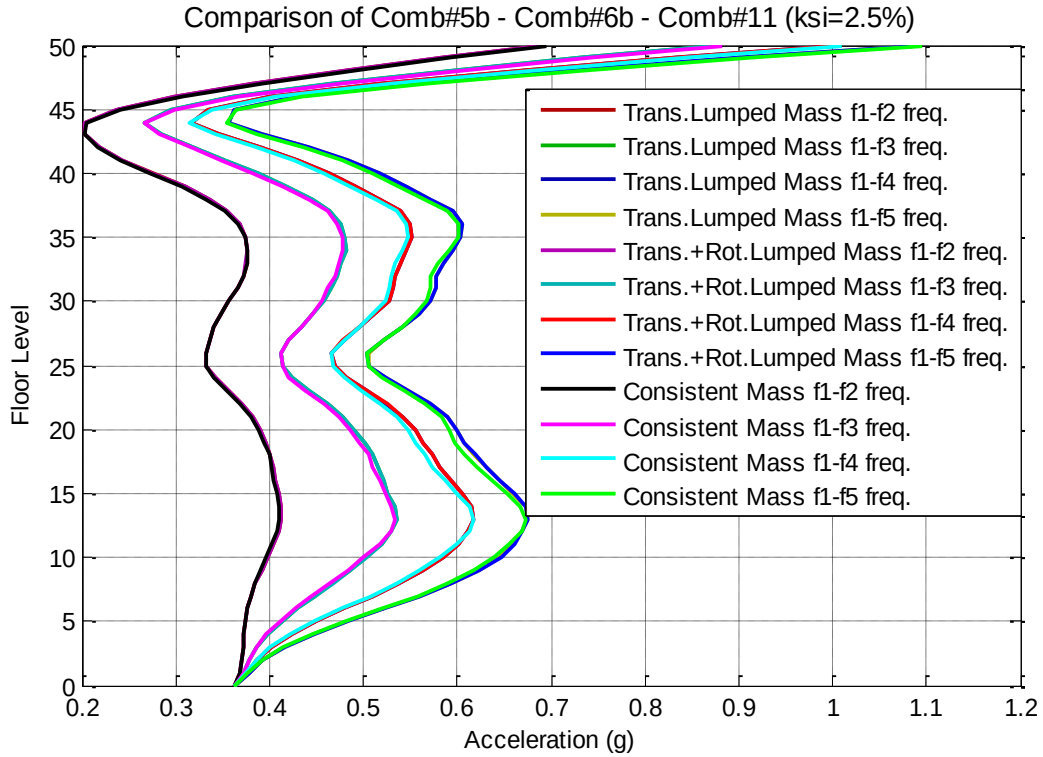

Figure 9.20. Total acceleration response comparison of Comb#5b – Comb#6b – Comb#11.

9.2.4. Comb#7 - Comb#8 - Comb#12 Comparison

In this case, different mass representations are compared for structural (rate-independent) damping with acceleration loading.

9.2.4.1. Drift Ratio Comparison.

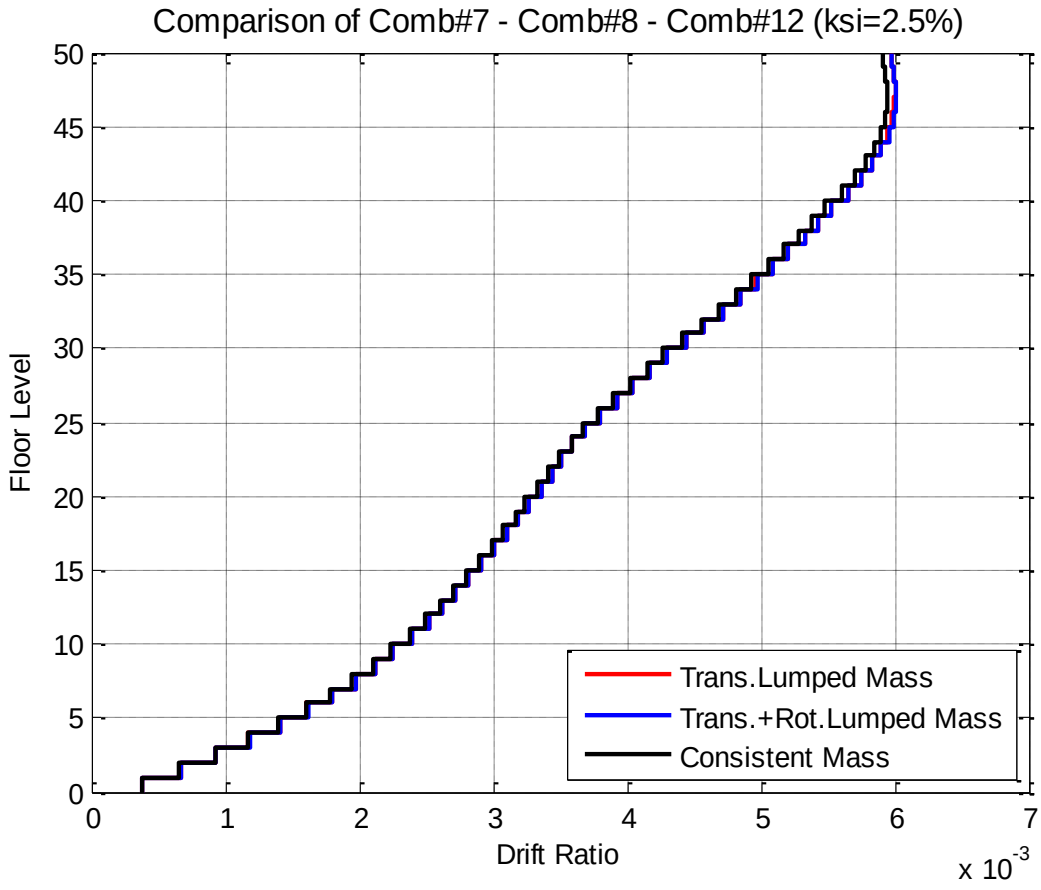

Figure 9.21. Drift ratio comparison Comb#7 – Comb#8 – Comb#12.

9.2.4.2. Total Acceleration Response Comparison. Structural damping case gives similar results in terms of differences between different mass systems to Rayleigh damping case.

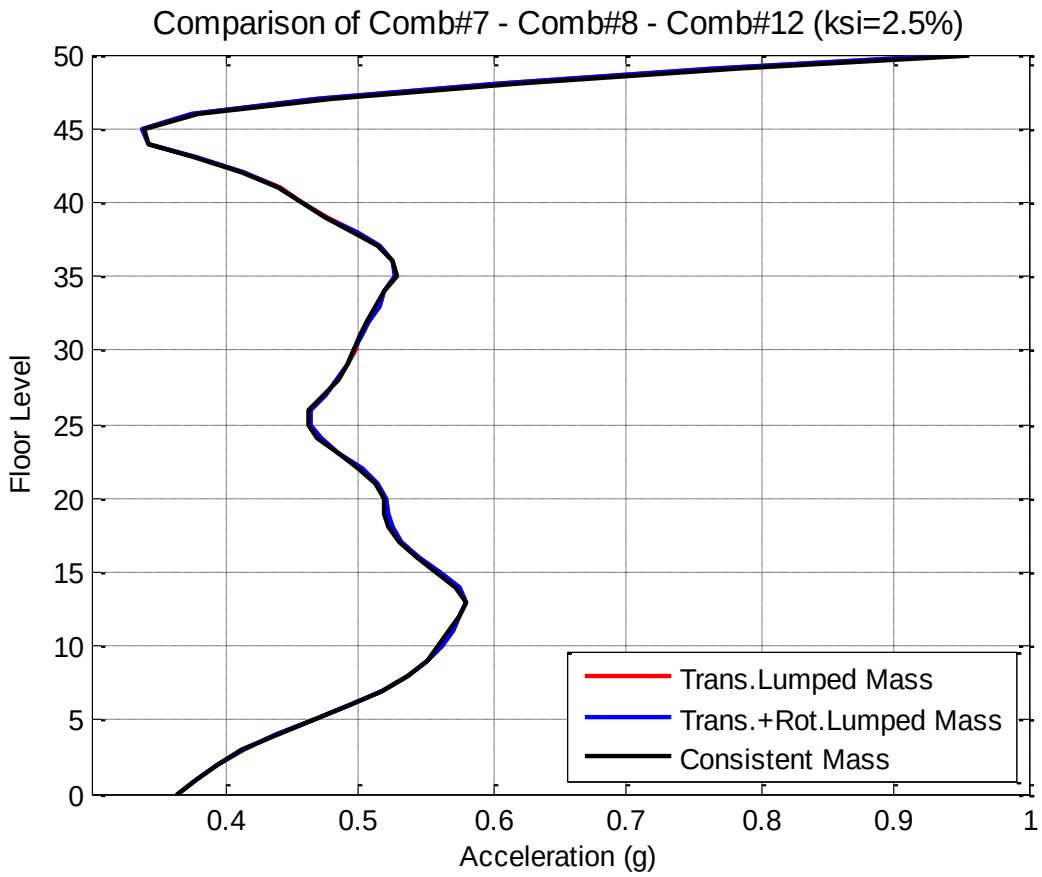

Figure 9.22. Total acceleration response comparison Comb#7 – Comb#8 – Comb#12.

9.3. Comparisons of Seismic Loading Representations for Mass and Damping Representations

9.3.1. Comb#1 - Comb#13 Comparison for ξ=2.5%

In this case, different seismic loading representations (ξ=2.5%) are compared for translational lumped mass system and mass proportional viscous damping.

9.3.1.1. Drift Ratio Comparison. One of the most expected case, undoubtedly, is acceleration and displacement loading case. Figure 9.23 shows that there is no difference between them.

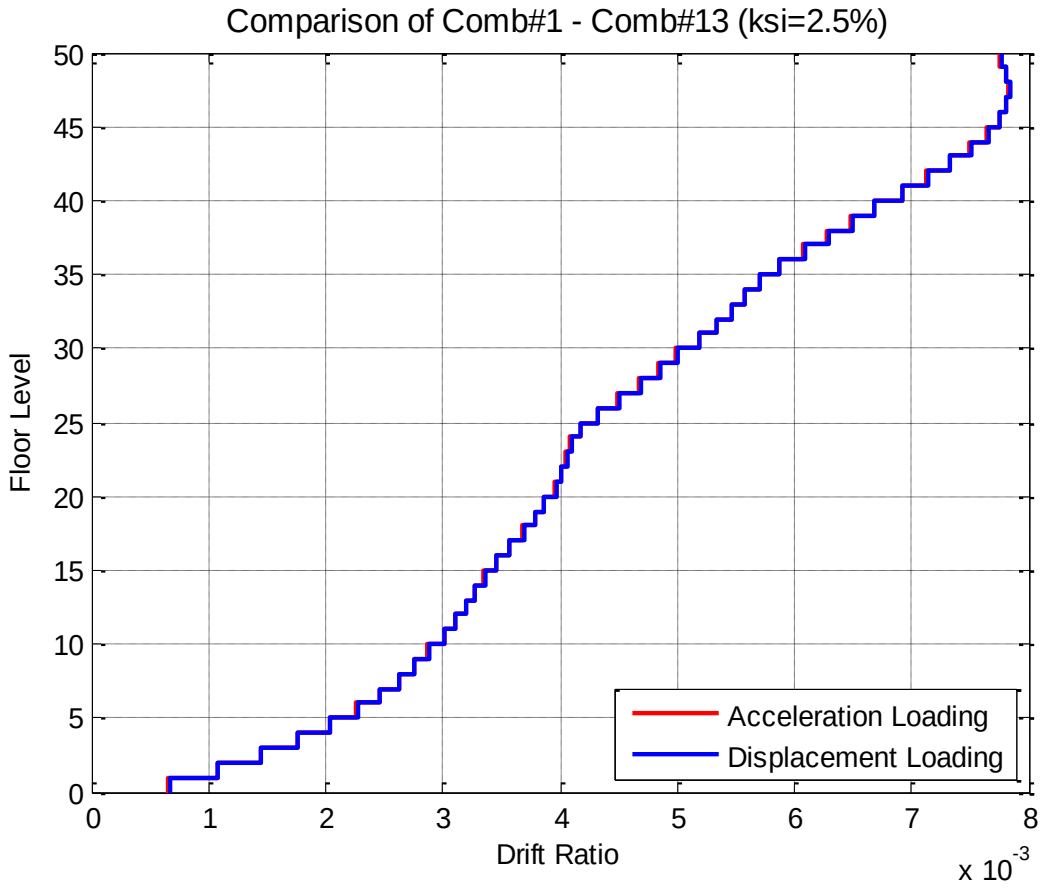

Figure 9.23. Drift ratio comparison Comb#1 – Comb#13.

9.3.1.2. Total Acceleration Response Comparison. Calculations of wave velocity via displacement loading formulation, it is said that this result is reasonable because wave velocity is approximately 1000 m/s. This major value indicates that wave completes its travel throughout the building so fast. It supports the lying idea of pseudo static transmission.

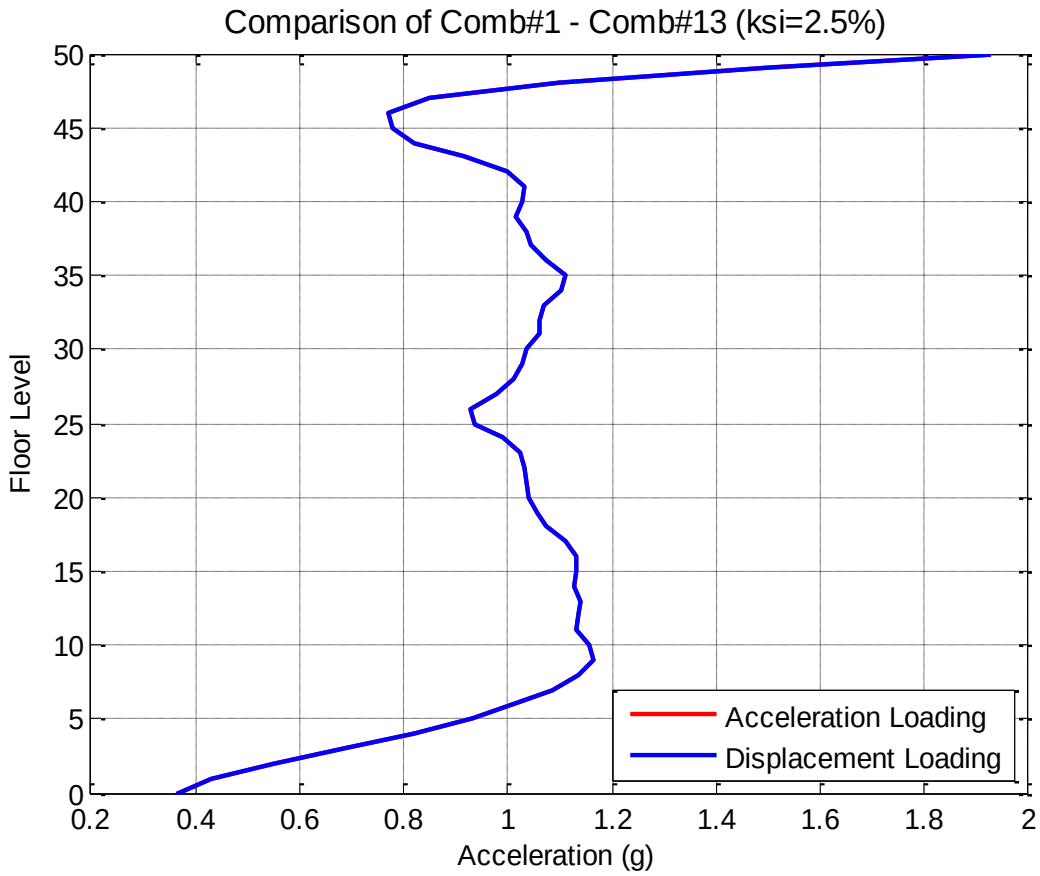

Figure 9.24. Total acceleration response comparison Comb#1 – Comb#13.

9.3.2. Comb#12 - Comb#24 Comparison for ξ=2.5%

In this case, different seismic loading representations (ξ=2.5%) are compared for consistent mass system and structural damping.

9.3.2.1. Drift Ratio Comparison.

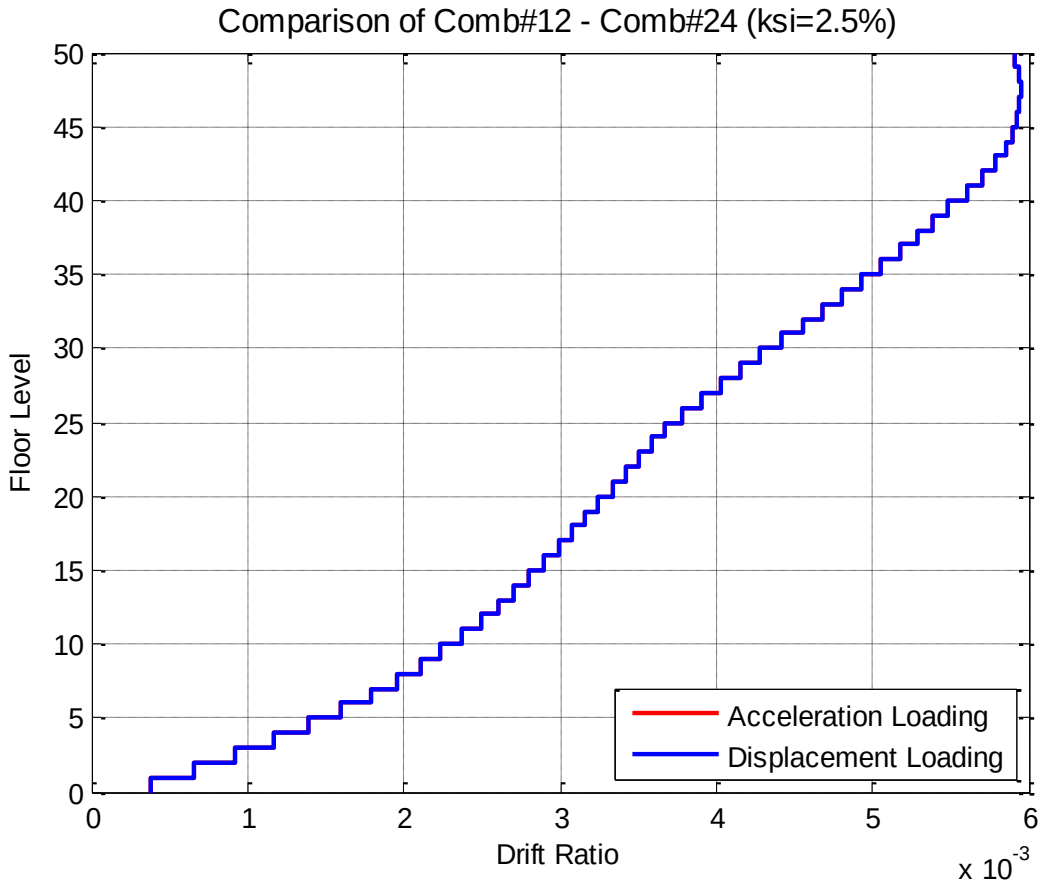

Figure 9.25. Drift ratio comparison Comb#12 – Comb#24.

9.3.2.2. Total Acceleration Response Comparison. For structural damping case, situation is the same for both total acceleration and displacement loading.

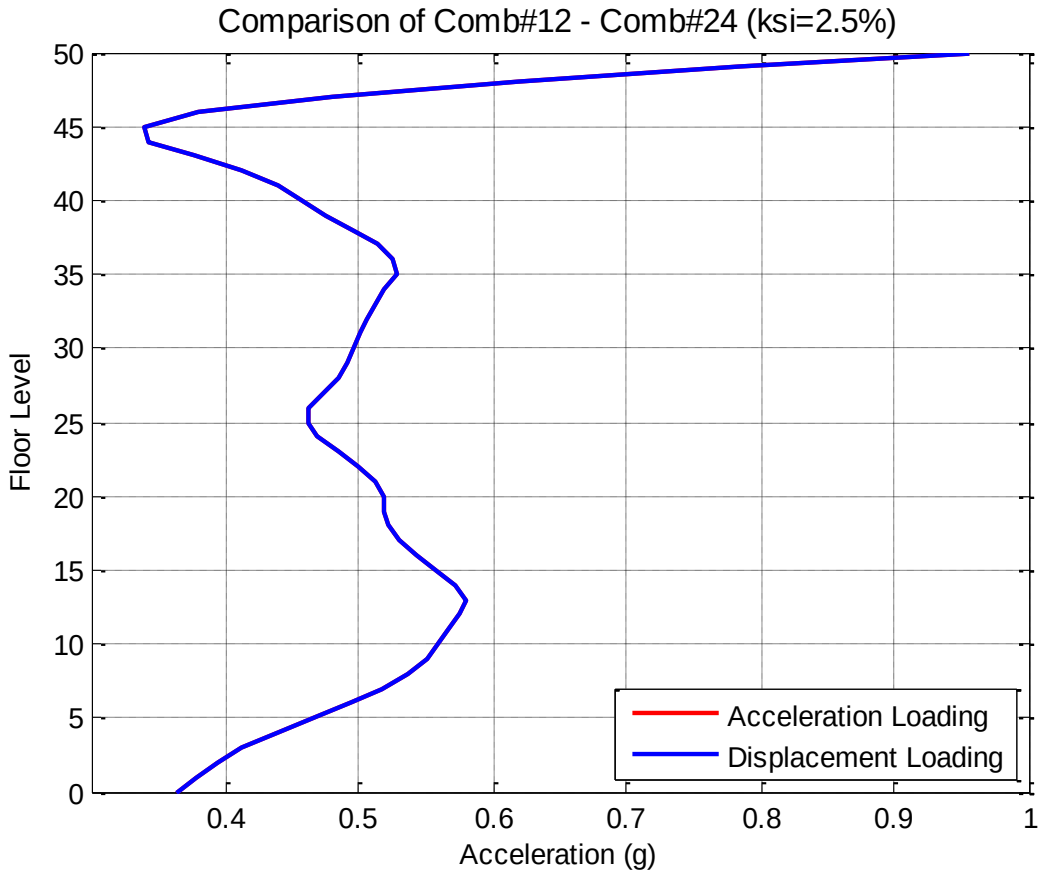

Figure 9.26. Total acceleration response comparison Comb#12 – Comb#24.

9.4. Effects of Different Damping Ratios on Mass Representations

In this case, effects of different damping ratios on the systems with different mass representations are investigated. Since the translational and rotational lumped mass system do not make difference with respect to ordinary translational lumped mass system, it is not incorporated into the comparisons herein.

9.4.1. Comb#1 - Comb#9 Comparison for ξ=1%, 2.5%, 5%

Effects of different (ξ=1%, ξ=2.5%, ξ=5%) damping ratios on the systems for different mass representations, in the case of mass proportional viscous damping with acceleration loading, are compared.

9.4.1.1. Drift Ratio Comparison.

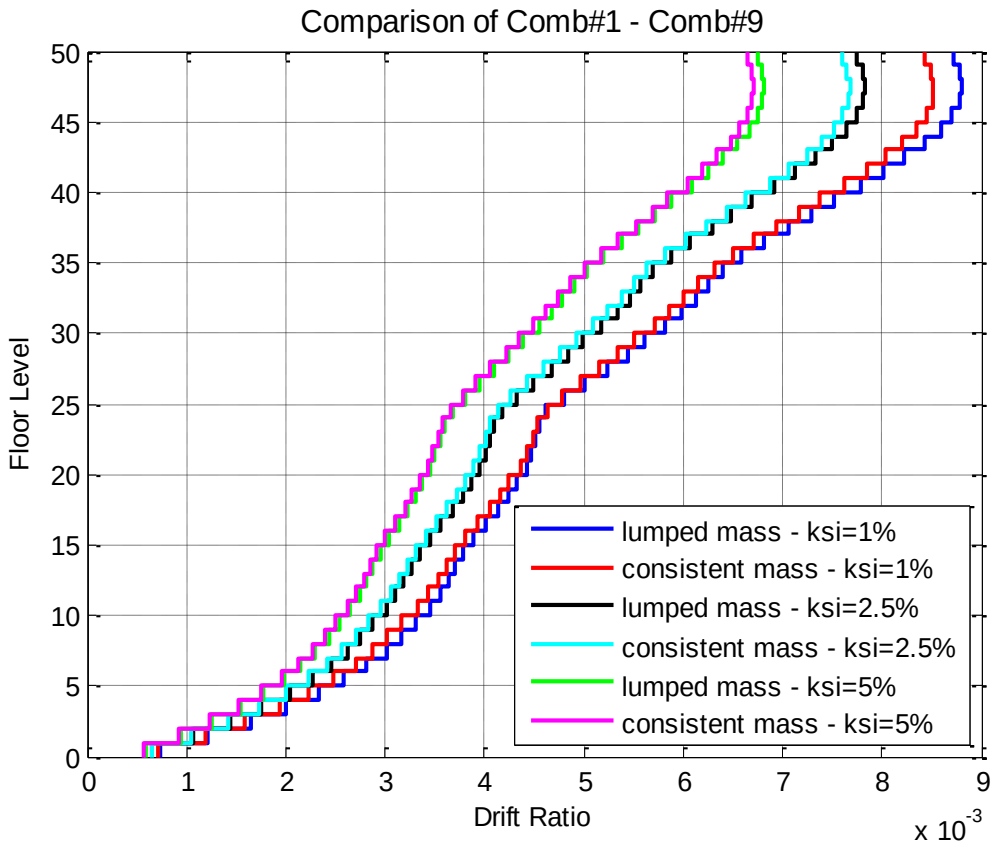

Figure 9.27. Drift ratio comparison Comb#1 – Comb#9.

9.4.1.2. Total Acceleration Response Comparison. Indisputably, small damping ratios generates higher response, and changing of damping ratios makes difference slightly between different mass systems for both drift and total acceleration responses. Rate of maximum responses between lumped mass and consistent mass system for both acceleration and drift is approximately 97%.

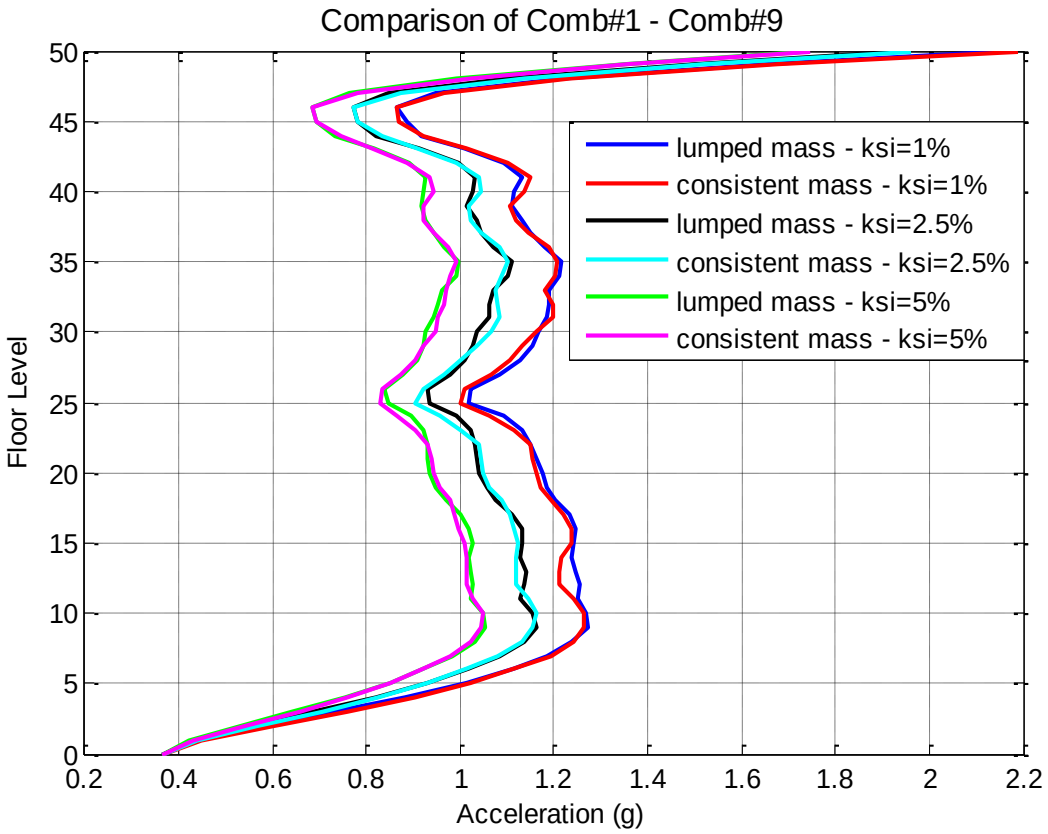

Figure 9.28. Total acceleration response comparison Comb#1 – Comb#9 (ξ=1%, ξ=2.5%, ξ=5%).

9.4.2. Comb#3 - Comb#10 Comparison for ξ=1%, 2.5%, 5%

Effects of different (ξ=1%, ξ=2.5%, ξ=5%) damping ratios on the systems for different mass representations in the case of stiffness proportional viscous damping with acceleration loading.

9.4.2.1. Drift Ratio Comparison.

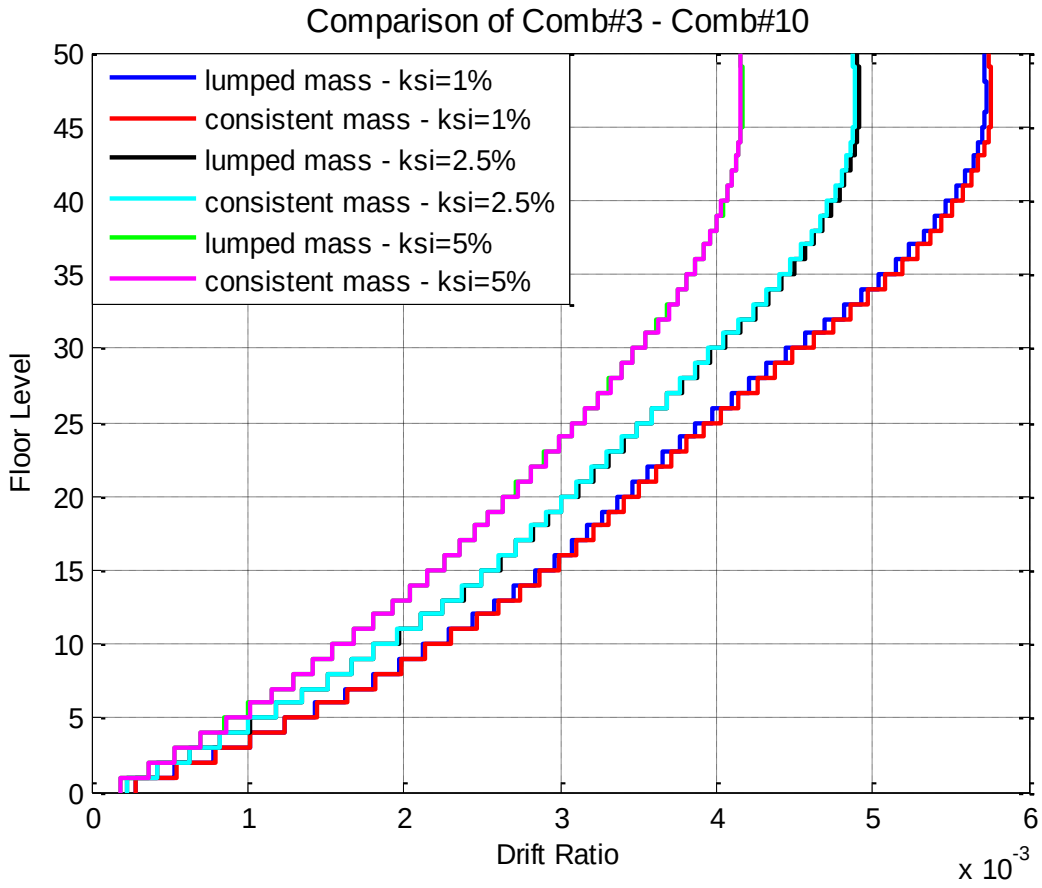

Figure 9.29. Drift ratio comparison Comb#3 – Comb#10 (ξ=1%, ξ=2.5%, ξ=5%).

9.4.2.2. Total Acceleration Response Comparison. Figure 9.29 and Figure 9.30 shows that difference between both total acceleration and drift responses are almost zero. Again, it is not possible to capture difference for stiffness proportional damping system.

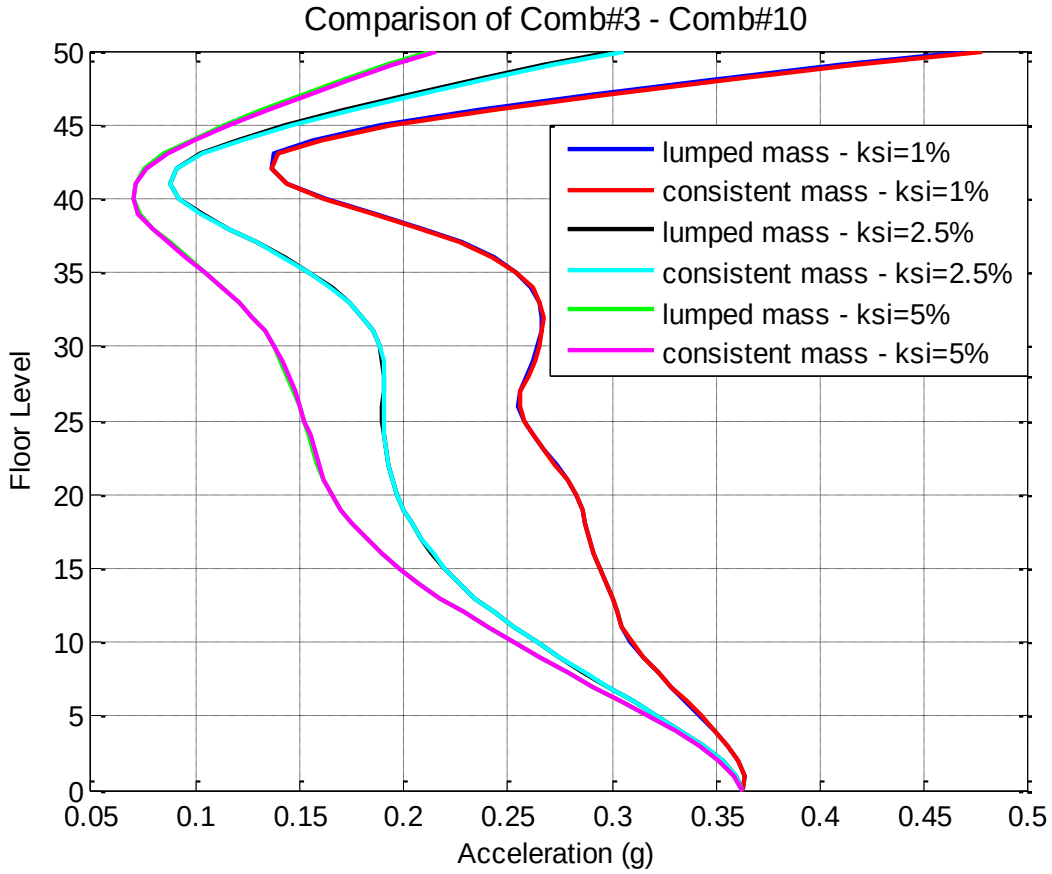

Figure 9.30. Total acceleration response comparison Comb#3 – Comb#10 (ξ=1%, ξ=2.5%, ξ=5%).

9.4.3. Comb#7 - Comb#12 Comparison for ξ=1%, 2.5%, 5%

Effects of different (ξ=1%, ξ=2.5%, ξ=5%) damping ratios on the systems for different mass representations in the case of structural damping with acceleration loading.

9.4.3.1. Drift Ratio Comparison.

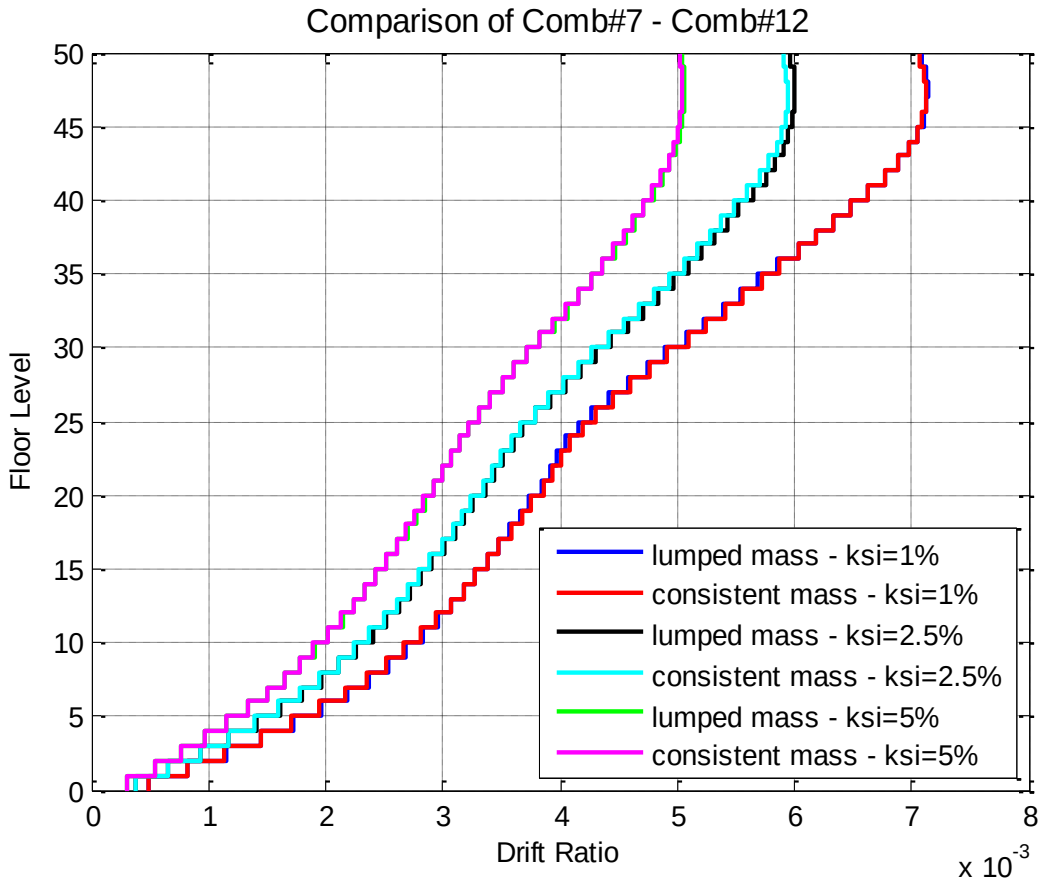

Figure 9.31. Drift ratio comparison Comb#7 – Comb#12 (ξ=1%, ξ=2.5%, ξ=5%).

9.4.3.2. Total Acceleration Response Comparison. The same trend is valid for structural damping case in terms of both drift and total acceleration responses.

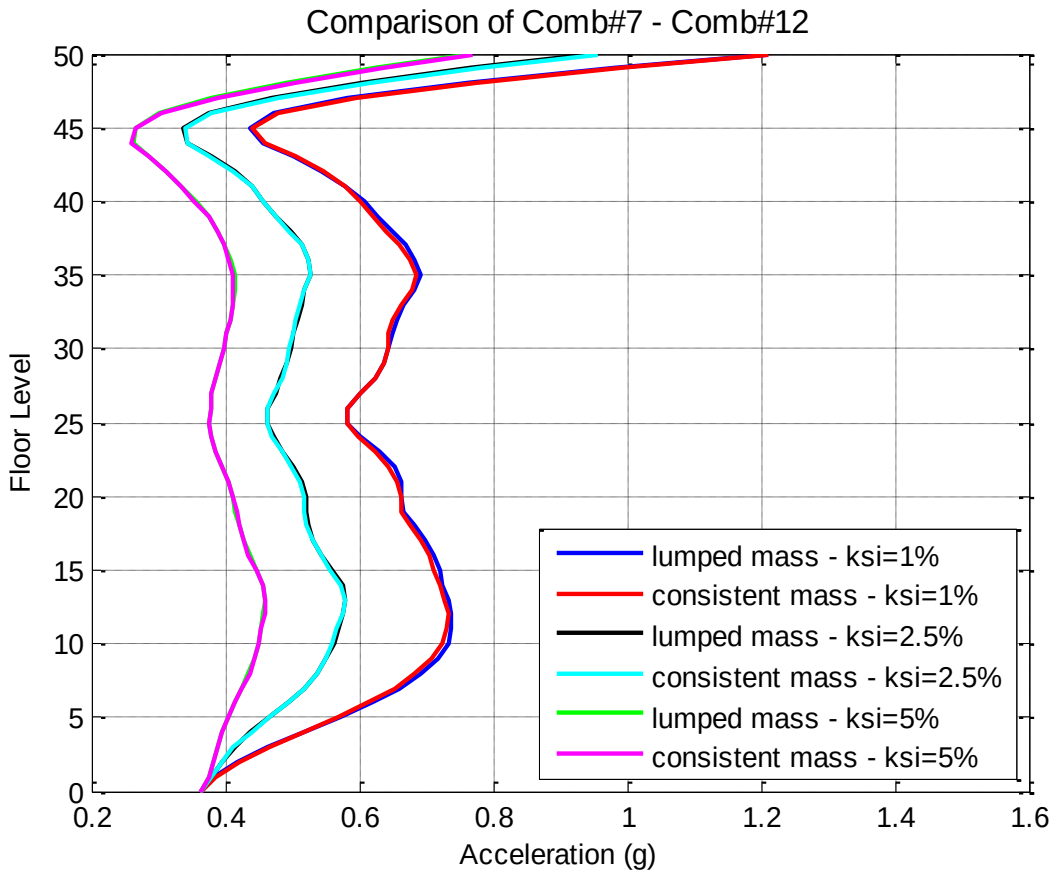

Figure 9.32. Total Acceleration response comparison Comb#7 – Comb#12 (ξ=1%, ξ=2.5%, ξ=5%).

9.5. Effects of Different Damping Ratios on Rayleigh and Structural Damping

9.5.1. Comb#5b - Comb#7 Comparison ξ=1%

In this case, two systems with mass and stiffness proportional (Rayleigh) viscous damping (different natural vibration frequencies are chosen for ξ=1%) and structural (rate-independent) damping are compared for lumped mass system with acceleration loading.

9.5.1.1. Drift Ratio Comparison.

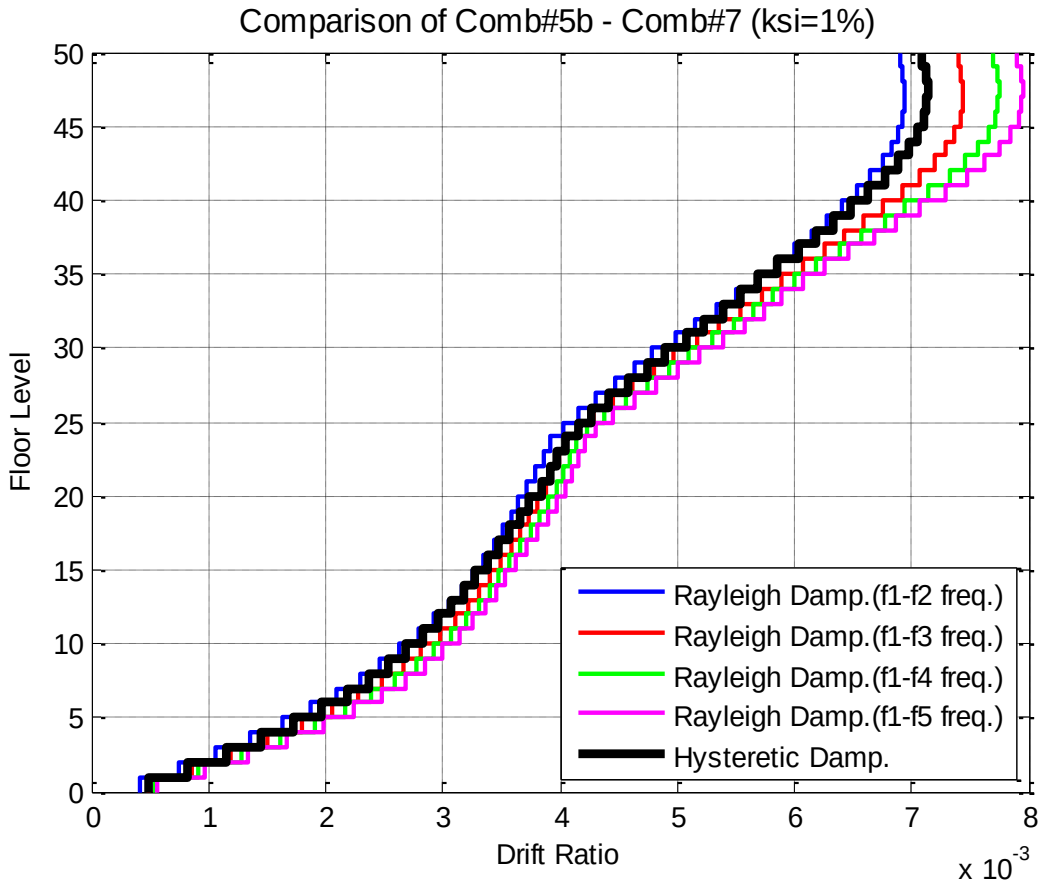

Figure 9.33. Drift ratio comparison Comb#5b – Comb#7 (ξ=1%).

9.5.1.2. Total Acceleration Response Comparison. This is other important comparison giving interesting results about effects of changing damping ratios. Maybe not essential for drift ratios but once it is evaluated in terms of acceleration responses, 1% damping ratio increase the acceleration responses in a remarkable level as compared with 2.5%. Trend of curve represented structural damping is almost matches with Rayleigh f1-f4 frequencies. At the lower levels, let's say until 5th story, structural damping response perfectly matches with Rayleigh f1-f5 frequencies.

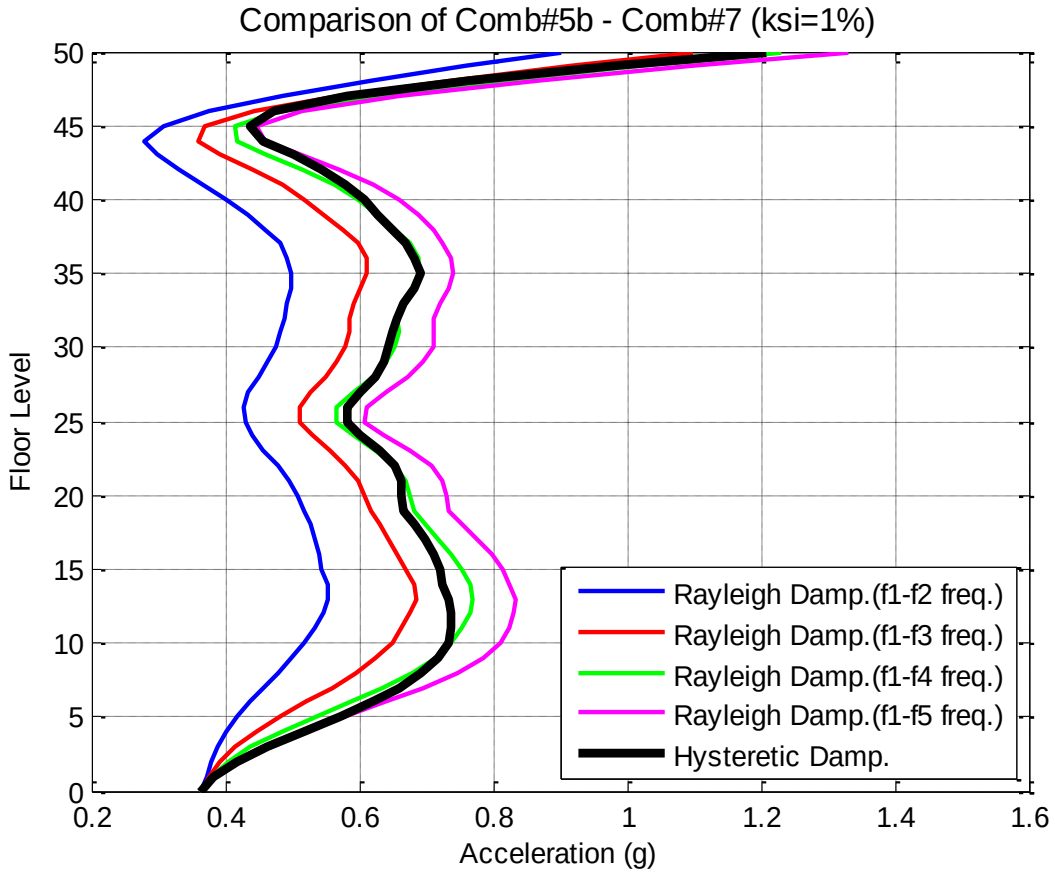

Figure 9.34. Total Acceleration response comparison Comb#5b – Comb#7 (ξ=1%).

When it is considered that regulations in the guidelines associated to tall buildings design procedures, 1% damping ratio is quite reasonable for such structures.

9.5.2. Comb#5b - Comb#7 Comparison ξ=5%

In this case, two systems with mass and stiffness proportional (Rayleigh) viscous damping (ξ=5% for different natural vibration frequencies chosen) and structural (rate-independent) damping are compared for lumped mass system with acceleration loading.

9.5.2.1. Drift Ratio Comparison. Since the bandwidth for drift ratios are quite narrow, changing of damping ratios cannot make much difference. For 5% damping ratio, it is observed that Rayleigh f1-f2 is almost perfectly matches with structural damping case.

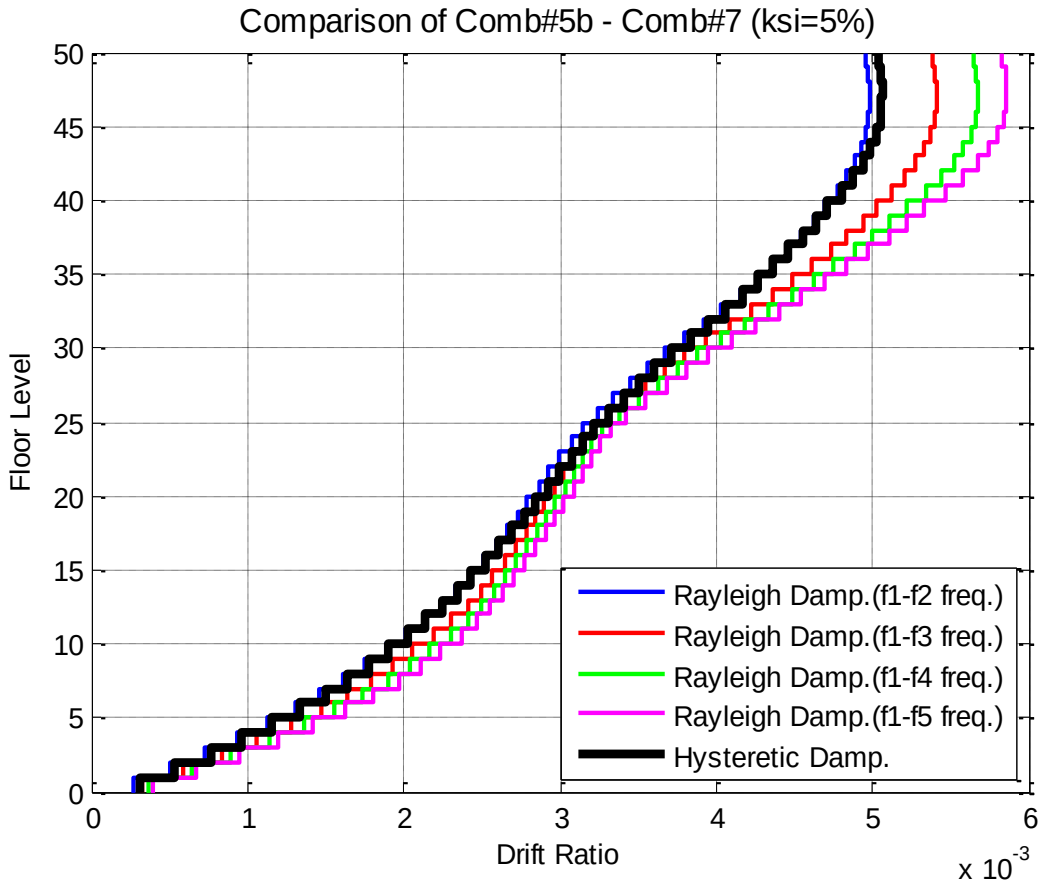

Figure 9.35. Drift ratio comparison Comb#5b – Comb#7 (ξ=5%).

9.5.2.2. Total Acceleration Response Comparison. For 5% damping ratio, structural damping is placed in the middle of Rayleigh f1-f3 and Rayleigh f1-f4.

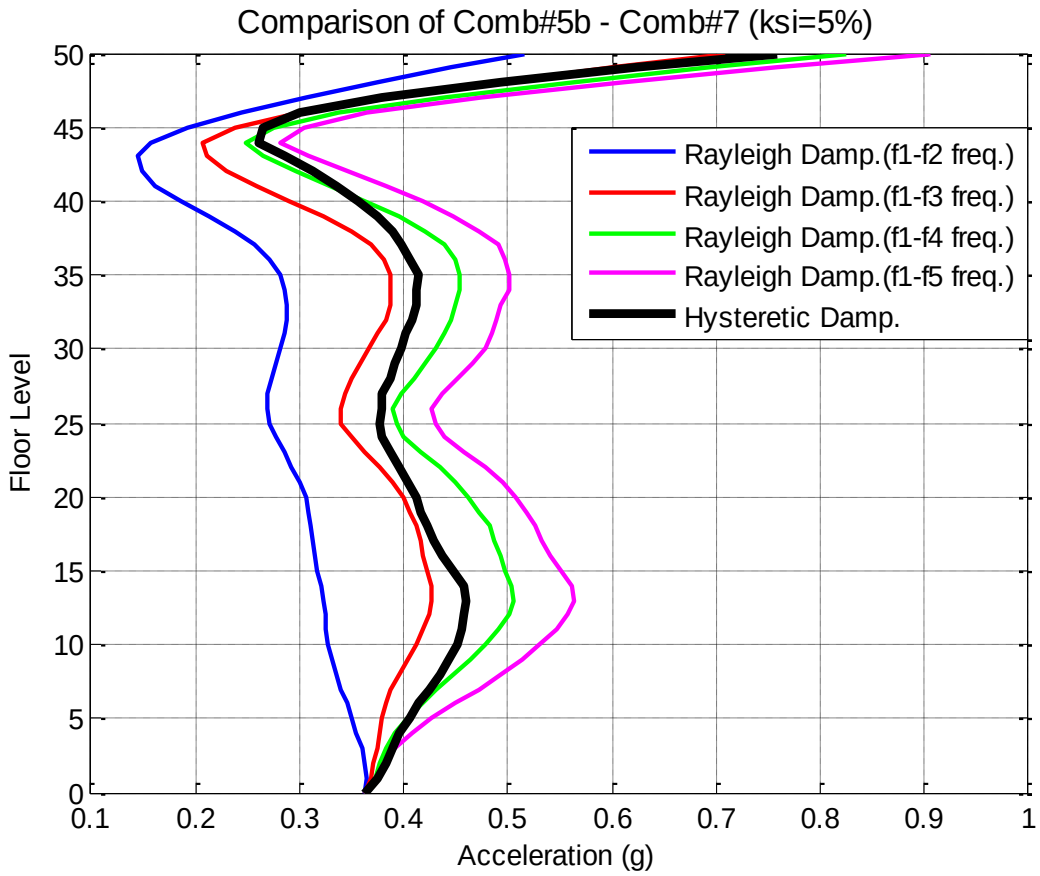

Figure 9.36. Drift ratio comparison Comb#5b – Comb#7 (ξ=5%).

10. CONCLUSION

The aim of this study, as it is mentioned before, is to investigate the very popular assumptions in structural earthquake engineering. As it is expected that most of them have not made remarkable differences, however, instructive and consistent knowledge have been captured.

Damping topic is placed on the top since most significant results are captured from that issue. The outcomes learned from this study in terms of damping topic can be outlined that so-called Rayleigh damping is very efficient method both practical usage and giving reliable results if the frequencies associated are chosen correctly. Studies show that choosing f1-f2 frequencies is enough to get correct drift ratios and it is almost independent from the damping ratio. However, for total acceleration response quantities, it is not valid. Even though, effects of different damping ratios are remarkable, author proposed that f1-f4 frequencies for Rayleigh damping should be chosen for such buildings independent from damping ratio roughly.

Another important issue that it is worth to mention here is significant difference between stiffness proportional damping and complex stiffness (structural) damping. This result presents explicitly the effect of phase shifting on seismic response.

Effects of mass representations have taken the second place. Translational and rotational lumped mass assumption is definitely identical with ordinary lumped mass approach. Thus, the idea of rigidly rotating floor masses has been discarded. Although the phase lag between consistent mass and lumped mass systems is seen in animations, since the maximum response quantities are not so different, only slight difference could have been captured from this comparison. Even so, author proposes consistent mass systems for the sake of integrity.

The last topic is related to validation of pseudo-static displacement assumption for tall buildings. The results show no difference, actually there is a very small difference but most probably, due to fact that it is caused by phase lags, it cannot be captured in drift or acceleration responses. Nevertheless, not only the sense of displacement loading but also

animations generated by using displacement formulations give a better understanding of wave travel throughout the building. Author thinks that it can be used as an educational material at least.

REFERENCES

1. Przemieniecki, J. S., *Theory of Matrix Structural Analysis*, McGraw-Hill Inc., USA, 1968.

2. American Society of Civil Engineers, *ASCE/SEI STANDARD 7-05: Minimum Design Loads for Buildings and Other Structures*, VA, USA, 2006.

3. Clough, R. W. and J. Penzien, *Dynamics of Structures*, 3rd Edition, Computer and Science Inc., Berkeley, CA, USA, 2003.

4. Chopra, A., *Dynamics of Structures – Theory and Applications to Earthquake Engineering*, 3th Edition, Pearson Education Inc., Upper Saddle River, NJ, USA, 2007.

5. Neumark, S., *Concept of Cmplex Stiffness Applied to Problems of Oscillations with Viscous and Hysteretic Damping*, HM Stationery Office, 1962.

6. Rijlaarsdam, D. J., *Modelling Damping in Linear Dynamic Systems*, 2005.

7. Wilson, Edward L., *Three-Dimensional Static and Dynamic Analysis of Structures – A Physical Approach with Emphasis on Earthquake Engineering*, 3rd Edition, Computer and Science Inc., Berkeley, CA, USA, 2002.

8. Aydinoglu, M. N., Y. M. Fahjan, *A Unified Formulation of the Piecewise Exact Method for Inelastic Seismic Demand Analysis Including the P-delta Effect*, Istanbul, Turkey, 2003.

9. Cooley, J. W., J. W. Tuckey, *An Algorithm for the Machine Calculation of Complex Fourier Series*, USA, 1965.

10. Safak, E., *Fourier Transform Lecture Notes*, Istanbul, Turkey, 2013.

11. Federal Emergency Management Agency and Applied Technology Council, *P-695: Quantification of Building Seismic Performance Factors*, WA, USA, 2009.

12. Los Angeles Tall Buildings Structural Design Council, *An Alternate Procedure for Seismic Analysis and Design of Tall Buildings Located in the Los Angeles Region*, LA, USA, 2011.

REFERENCES NOT CITED

13. Snieder, R., and E. Şafak, "Extracting the Building Response Using Seismic Interferometry: Theory and Application to the Millikan Library in Pasadena, California" *Bulletin of the Seismological Society of America*, 2006.

14. Safak, E., "Wave-propagation Formulation of Seismic Response of Multistory Buildings" *Journal of Structural Engineering*, 1999.

15. Safak, E., "Propagation of Seismic Waves in Tall Buildings" *The Structural Design of Tall Buildings*, 1998.

16. Safak, E., E. Cakti, and Y. Kaya, "Seismic Wave Velocities in Historical Structures: A New Parameter for Identification and Damage Detection" *Proceedings of* (IOMAC 2009) *the 3rd International Modal Analysis Conference, Ancona*, Italy, 2009.

17. Miranda, E., and S.D. Akkar, "Generalized Interstory Drift Spectrum", *Journal of Structural Engineering*, 2006.

18. Reinoso, E., and E. Miranda, "Estimation of Floor Acceleration Demands in High-rise Buildings During Earthquakes", *The Structural Design of Tall and Special Buildings*, 2005.

19. Liu, Y., and Zhitao L., "Methods of Enforcing Earthquake Base Motions in Seismic Analysis of Structures", *Engineering Structures*, 2010.